

Foam management in distillation plants

**Dissertation zur Erlangung des Doktorgrades der
Naturwissenschaften (Dr. rer. nat.)**

**Fakultät Naturwissenschaften
Universität Hohenheim**

Institut für Lebensmittelwissenschaft und Biotechnologie
Fachgebiet Hefegenetik und Gärungstechnologie

vorgelegt von

Daniel Heller

aus Waiblingen

2022

Dekan bzw. Dekanin: Prof. Dr. Uwe Beifuß
1. berichtende Person: Prof. Dr. Ralf Kölling
2. berichtende Person: Prof. Dr.-Ing. Reinhard Kohlus
Eingereicht am: 17.10.2022
Mündliche Prüfung am: 03.04.2023

Die vorliegende Arbeit wurde am (10.02.2023) von der Fakultät Naturwissenschaften der Universität Hohenheim als „Dissertation zur Erlangung des Doktorgrades der Naturwissenschaften“ angenommen.

“Measurement is the first step that leads to control and eventually to improvement. If you can’t measure something, you can’t understand it. If you can’t understand it, you can’t control it. If you can’t control it, you can’t improve it.”

– H. James Harrington

Table of Contents

Table of Contents	IV
List of Figures	VIII
List of Tables.....	XII
Preliminary remarks	XIII
Full papers	XIII
1. Introduction	1
1.1. Distillation	2
1.2. Volatile compounds.....	4
1.3. Foam problematic	6
1.4. Foam & Liquid Fraction	8
1.5. Distillation reproducibility	10
1.6. Thesis outline.....	11
2. Reproducibility of fruit spirits.....	13
Abstract	13
Keywords	14
2.1. Introduction	14
2.2. Materials and Methods	16
2.2.1. Batch distillation system	16
2.2.3. Mash preparation and fermentation.....	18
2.2.4. Product analysis.....	19
2.2.5. Data analysis	19
2.3. Results & Discussion.....	20
2.3.1. Distillation process parameters	20
2.3.2. Volatile compound composition of product fractions.....	27
2.4. Conclusion	33
Declarations.....	33
3. A minimal-invasive method for the evaluation of liquid fractions in foams with a point level sensor	34
Keywords	34
3.1. Introduction	35
3.2. Experimental setups and methods	36

3.2.1.	Variation of immersion depth and container materials	36
3.2.2.	Measurement setup with conductivity sensors and capacitive level sensor	38
3.3.	Results and Discussion	40
3.3.1.	Immersion Depth and Sensor Surroundings.....	40
3.3.2.	Surfactants and Solvents	41
3.3.3.	Correlation of Water Content Fractions of Foam with <i>SR</i>	43
3.4.	Summary and Outlook.....	45
	Acknowledgment	46
	Symbols used.....	46
4.	Foam-resilient distillation processes - Influence of pentosan and thermal energy input on foam accumulation in rye mash distillation	48
	Abstract	48
	Keywords	48
4.1.	Introduction	48
4.2.	Material and methods	50
4.2.1.	Mash preparation.....	50
4.2.2.	Substrate characterisation.....	52
4.2.3.	Pentosan degradation effects	52
4.2.4.	Foam accumulation experiments.....	53
4.2.5.	Statistical analysis	54
4.3.	Results and Discussion	54
4.3.1.	Substrate characteristics	54
4.3.2.	Pentosan conversion	55
4.3.3.	Effects of pentosan conversion on mash viscosity.....	55
4.3.4.	Effects of pentosan conversion on foam accumulation.....	55
4.3.5.	Unspecific protein degradation	56
4.3.6.	Effects of thermal energy input on foam accumulation	57
4.3.7.	Critical temperature range	57
4.4.	Conclusion	58
	Declarations.....	59
5.	Tackling foam-based process disruptions in spirit distillation by thermal energy input adaptations.....	60
	Abstract	60
	Keywords	60

5.1.	Introduction	61
5.2.	Materials and methods	62
5.2.1.	Distillation system	62
5.2.2.	Experimental setup	63
5.2.3.	Sampling	65
5.2.4.	Raw materials and mash preparation	65
5.2.5.	Substrate characteristics	66
5.2.6.	Distillate product analysis	66
5.2.7.	Statistical analysis	67
5.3.	Results and discussion	67
5.3.1.	Substrate characteristics	67
5.3.2.	Effects of different heating profiles (first test series)	68
5.3.3.	Effects of different heating profiles (second test series)	72
5.4.	Conclusion	77
	Declarations	77
6.	Resonant Ultrasonic Defoaming in aqueous evaporation / boiling processes at different size scales	78
	Abstract	78
	Keywords	79
6.1.	Introduction	79
6.2.	Material and Methods	80
6.2.1.	Fluids	80
6.2.2.	Ultrasound frequency	80
6.2.3.	Ultrasound systems	81
6.2.4.	Mini-scale setup	82
6.2.5.	Lab-scale setup	83
6.2.6.	Column still	84
6.2.7.	Determination of foam height and lamella length	85
6.3.	Results	85
6.3.1.	Defoaming beer wort in beaker tests	85
6.3.2.	Defoaming at different specific heat input and foam heights at lab-scale	86
6.3.3.	Implementation to a column still	89
6.3.4.	Discussion of ultrasonic effects	89

6.4. Conclusion	91
Supporting Information	92
Acknowledgment	92
Symbols used.....	92
7. Concluding remarks	94
7.1. Reproducibility: operating conditions and foam formation.....	95
7.2. Substrate-based factors influencing foam formation.....	96
7.3. Passive process parameters.....	97
7.4. Active foam management.....	97
7.5. Economic relevance of the results	98
Summary	99
Zusammenfassung.....	101
References	103
Acknowledgments.....	122
Eidesstattliche Versicherung	123
Curriculum Vitae.....	124

List of Figures

Figure 1. Vapor-liquid equilibrium of binary water-ethanol mixture at atmospheric pressure with x_F alcohol content of liquid phase, x_D alcohol content of gas phase and A azeotropic point. Source: [14].....	3
Figure 2. Rectification coefficients of compounds in ethanol-water mixtures, (A) 1-pentanol, (B) 3-methylbutyl acetate, (C) ethyl acetate, (D) methyl acetate. Source: [15].....	5
Figure 3. Distribution of volatile compounds in head, heart and tail fraction in spirit distillation with alembic distillation (full line) and column distillation (dashed line), * indicates the area of maximum concentration in the fraction. Source: [6].....	6
Figure 4. Graphical illustration of liquid fraction in foam. Source: [75]	10
Figure 5. Instrumentation diagram of the batch distillation system equipped with rectification column (A), copper packing (B) and product cooler (C). FCR = regulated valve for thermal energy input, TR = temperature sensors, FR = flowmeters, black arrow indicates point of Q1-Q3 regulation.....	17
Figure 6. Monitored distillation process parameters of repeated wine mash distillation processes A-C. Each data point was averaged over 60 seconds for better visualization.	23
Figure 7. Monitored distillation process parameters of repeated Williams pear mash distillation processes D-F. Each data point was averaged over 60 seconds for better visualization.	24
Figure 8. Monitored distillation process parameters of repeated plum mash distillation processes G-H. Each data point was averaged over 60 seconds for better visualization.....	25
Figure 9. RSD values of monitored process parameters in duplicated distillation runs A-H. Each parameter considered data of the whole distillation run. Note logarithmical x-axis scaling.....	26
Figure 10. Volatile compound concentrations in distillate fractions produced by distillation profiles A-C performed in duplicates. Note left logarithmical y-axis scaling. aa = anhydrous alcohol	28
Figure 11. Volatile compound concentrations in distillate fractions produced by distillation profiles D-F performed in duplicates. Note left logarithmical y-axis scaling. aa = anhydrous alcohol	29
Figure 12. Volatile compound concentrations in distillate fractions produced by distillation profiles G-H performed in duplicates. Note left logarithmical y-axis scaling. aa = anhydrous alcohol	30

Figure 13. RSD values based on volatile compound concentrations in product fractions sampled during replicated distillation profiles A-H. Each box plot considered data of all sampled fractions. Note logarithmical x-axis scaling	32
Figure 14. Measurement setups for various materials, immersion depth (ImD), and beaker diameters to characterize the SR of the liquid with the capacity point level sensor [136]	37
Figure 15. Schematic drawing and photo of the experimental setup used for correlating level sensor signals and liquid fractions of foams via conductivity measurements.....	39
Figure 16. Experimental data of sweep range (SR) as a function of immersion depth (ImD) of the sensor in addition to varied beaker materials with different beaker diameters at 14 °C in a liquid SDS/water mixture.....	41
Figure 17. Influence of the anionic surfactant SDS on the normalized SR (nSR) of a full-immersed sensor tip, in PVC surroundings at 14 °C.....	42
Figure 18. Experimental data of Sweep Range (SR) measured in various liquid mixtures at 18 °C.....	43
Figure 19. Experimental data of normalized Sweep Range (nSR) as a function of liquid fraction	44
Figure 20. Representation of the frequency of deviations (left) and the dependence of the deviation on the bubble size (right).....	45
Figure 21. Flow chart of rye mash preparation	51
Figure 22. Maximum foam accumulation levels (primary y-axis) and viscosity (secondary y-axis) of nine rye mashes in relation to pentosan conversion (x-axis), added pentosanase from left to right: 0.0; 0.1; 0.2; 0.8; 1.0; 1.2; 1.6; 2.0; 4.0 mL/kg (n = 3)	56
Figure 23. Maximum foam accumulation levels in rye mash distillation performed with different thermal energy inputs and different pentosanase concentrations (n = 3)	57
Figure 24. Foam accumulation levels and mash temperature during distillation of 54 rye mashes, grey line indicates 3 cm foam level	58
Figure 25. Instrumentation diagram of the batch distillation system equipped with rectification column (a), copper catalyser (b) and product condenser (c). 1: Temperature sensor ‘Mash’; 2: Temperature sensor ‘Headspace’; 3: Temperature sensor ‘Tray 1’; 4: Temperature sensor ‘Tray 2’; 5: Temperature sensor ‘Tray 3’; 6: Flow sensor ‘Reflux’; 7: Flow sensor ‘Product’; 8: Level sensors ‘Foam height’	63
Figure 26. Heating profile of experiments in the first (left) and second (right) test series	64

Figure 27. Distillation performance of control (a) and heating profile HP1.3 (b). Vertical, black arrow indicates excessive foam formation to reach the first trays.....	69
Figure 28. Distillation process with reduced thermal energy input at 90 °C mash temperature; HP1.4.....	70
Figure 29. Concentration of Ethanol (a), Methanol (b), Acetaldehyde (c) and Ethyl acetate (d) in the first fractions with control and modified heating profiles with reduced thermal energy input (HP1.1, HP1.2, HP1.3, HP1.4).....	71
Figure 30. Distillation process of rye mash with control (a) and HP2.1 (b). Vertical, black arrow indicates overflow of foam onto trays.....	74
Figure 31. Distillation process of Bartlett pear mash with control (a) and HP2.3 (b)	75
Figure 32. Ethanol recovery of rye mash (a) and Bartlett pear mash (b) distillation with heating profiles control, HP2.2 and HP2.1 or HP2.3.	76
Figure 33. Measured electrical impedance Z (a) and phase angle (b) in frequency range between 20 kHz and 200 kHz. Local minima and maxima in a) indicate the transducers mechanical resonance and antiresonance, respectively.....	82
Figure 34. Schematic setup of beaker test showing wave propagation through liquid bulk	82
Figure 35. Lab-scale setup with ultrasound actuator clamped on metal wall	83
Figure 36. Schematic sequence of the test series by alternating heat input and ultrasound powers. Referencing foam heights and foam heights during sonication were measured within each heating step	84
Figure 37. Sketch of the batch copper still with sieve tray column and dephlegmator (A), copper catalyst (B) and product cooler (C), ultrasonic actuators (US) and all installed sensors	84
Figure 38. Temporal foam decay of boiling wort in waterborne ultrasound with a frequency sweep 40-168 kHz, at modified power a); and lengths of wall bounded Plateau borders before and 6 s after the start of sonication at 10 W, n=50 lamella.	86
Figure 39. Mean equilibrium foam heights, averaged over 4 min without insonication at different heat inputs, n =3	87
Figure 40. Separation of foam of beer wort in a fine-pored foam on the top and a coarse-pored foam layer at the bottom at incident heat input 250 WL ⁻¹	88
Figure 41. Mean equilibrium foam heights normalized to individual reference foam height for beer wort a), rye mash b) and SAS c).....	88

Figure 42. Comparison between process with ultrasonic foam suppression and a reference process without defoamers. A temperature difference $< 2^{\circ}\text{C}$ between temperature of headspace and of mash indicates flooding of the headspace with foam and reaching the sensors. Sonication suppresses the foam formation leading to a decrease of the temperature in the headspace and in the first and second tray again..... 89

Figure 43. Overview of foam formation under boiling condition, its causes (black), promoting factors (dark grey) and foam management methods (light grey) with their place of action 95

List of Tables

Table 1. Distillation profile parameters.....	18
Table 2. Substrate characteristics	19
Table 3. Parameters of the logarithmic fit regarding nSR as a function of liquid fraction (ϕ)	44
Table 4. Substrate characteristics of rye mash	54
Table 5. Process parameters for experiments in the test series	65
Table 6. Analyzed volatile compounds in the fractionated distillates.....	67
Table 7. Mean values and standard deviations of substrate characteristics of each mash batch.	68
Table 8. Density, viscosity, and surface tension given for beer wort, rye mash, SAS-solution (0.1 %). Rye mash displays shear thinning rheological properties, thus the viscosity value for rye mash is given at the maximum shear rate. * Measurements at 20 °C, ** Reference values of water have been used.	80
Table 9. Calculated resonant frequency of aqueous foams with a mean bubble radius of 1 mm for liquid fractions between those of spherical and polyhedral bubbles	81
Table 10. Summary of applied actuator power inputs and ratio of power to cross-section area	90

Preliminary remarks

The work presented in this thesis is a selection of papers published in international peer-reviewed journals, which are listed below.

Full papers

First author

Heller D, Einfalt D. Reproducibility of Fruit Spirit Distillation Processes. *Beverages*, 8(2), 20 (2022). <https://doi.org/10.3390/beverages8020020>

Contribution Conceptualization, Methodology, Investigation, and Writing (review & editing)

Heller, D., Einfalt, D. Foam-Resilient Distillation Processes—Influence of Pentosan and Thermal Energy Input on Foam Accumulation in Rye Mash Distillation. *Food Bioprocess Technol* 14, 1640–1647 (2021). <https://doi.org/10.1007/s11947-021-02660-9>

Contribution Conceptualization, Methodology, Investigation, Formal Analysis, and Writing (Original Draft)

Heller, D., Roj, S., Switulla, J., Kölling, R. and Einfalt, D. Tackling Foam-Based Process Disruptions in Spirit Distillation by Thermal Energy Input Adaptations. *Food Bioprocess Technol* 15, 821–832 (2022). <https://doi.org/10.1007/s11947-022-02785-5>

Contribution Conceptualization, Methodology, Investigation, Formal Analysis, and Writing (Original Draft)

Co-author

Staud, R., Heller, D., Knüpfer, L., Heitkam, S., Einfalt, D., Jasch, K. and Scholl, S. Minimal-Invasive Method for the Evaluation of Liquid Fractions in Foams with a Point Level Sensor. *Chem. Eng. Technol* (2022). <https://doi.org/10.1002/ceat.202200072>

Contribution Conceptualization, investigation (Correlation of Liquid fraction/SR), statistical analysis, Writing Draft (Introduction, Correlation liquid fraction/SR)

Thünnesen, J., Gerstenberg, C., Heller, D., Leuner, H., Einfalt, D., McHardy, C., Gatternig, B., Rauh, C., Repke, J. and Delgado, A. Resonant Ultrasonic Defoaming in Aqueous Evaporation/Boiling Processes at Different Size Scales. *Chem. Eng. Technol* (2022). <https://doi.org/10.1002/ceat.202200068>

Contribution Investigation (Column still), Formal Analysis (Data Column still)

1. Introduction

Each time a new process is developed, process-related problems emerge that were previously unknown or not considered. As a result, the nature of processes is to be constantly subject to optimization and improvement, as well as adaptation to work around problems. The same applies to distillation.

Distillation is one of the oldest used methods for the separation of a liquid mixture [1] utilizing selective evaporation and subsequent condensation. The process of distillation traces back more than 5000 years [2]. Since then, distillation has constantly been improved upon and is now one of the best investigated and understood processes. Therefore, it is not surprising that distillation is widely used in many industry sectors, i.e. chemical, pharmaceutical, biotechnology, and food industries.

The application of distillation for producing high-proof spirits in Europe goes back to two men. In the 12th century, Magister Salernus of the Salerno School documented the first recipe for producing brandy by fractional distillation of alcoholic wine. In the 13th century, Albertus Magnus further developed the distillation of wine. Their research and developments laid the foundation for the distillation of spirits and ensured that distillates were widely used in medicine in the coming centuries. [2]

Additionally, during this time it became the norm to drink distilled, high-proof alcohol as a stimulant. The consumption of spirits became the main driver of research, as well as the improvement of distillation and distillation equipment in general [1]. Some of the most important contributions were made by Brunschwyk [3], Ryff [4], and French [5]. The continuous improvement of the distillation equipment for the production of spirits culminated in column stills, which can be traced back mainly to Jean-Baptiste Cellier-Blumenthal, and are the most used distillation system in Germany for spirit drink production today [6].

The widespread consumption of spirits caused the diversification of spirits. In many countries high-proof beverages with a distinctive taste were developed, be it whisky from the UK, cognac from France, grappa from Italy, palinka from Hungary, or vodka from Russia. Due to the availability of raw materials, mainly fruit spirits have been produced and consumed in Germany.

Currently, there are about 17,800 spirits distilleries [7] with a turnover of 2.28 billion €/a and production output of 534 million bottles [8] in Germany. Due to the increased competitive situation [9] and the abolition of the Branntweinmonopolgesetz in 2017, the quality of the products produced is becoming increasingly more important [10,11]. However, it is repeatedly shown at awards that a considerable proportion of the distillates submitted have quality deficiencies [12,13]. This indicates that the current distillation process and the equipment used continue to require further improvements.

1.1. Distillation

An overview of distillation is given by Kirschbaum [14], Spaho [6] and Pieper et al. [15]. The relevant knowledge is summarized below.

Although distillation has been applied for the last 5000 years, the fundamental setup is always consistent. Distillation is the evaporation followed by the condensation thereof. Therefore, a distillation system consists at least of a vessel for heating a mixture of liquids and a condenser to collect the created vapor, as well as a pipe to transfer the vapor from the vessel to the condenser.

When liquids containing alcohol are heated in such a vessel, the boiling point depends on the alcohol content of the liquid. The boiling point is reached when the vapor pressure of the liquid, which rises during heating, is equal to the atmospheric pressure. For pure alcohol, this state is reached at a temperature of 78.3 °C, while for pure water, this state occurs at 100°C. In an alcohol/water mixture, the boiling point is always between these two temperature values, depending on the mixing ratio with one exception. At an alcohol content of 97.2 % vol, the boiling point of an alcohol/water mixture is 78.15 °C.

The created vapor by heating an alcohol/water mixture above its boiling point is like the liquid, always an alcohol/water mixture. The composition of the vapor is determined by the alcohol content of the liquid and its boiling temperature, respectively. The most important effect of the distillation of alcohol is that when highly volatile compounds (alcohol) and low-volatile compounds (water) mixtures are heated, the created vapor is enriched in the highly volatile compounds. Accordingly, the proportion of the low-volatile compounds in the remaining liquid increases.

The maximum achievable enrichment of alcohol in the vapor phase is limited by the alcohol content of the given liquid. For example, with an alcohol content of 10 % vol in the liquid phase present, a maximum enrichment with a factor of 3.27 can be achieved to an alcohol content of 32.7 % vol. By plotting the alcohol content of the emerging vapor phase against the alcohol content of the corresponding liquid phase, *Figure 1* is obtained.

To achieve a higher enrichment in alcohol or higher alcohol concentration in the distillate, respectively, another distillation of the distillate is required. To distinguish between single and double distilled spirits, different terms are used. They are called raw spirits after one distillation and fine spirits after two or more distillations. In the previously given example with a given 10 % vol alcohol/water mixture, at least four distillations are required to reach an alcohol concentration of > 80 % vol. But this is only the case if the vapor-liquid equilibrium would be consistent during distillation. However, in a simple distillation setup, the enrichment is reduced over time due to the decreasing alcohol content in the liquid phase.

Besides, there is also a physical limit on the enrichment of alcohol by multiple distillations. If the alcohol-water mixture reaches an alcohol content of 97.2 % vol, alcohol and water form an azeotropic mixture (*Figure 1 A*). This means, that the emerging vapor has the same composition

as the liquid from which it evaporates. Accordingly, an increase in the alcohol content of such a mixture is no longer possible by distillation.

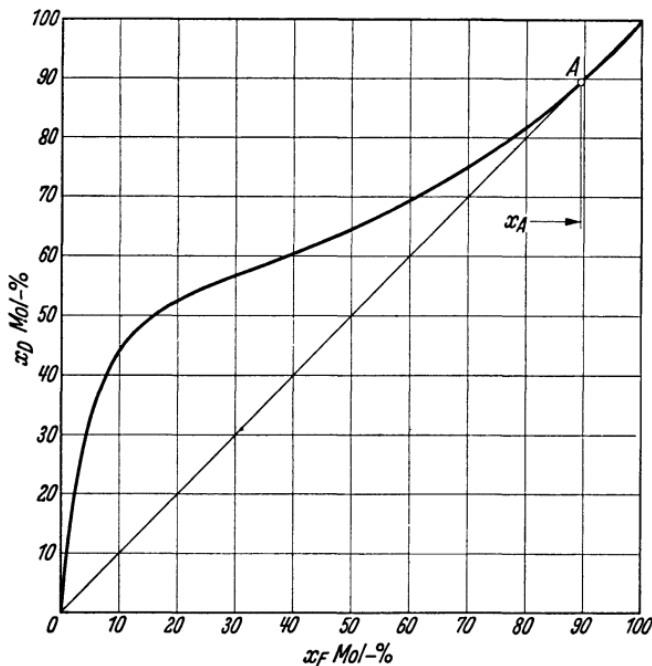


Figure 1. Vapor-liquid equilibrium of binary water-ethanol mixture at atmospheric pressure with x_F alcohol content of liquid phase, x_D alcohol content of gas phase and A azeotropic point. Source: [14].

To perform multiple distillations in a single step, so-called distillation columns were invented. Compared to the simple distillation systems, which are also called alembic style distillation or alembic pot stills, pot stills with distillation columns or column stills have the advantage that several distillations are performed in one distillation step and the vapor-liquid equilibrium can be kept constant for a longer period.

To achieve multiple distillations in one step a column with internals and a condenser at the top is introduced after the heating vessel. The condenser at the upper end of the column, i.e. after the uppermost internal, condenses rising vapor and ensures a countercurrent of liquid. For this reason, this type of distillation is called countercurrent distillation, in contrast to the pot still which works according to the co-current principle. By generating the countercurrent, the descending liquid stream at boiling temperature is constantly fed against the upward rising vapor stream. As a result, the down-flowing stream increases in low-volatility compounds, while the up-flowing stream increases in high-volatility compounds. This leads to an accumulation of alcohol in the vapor. Accordingly, the temperature in such a column also decreases from the bottom to the top, since a larger proportion of water precipitates at the bottom, while concentrated alcohol is present at the top.

Internals are used to increase the liquid-vapor interaction of the downflowing liquid with the upward rising vapor stream. This increases the exchange of volatile compounds between the two phases. Commonly used internals in spirit distillation are trays, either sieve or bubble cap

trays. However also structured and unstructured packing can be found. On trays down-streaming liquid is collected. Overflow pipes allow excess liquid to drain onto trays below. The rising vapor is directed through the liquid phase on the tray ensuring close contact between the liquid and vapor phases. In packings the downflowing liquid is distributed over the large surface area of the packing. The rising vapor passes through the packing and is hereby in close contact with this large surface of the liquid.

The separation of alcohol and water by heating-induced evaporation of mostly highly volatile compounds in such a distillation system is also called rectification [16]. However modern distillation systems in spirit production use additional dephlegmation to separate alcohol and water [15]. In contrast to rectification, dephlegmation separates alcohol and water by cooling-induced condensation of mostly low volatile compounds. For this purpose, a partial condenser is introduced at the top of the column instead of a full condenser. On the one hand, this provides the necessary reflux into the column for rectification, and on the other hand, the alcohol is enriched by the partial condensation of low volatile compounds (=dephlegmation). A distillation system that is based solely on this type of enrichment is the so-called Pistorius basin, which is rarely used today.

1.2. Volatile compounds

So far, only a two-phase mixture of substances or a binary mixture of substances have been considered. Although water and alcohol account for over 99% of the ingredients in spirits, the alcohol-containing mashes have a large number of other volatile substances present, which are also partly distilled and present in the final spirit. The < 1% is composed of several volatile aroma compounds from the original raw material, as well as volatile compounds formed during fermentation by the yeast *Saccharomyces cerevisiae* or during distillation [17–25]. These compounds include higher alcohols, esters, carbonyl compounds, and fatty acids [15,17]. In total, several hundred volatile constituents are found in distillates, but only a very limited number of them influence the aroma of the fruit spirit and thus play a decisive role in the quality of the product [18,26]. The challenge during distillation is to separate typical aroma compounds of the fermented fruit from undesirable aroma compounds that are negatively correlated with the overall aroma.

Due to the abundance of volatile compounds, several effects have to be considered during their distillation: the compositions and concentrations of the compounds change continuously with time, the compounds interact with themselves and each other, and the volatility of the compounds is highly dependent on the ethanol content in the liquid phase from which they evaporate [6,27]. The latter effect, in particular, is of critical relevance and is referred to as ‘relative volatility’ or ‘rectification coefficient’. It indicates the ratio in which the compound is enriched in the vapor phase or depleted in the liquid phase, depending on the prevailing ethanol concentration (*Figure 2*). For example, in a 10 %vol ethanol solution, 1-pentanol accumulates in the vapor phase in a ratio of 3:1. If the ethanol concentration is increased to 40 %vol, the vapor and liquid contain equal proportions of 1-pentanol. At an ethanol concentration of 70

% vol, 1-pentanol accumulates in the vapor phase in a ratio of 0.75:1 and therefore remains in larger proportions in the liquid phase.

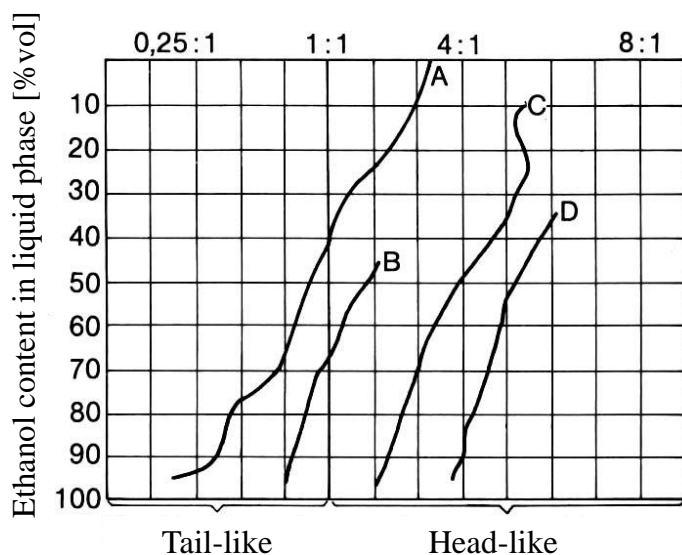


Figure 2. Rectification coefficients of compounds in ethanol-water mixtures, (A) 1-pentanol, (B) 3-methylbutyl acetate, (C) ethyl acetate, (D) methyl acetate. Source: [15].

With the rectification coefficient, the behavior of volatile compounds during distillation with trays can be predicted very well, since on each tray, in theory, a complete condensation of the vapor takes place with a renewed evaporation. Thus, the concentration of volatile compounds in the rising vapor always results from the ethanol concentration of the underlying tray.

In addition, the rectification coefficient indicates that some volatile compounds will be always enriched independent of the ethanol concentration (*Figure 2 C & D*), while others show a differentiated distillation behavior depending on the ethanol content (*Figure 2 A & B*). Volatile compounds showing the first behavior will always be the first to be distilled. While volatile compounds showing the latter distillation behavior will only distillate when the ethanol content decreases under a certain threshold. This enables the fractionation of the obtained distillate in head, heart, and tail.

A fractionation in head, heart, and tail is possible with all distillation systems. However, the fractionation behavior of volatile compounds differs in alembic pot stills and pot stills with columns (*Figure 3*) [6]. Various works [28–32] have already extensively compared countercurrent with co-current distillation and showed that the main reason for this is the differences in ethanol concentration. While distillations with column stills generally yield a higher ethanol concentration of 70-87 % vol in head and heart fraction, distillations in alembic pot stills yield ethanol concentration of 15-25 % vol depending on the alcohol content of the mash or 60-70 % vol if the raw spirit is distilled. In addition, these works showed that besides ethanol concentration, significant differences in the composition of volatile compounds and aroma compounds can result from other distillation process parameters.

Especially important regarding the composition of volatile compounds in countercurrent distillation is the cooling rate of the partial condenser or the dephlegmation rate, respectively [33–36]. The higher the cooling rate the higher the thermal barrier, which provides resistance to the vapor to pass on towards the product cooler. This leads to higher internal reflux and an increase in highly volatile compounds by cooling-induced condensation of low volatile compounds in the vapor.

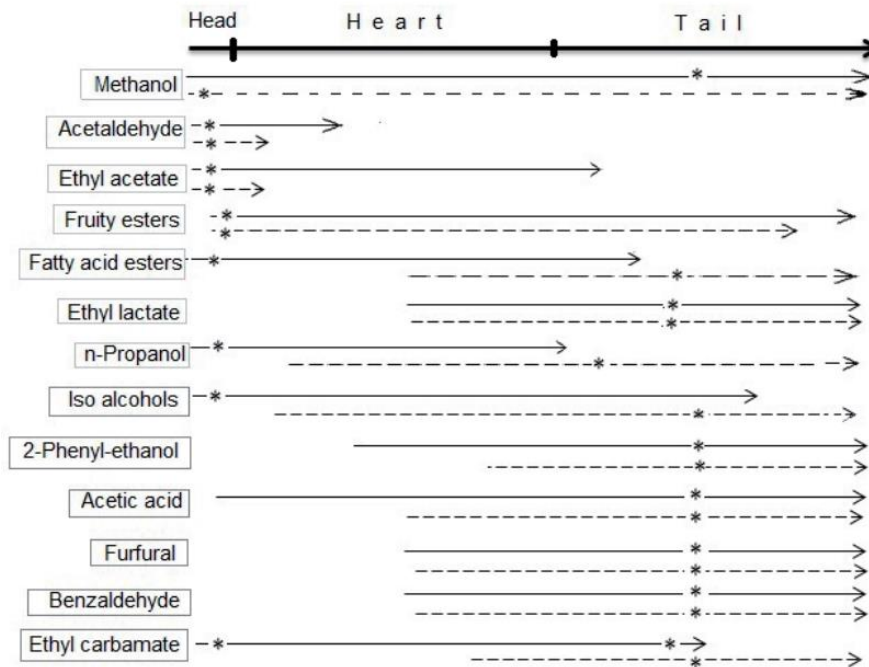


Figure 3. Distribution of volatile compounds in head, heart, and tail fraction in spirit distillation with alembic distillation (full line) and column distillation (dashed line), * indicates the area of maximum concentration in the fraction. Source: [6].

1.3. Foam problematic

In many industrial processes accumulating foam levels are a common cause of malfunction and process failures. Due to the inherent foaming properties of foodstuffs, especially due to the presence of proteins and polysaccharides [37–41], many processes in the food and beverage industry are subject to foaming problems [42–45]. This is equally the case in the spirits industry, where a large variety of different substrates, each having a specific composition regarding protein and polysaccharides and a specific foaming property, are processed. Some substrates with especially enhanced foam formation capacities are mentioned in the literature [15]. Within fruit-based substrates, these include cherry, Bartlett pears, and wine lees. Within cereal substrates in particular rye mashes are regarded as exhibiting strong foam formation. However, substrate properties are not solely responsible for excessive foaming. Inadequate operational process management and technical faults are two major contributors to various foam-related process problems [46].

For processes including thermal separation, an efficient phase transition from the liquid to the gaseous phase is essential. Foam forms and accumulates at the boundary layer between the liquid and gaseous phase, thus impairing an efficient phase transition. This is particularly unfavorable in such processes and is one of the main problems in the distillation industry [46]. Besides impairing phase transition, accumulating foam levels transport liquid and solids from the mash into plant sections that are normally only reached by 'purified' ethanol enriched vapor or the corresponding condensate. This leads to increased cleaning efforts and increased maintenance costs [15,47]. In severe cases excessive accumulating foam levels even discharge from the distillation system into the distillate and cause contamination of the valuable product, thus impairing the product quality [15,47]. Subsequently, cost-intensive cleaning steps e.g. filtration or an additional distillation have to be carried out to remove the contamination and restore the quality of the distillate. Additionally, to stop spillage of excessive foam formation into the distillate, a partial or complete process shutdown is necessary [47,48]. A shutdown requires a subsequent restart of the process with corresponding costs for cleaning the system, energy costs for reheating the mash, and energy costs to regain separation efficiency.

However, even foam levels, which do not spill into the distillate, can already reduce the distillate's quality. As foam rises to the trays or internals of the column, its separation efficiency is reduced by the carryover of liquid from the heating vessel. This leads to a reduction in the alcohol concentration by carry-over of liquid that would otherwise be separated by distillation and can accordingly negatively influence the aroma profile of the distillate by changing the distilling behavior of volatile compounds [46,47,49]. Another effect reducing the separation efficiency of a distillation system is the creation of micro droplets or mist by rupturing of the foam bubbles [47]. These microdroplets are entrained by the rising vapor and thus reach the trays and the distillate while missing a separation step. Miller [47] states that these droplets 'are thought to have flavor impact by mixing some small fraction of the pot liquid with the condensate, out of equilibrium'. However, no clear research results could be found to support this hypothesis.

Other problems regarding foam formation in distillation processes include increased pressure losses and a reduction in the possible throughput [46]. However, both of these problems are mainly concerning large continuous working distillation plants and do not play a major role in batch distillation systems.

The foam problem resulted in several adaptations of distillation systems. Because a carryover of the liquid phase to a higher tray causes a back-mixing of the liquid and thus canceling the separation work performed, tray distances of at least 200 to 300 mm are usually observed in distillation columns [50]. In Scottish pot stills elongated swan necks were introduced to prevent the carry-over of foam and to reduce the transfer of micro droplets into the distillate [47,49]. Similarly, large helmets or increased heating vessel size were introduced in other regions [15,51]. Otherwise, a reduced filling of the heating vessel of 25% to 50% is common [15]. Another adaptation of distillation systems includes the introduction of a foam retention installation between the heating vessel and the column or the spirit pipe. When foam reaches these foam retention devices, the upward motion of the foam is converted into a rotational motion by a horizontally bent tube, causing the foam to partially disintegrate [15,52]. However,

all of these measures increase manufacturing costs or require a larger distillation device having a higher surface area, which is associated with higher process costs due to additional surface area heat radiation.

Currently, a common strategy to reduce foam accumulation in distillation plants is the addition of chemical antifoam based on mineral or silicone oil [53]. These chemical defoamers replace or modify surface-active stabilizers, reduce the surface viscosity and the elasticity of the foam and hereby increase film thinning and stretching deformations that precede bubble bursting [53–55]. Because of this ability, which is substrate-independent, chemical defoamers are reliable and widely used foam inhibitors in the distillation industry [56]. However, there are also some negative aspects. In the stillage remaining, mineral or silicone oil-based defoamers enter the environment via the wastewater chain causing environmental concerns [57,58]. In natural water bodies they have negative effects on oxygen transfer rates, influence microorganisms, and impair biodegradation processes [58]. Because of their resistance to environmental degradation, they are poorly biodegradable and remain over a long period in the environment [57,59]. Therefore, chemical defoamers are under tight regulatory pressure, especially in environmentally sensitive areas [59].

In other industrial processes mechanical, thermal, and acoustic methods for active, physical foam destruction are deployed [60–62]. These involve foam destruction by thermal effects, either freezing or heating via a hot contact surface, steam, infrared arrays or hot air, rotating internals, spraying with water or with the foam immanent liquid, and the use of ultrasonic technology [60]. However, all of these methods are associated with high investment costs and bear the risk of secondary foams formation, which could cause flooding [60,63,64]. To date, no application of these methods in spirit distillation has been described in the literature.

In general, research regarding process-related measures to reduce foam formation in spirit distillation systems is scarce. So far there are studies on the dependency of the heating vessel size and vapor flow rate on foam accumulation [51], as well as an unspecific, heuristic recommendation to reduce thermal energy input at critical foam-prominent temperature ranges with associated process retardation [15]. However, both sources state, that excessive foam formation may happen despite the implemented management strategies.

1.4. Foam & Liquid Fraction

To deploy a reliable foam management, other problems must be addressed beforehand. First, it is important to gain excessive information about the accumulation of foam, its mechanism, and factors that influence it. For a successful foam management, it is also necessary to know about the foam structure that is present [61,65]. Only then a foam management consisting of passive measures, e.g. adjustment of the heating power, and/or active measures, e.g. ultrasound can be implemented.

In general liquid foams are defined as a nonpermanent form of gas bubbles separated by thin films of a liquid continuous phase [37,43,66]. The thin films, also called lamellae, between the

bubbles are connected via plateau borders containing the bulk of the liquid phase. Besides a mostly aqueous fluid, the continuous liquid phase contains surface active molecules called surfactants, which stabilize the liquid films. In foodstuffs like mashes, the continuous liquid phase may as well carry solid particles, which could stabilize the liquid films between bubbles [62,67].

In distillation processes the formation of foam occurs on three occasions [37]. Either a liquid is saturated with a gas, e.g. by fermentation, and the gas is expelled by a change in pressure, a gas phase in the liquid is created by heating induced evaporation and is expelled or gas is introduced into the liquid by mechanical processing, e.g. by vigorous stirring, pumping. In all cases, however, the foaming capacity of the liquid is relevant for foam formation. The foaming capacity of a liquid is directly dependent on its physical properties. Important physical parameters with direct or indirect effects on foamability include density, surface tension, wetting angle, and specific thermal capacity, in addition to rheological properties [68–70]. The physical properties of a foamable liquid are strongly influenced by various dissolved substances in the liquid. These are either substances increasing the viscosity or the previously mentioned surfactants, which influence the surface tension. In foodstuff proteins, cellulose derivatives, polyphenols, and polysaccharides are therefore of major importance for foam formation [60,71,72]. The physical properties of the liquid influence the foaming capacity, but also have a direct influence on the foam itself, its appearance, and structure.

To characterize and categorize foams, different structural and geometric properties are used, like the bubble size or the polydispersity [73]. A crucial role in determining the foam structure and its stability is played by the gas or the liquid fraction, respectively [73,74].

The liquid fraction represents the ratio of the liquid's volume to the total foam volume. Foams are roughly separated into dry foams, having a low liquid fraction, and wet foams, having a high liquid fraction. Dry foams are very rigid, while wetter foams lose rigidity [74]. In drier foams with a gas fraction of > 0.75 [37] the bubbles are in close contact and deform one another, causing them to have an increasingly polyhedral shape (Figure 4). On the other hand, if the liquid fraction increases the bubbles become increasingly spherical. At a critical liquid fraction, the bubbles lose contact (jamming transition) and the rigidity of the foam decreases [37,74]. However, for an effective foam management rigid, dry foam is favorable because it is easier to destroy by mechanical stress [74].

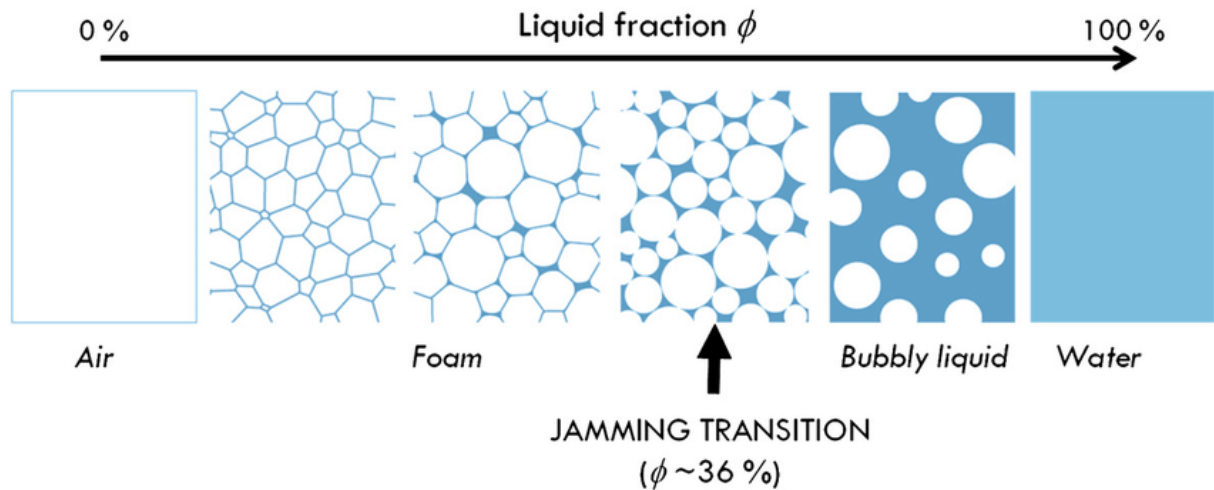


Figure 4. Graphical illustration of liquid fraction in foam. Source: [75].

As long as no new liquid is added the liquid fraction naturally, constantly decreases due to the drainage of liquid during aging of foams. The decrease in liquid fraction leads to bursting of the thin layers between individual bubbles and hereby to coalescence. Additionally, the diffusion of gas from dissolving small to growing large bubbles, the so-called Ostwald ripening, is accelerated. The gas exchange takes place through the liquid thin film, if the liquid fraction decreases, the thin film thickness also decreases promoting a faster diffusion. However, in a process such as distillation, new foam is constantly being formed limiting the effects of aging.

Nevertheless, due to the formation of new foam and the drainage of liquid, the liquid fraction is in a constant state of change. Since it is largely responsible for the foam structure and stability, it is an important parameter for effective foam management. Currently, there are several ways to measure the liquid fraction in foams, be it by electrical conductivity, optical transmission, surface fraction by imaging light reflection, ultrasound, X-ray radiography, or neutron imaging [76–85]. However, all of these methods have characteristics that make them unsuitable for use in industrial plants, e.g. they require non-conductive vessels, transparent walls, the measuring device is too large, or they are simply too expensive. A new constant, reliable determination of the liquid fraction in industrial plants by a straightforward method is therefore necessary.

1.5. Distillation reproducibility

Besides excess information on foam accumulation and foam structure, it is important to quantify the effects of an anti-foam measure to implement a successful foam management. This includes on the one hand influences on the foam and on the other hand influences on the product and the processes. To exclude external uncontrollable influences and thus relate the observed differences solely to different experiment variables, the development of a reproducible distillation process is necessary [28].

Spirit distillations are influenced by many external and internal parameters, which affect the reproducibility of distillations.

Directly controlled parameters in the process are the heating power and the cooling rate of the dephlegmator in pot stills with columns. These two parameters control the evaporation rate and the reflux in the column. This in turn has an influence on the separation efficiency and thus on the composition of the distillate [32,86–89]. External factors also play an important role. For example, the ambient temperature also causes reflux [28]. While this accounts for a small proportion compared to the actively generated reflux in column stills, it is the main cause of reflux in alembic pot stills. Other external influences on evaporation behavior are the air pressure and the humidity of the air [28]. Also, properties of the substrate or the mash, respectively, influence the distillation process, e.g. ethanol content.

To achieve comparable results, all these parameters must be considered. Looking at other processes apart from spirits distillation, extensive process control and monitoring offer the chance to quantify effects of external influences and enable an improved regulation of process parameters, thus increasing the reproducibility of processes and even leading to process reformations [90–92].

1.6. Thesis outline

The present thesis addresses the formation and destruction of foam under boiling and evaporation conditions in distillation processes. The aim is to develop methods for foam control and inhibition, and to determine substrate-specific foam-promoting properties of mashes.

As a basis, a batch distillation column has to be modified such that the lack of reproducibility in spirit distillation is overcome. Therefore, a distillation plant has to be digitalized, and extensive instrumentation and control equipment has to be installed. This eliminates variable operational influences and allows the quantification of external influences. The extension of the distillation plant needs to include sensors constantly measuring foam properties to gain excessive knowledge about foam formation, destruction, and structure in distillation plants. On the one hand, this allows the instantaneous evaluation of the effectiveness of foam management methods and on the other hand to generate data regarding the structural changes in the foam for future simulation research. Because an applicable method for determining the liquid fraction of foams in industrial plants, which is a major factor influencing the foam structure, is still missing, a new minimally invasive method for determining the liquid content is needed.

All of this serves to investigate and quantify different operating conditions including active and passive foam management methods and their influence on foam formation. Passive methods describe the adjustment of process parameters without active intervention in the process itself. While active methods include a severe intervention in the process either by introducing mechanical or thermal actors.

The development of passive methods for foam management is based on the working hypothesis that process parameters have a decisive influence on the foam dynamics under boiling conditions. Because foam formation has a complex causal relationship with process parameters, suitable modes of operation can be found to avoid foam-induced disturbances in distillation processes. As the most important process parameter the main focus is on the thermal energy input. By defined variation of the thermal energy input and the resulting varied heating profiles, heating effects on foam formation with different substrates can be investigated. Subsequent heating profiles with minimum foam formation on a substrate-specific basis can be developed. Additionally, foam-promoting temperature ranges in distillation systems can be deduced. The findings on heating can be further developed to derive general recommendations regarding foam dynamics under boiling conditions in distillation systems. However, the factors energy demand, processing time, and product quality must be urgently considered.

Besides passive foam management methods, active, physical foam-regulating or -destroying mechanisms have to be investigated and their effects systematically verified. For the application in a distillation system, such methods are used whose effectiveness and advantageous mode of operation have been demonstrated on a laboratory scale or based on simulation studies. The focus of research here is the use of ultrasound, as its use has fewer disadvantages compared to other thermal or mechanical foam destruction methods [60]. A destructive effect of ultrasound on foam accumulation in distillation systems is expected. The use of ultrasound to destroy foam could have an impact on the resulting product, due to the creation of micro droplets by bubble bursting.

To complete the research of foam formations in distillation systems, in addition to active and passive foam management measures substrate-specific physical factors that contribute to foam formation have to be investigated on a laboratory scale. In particular, substrates with a strong foaming tendency will be investigated. The working hypothesis is that the rheological properties of substrates, derived from specific ingredients like proteins and polysaccharides, contribute to different foaming capacities of substrates. Such ingredients, which enable substrates to cause large foam formations, are to be detected and, if possible, selectively removed. By doing this, the formation of foam can be inhibited, and/or the stability of foams can be impaired.

These three approaches, foam inhibition by selective removal of foam-promoting substances, passive foam inhibition and reduction by adaption of process parameters, and active foam destruction, constitute a comprehensive arsenal of foam management and control methods. By developing and designing such methods process malfunctions due to foam formations can be avoided in the future. This allows energy- and resource-efficient operation of the distillation systems even under foam risky conditions. In the following, an insight into the research regarding foam dynamics, and the development of methods for foam control in distillation plants of the spirits industry is provided.

2. Reproducibility of fruit spirits

Daniel Heller and Daniel Einfalt*

University of Hohenheim; Institute of Food Science and Biotechnology; Yeast Genetics and Fermentation Technology; Garbenstraße 23; Stuttgart 70599; Germany

*Correspondence: daniel.einfalt@uni-hohenheim.de (D.E.); Tel.: +49 711 459 23353

Abstract

Fruit spirit distillations processes are based on physical principles of heat and mass transfer. These principles are decisive for the separation of desired and undesired aroma compounds which affects the quality of the distilled product. It is mandatory to control heat and mass transfer parameters to be able to perform fruit spirit distillation processes in a reproducible manner and to achieve equal products with similar volatile compound compositions repeatedly. Up to now, only limited information is available on the magnitude of reproducibility errors since fruit spirit distillation columns are typically not equipped with suitable control or monitoring technique. We upgraded a batch distillation column with digitized instrumentation and control technique to be able to control crucial parameters such as thermal energy inputs and reflux rates. The aim of this study was to identify whether control over two distillation parameters has the potential to perform distillation processes repeatedly. This study analyzed the magnitude of reproducibility errors for (i) six monitored distillation process parameters and (ii) 13 quantified volatile compounds in the product between duplicated distillation runs performed with equal setups. A total of eight different distillations were performed in duplicates (n=16), while the six distillation parameters were monitored and logged every ten seconds. The produced distillates were equally subsampled into 20 fractions and each fraction analyzed for 13 volatile compound concentrations. Based on a data set of 28,600 monitored duplicate distillation process data points, this study showed that process parameters can indeed be replicated with a median relative standard deviation (RSD) of <0.1% to 7.0% when two crucial process parameters are controlled. The comparison of 1,540 volatile compound concentrations in the product fractions showed a reproducibility error with an average median RSD of $9.0 \pm 8.0\%$. This showed that by gaining control over thermal energy input and reflux rates the reproducibility of fruit spirit distillation processes and their associated products can largely be met. It is advisable to equip distillation columns with suitable control technique to be able to perform fruit spirit distillations reproducibly.

Keywords

batch distillation column; thermal energy input; rectification column; relative standard deviation; reproducibility error

2.1. Introduction

Fruit spirits are consumed in several countries all over the world. The pre-tax turnover for the distillation industry in the EU is estimated to 26.5 billion € [93]. In Germany there are 14,671 small and medium-sized (SME) distilleries that in the year 2018 produced 3.8 million L ethanol [94]. Both distillers and consumers would like to achieve products with consistently high quality in a reproducible manner. The quality of distillates depends on several aspects such as fruit quality, mashing, fermentation, distillation parameters and aging. The Federation of German Food and Drink Industries considers food and drink quality to be the most important factor for consumer decisions [11]. They also stated that through innovations in quality improvement, food manufacturers have been able to increase product sales by 2.2 percent annually over the past twelve years. Investments to increase the product quality in the European spirits industries have therefore the potential to increase sales volumes by 583 million € annually. Overall, the most important quality marker for distilled beverages is the aroma, which is defined by the volatile compound composition of the product [18]. It is known that the distillation process itself does have a major impact on the volatile compound composition of the product and therefore its quality [32,95].

In general, fruit spirit distillation processes are based on physical principles of heat and mass transfers which are decisive for the separation of desired and undesired aroma compounds [96,97]. The process principles are similar for each batch distillation process and can be categorized into consecutive process sequences. Initially the process starts with heating a fermented fruit mash in the reboiler of the still. Due to the constant thermal energy input a multicomponent vapor which contains ethanol, water and various other volatile compounds (congeners) evaporates to the top of the column [6]. The evaporation rate can be controlled by the thermal energy input [98,99]. These vapors condense when they get in contact with cooler surface areas which causes a liquid reflux that flows downwards again [90]. This evaporation/condensation process is crucial for the separation of substances with different volatilities [6,90,96,97,100]. Substances with low boiling points become enriched in the vapor phase while compounds with higher boiling points concentrate in the liquid phase. A recent study to investigate the best distillation technique for improving the quality of apricot brandies also concluded that the right balance between heating parameters, which determines evaporation rates, and reflux conditions has a decisive role to gain improved product qualities [101]. This indicates that it is important to control and monitor both process parameters in fruit spirit distillation processes.

During the distillation run ethanol and water are the two main components which support the carryover of other volatile compounds. This carryover is influenced by the relative volatility of

each compound in respect to the present ethanol and water concentration [6,96,102]. The concentration of ethanol in ethanol-water mixtures can be determined by measuring the temperature under boiling conditions [103]. The monitoring of temperatures in the distillation device is therefore additionally important to be able to estimate and control the carryover of volatile compounds in regard to the apparent ethanol concentration.

In chemical industries distillation accounts for 90-95% of all separations processes [104]. The separation of multicomponent mixtures is known to be challenging but includes some of world's largest and most profitable separations, such as crude oil fractionation, hydrocarbon separation from steam cracking, and natural gas liquids separation. In order to separate a multicomponent mixture that contains n components into n product streams, each enriched in one of the components, a sequence of distillation columns known as a distillation configuration is required [91]. Such distillation setups are equipped with extensive process control and monitoring that enable the regulation of evaporation rates and reflux streams [90,91]. Similar control strategies could be transferred to fruit spirit distillation processes to be able to investigate distillative separation processes in more detail. Bastidas et al. [105] also transferred thermodynamic models and unit operation data from a fuel production plant to evaluate optimized wine distillation processes by simulation models. They also stated that deep knowledge and understanding of the fuel ethanol process, allows identifying the main operation conditions of the process in order to keep product flowrate and quality in the desired values.

Industrial fruit spirit production is mainly performed with two different distillation systems, the traditional Charentais alembic stills and modern batch distillation columns [6]. In alembics, internal reflux is caused by condensation in the head and the swan neck, which mainly depends on external temperature. This reflux can only be modified by regulation of the thermal energy input in the boiler and therefore is a very limited system in terms of control and modification during the distillation process. On the other hand, modern batch distillation columns are equipped with an additional internal partial condenser, which can be controlled and operated independently. This allows a rather simple control of the internal reflux by adjusting the cooling water flow rate of the partial condenser [28,86]. The condensate can be collected on the trays and the vapor from the lower tray must pass through the holes and therefore through the reflux condensate, causing rectification and therefore more efficient separation of the different volatile components [100].

The dephlegmator works as a thermal barrier that provides resistance to the distillate vapors to pass on towards product cooler. The mass transfer of vapor to exit the distillation column is mainly influenced by the cooling power of the dephlegmator and the thermal energy input to the distillation column [101,106]. This indicates the importance to regulate and monitor both parameters to have the ability to control mass transfer rates.

Earlier studies already focused on product differences between both distillation systems [28,86,107]. It was shown that the internal reflux rates as well as the thermal energy input are two important parameters that control volatile concentrations and, in-terms, aroma attributes in the final product [32,88,89,107,108]. Despite their importance, very limited information on both parameters is available in scientific publications dealing with fruit spirit distillations [109].

García-Llobodanin et al. [28] emphasized the importance of both parameters and considered that 'they are severely affected by heat loss, ambient temperature, cooling water flow rates and temperatures.' They concluded that there is a prominent lack of control of these operation variables which leads to a lack of reproducibility of fruit spirit distillation processes, which also significantly affects the volatile composition of the produced spirits.

We upgraded a 120 L batch distillation column with digitized instrumentation and control technique in order to gain control over the crucial process parameters thermal energy input and reflux rates and to monitor six distillation parameters. We hypothesized that reproducible fruit spirit distillation processes and products can largely be gained when the two crucial process parameters can be controlled and monitored. The aim of this study was to identify the magnitude of reproducibility errors for (i) six distillation process parameters and (ii) 13 volatile compound compositions in the product in repeatedly performed distillations, when two process parameters are controlled during the distillation process.

2.2. Materials and Methods

2.2.1. Batch distillation system

This study was performed with a steam heated copper batch still (Carl GmbH, Eislingen, Germany) equipped with a 120 L reboiler, three sieve trays, rectification column with partial condenser, a separate reactive copper packing and a product cooler (*Figure 5*). The system was upgraded with digitized technical sensors in order to control and monitor thermal energy input, temperatures at four different positions, internal reflux induced by the partial condenser and product volume flow rate. All controllers and sensors were calibrated by the batch still producer ($R^2 \geq 0.95$). The crucial process parameter thermal energy input was controlled by an electro-pneumatic valve positioner (SP400, Spirax-Sarco Engineering plc, Cheltenham, UK). The crucial process parameter internal reflux rate was monitored via a Coriolis flowmeter (Emerson micro motion H series, St. Louis, USA) and indirectly controlled (SM6120 flowmeter, Ifm electronic GmbH, Essen, Germany) by adjusting the cooling water flow rate to the partial condenser. For this investigation, the cooling water flow rate to the partial condenser was kept constant at 2.0 L/min. Additional process monitoring was performed by four PT100 temperature sensors and an additional Coriolis flowmeter (Emerson micro motion H series, St. Louis, USA) for determination of product volume flow rates. The cooling water flow rate for the product cooler was constantly set to 7.0 L/min. All control and monitor data were logged every 10 sec and stored via a manufactured automation system (DPC500, Carl GmbH, Eislingen, Germany). After each distillation run, data were transferred to Excel (Microsoft Office 2010, Microsoft Corporation, Redmond, DC, USA). To avoid illegible diagrams on distillation process parameters, we averaged mean values and standard deviations of six consecutive logging points and present it as one data point (*Figure 6-Figure 8*). The distillation system contained additional technical sensors which were not considered in this study. More specifics to the digitized distillation system are given in Heller et al. [99].

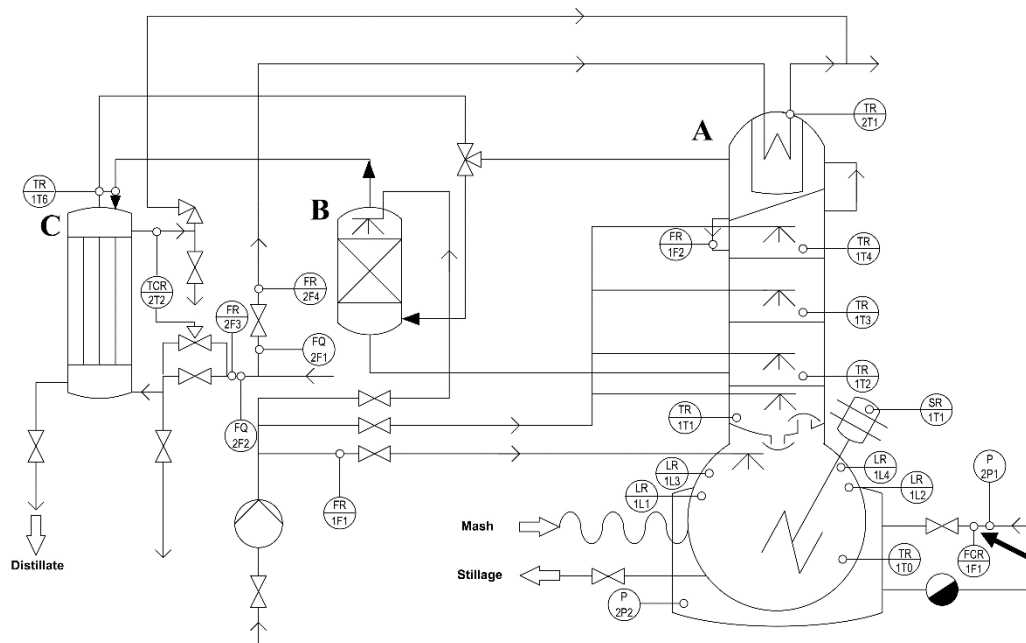


Figure 5. Instrumentation diagram of the batch distillation system equipped with rectification column (A), copper packing (B) and product cooler (C). FCR = regulated valve for thermal energy input, TR = temperature sensors, FR = flowmeters, black arrow indicates point of Q1-Q3 regulation.

2.2.2. Experimental setup

Eight different distillation profiles (A-H) were performed in duplicates ($n=16$) while thermal energy input was adjusted (*Table 1*). Every distillation run of the duplicates was performed with 100 L fermented fruit mash of the same batch. The distillation profiles started off with an initial thermal energy input of 450.0 W/L. When mash temperature reached 90.0 °C the thermal energy input was reduced to a defined value (Q1). When the third tray of the rectification column reached a temperature of 75.0 °C the thermal energy input was adapted again to a different value (Q2). From this point on thermal energy input constantly increased by a defined value (Q3) until the product flow began to run. Subsequently the DPC500 automation system regulated the thermal energy input to hold a constant product flow rate of 10.0 ± 0.5 L/h. These different distillation profiles were performed in order to simulate different distillation conditions, such as fast distillation or different internal reflux intensities, induced by variations in thermal energy input. Mean and relative standard deviations (RSD) were calculated from two distillation replicates.

Table 1. Distillation profile parameters

Distillation profile	fermented mash	adaptation Q1 (W/L)	adaptation Q2 (W/L)	adaptation Q3 (W/L/h)
A	wine	134.0 ± 1.0	134.0 ± 1.0	46.0 ± 2.0
B	wine	43.0 ± 1.0	59.0 ± 1.0	121.0 ± 2.0
C	wine	43.0 ± 1.0	59.0 ± 1.0	161.0 ± 2.0
D	pear	134.0 ± 1.0	134.0 ± 1.0	46.0 ± 2.0
E	pear	43.0 ± 1.0	59.0 ± 1.0	121.0 ± 2.0
F	pear	43.0 ± 1.0	59.0 ± 1.0	161.0 ± 2.0
G	plum	134.0 ± 1.0	134.0 ± 1.0	46.0 ± 2.0
H	plum	43.0 ± 1.0	134.0 ± 1.0	46.0 ± 2.0

2.2.3. Mash preparation and fermentation

Red wine was ordered from research facility Plant Product Quality (University of Hohenheim, Stuttgart, Germany). Williams pears (*Pyrus communis* L.) were purchased from Kaiser Destillerie-Obstweinkellerei (Salach, Germany). Plums (*Prunus domestica* subsp. *domestica* L.) originated from agricultural farm Heidfeldhof (University of Hohenheim, Stuttgart, Germany). Substrate characteristics (*Table 2*) included determination of total solids and ash as described in VDLUFA [110] and ICC [111], respectively. Total carbohydrates were quantified via phenol–sulfuric acid method [30]. Total protein concentrations were analyzed using the method by Bradford [112]. Total phenol determination was performed as described in Lim et al [113]. pH and conductivity were measured via multimeter (HQ40D, Hach, Loveland, USA).

For mash preparation, Williams pears were water-cleaned, fruit mill shredded (Helmut Rink GmbH, Amtzell, Germany) and transferred to a 1,000 L stainless steel tank. The pH was lowered to 3.1 by phosphoric and lactic acid addition (product no. 5862, Schliessmann, Schwäbisch Hall, Germany). Additionally, 10.0 mL/hL pectin lyase (IUB 4.2.2.10, Schliessmann, Schwäbisch Hall, Germany) were applied to the mash in order to ensure sufficient substrate liquefaction. 20.0 g/hL selected yeast (*Saccharomyces cerevisiae*) strains (Aroma plus, Schliessmann, Schwäbisch Hall, Germany) were added to start mash fermentation.

For plum mash preparation all plums were thoroughly mixed with a mixing drill (product no. 6681, Schliessmann, Schwäbisch Hall, Germany). The mixing drill was used in order to achieve disintegrated fruits but prevent excessive seed abrasion or seed destruction. The disintegrated fruits were subsequently pumped to a 1,000 L stainless steel tank, pH adjusted to 3.0 (product no. 5862, Schliessmann, Schwäbisch Hall, Germany) and inoculated with 0.15 g/L selected yeast strains (Aroma Plus, product no 5828, Schliessmann, Schwäbisch Hall, Germany). 5.0 mL/hL pectin lyase enzyme (IUB 4.2.2.10, Schliessmann, Schwäbisch Hall, Germany) was also added to enhance liquefaction of the mash. All mashes were thoroughly mixed and pH readjusted after 24 h. Similar mash preparation procedures were described by Liebminger et al. [106]. Mash fermentations were performed for 21 days at 20°C room temperature.

Table 2. Substrate characteristics

	Total solids	Ash	Total carbohydrates	Total proteins	Total phenols	pH	Conductivity
	[% FM]	[% DS]	[g/L]	[g/L]	[mg/L]		[mS/cm]
wine	1.9 ± 0	38.3 ± 0.2	4.2 ± 0.4	0.1 ± 0	2.8 ± 0	5.5	5.5 ± 0
pears	5.6 ± 0.2	4.5 ± 0.1	16.4 ± 0.6	0.6 ± 0	2.8 ± 0.2	3.3	2.3 ± 0.1
plums	8.6 ± 0.6	5.8 ± 0.5	4.5 ± 0.5	0.4 ± 0.1	1.4 ± 0.1	3.5	3.5 ± 0.1

2.2.4. Product analysis

The produced distillates were collected in 20 defined fractions for subsequent analysis. Sampling was performed every 100 mL for the first ten fractions, while fractions 11 – 15 were sampled every 200 mL and fractions 16 – 20 were sampled every 1,000 mL. Additional distillate was collected as an undefined final fraction and not considered in this study. Williams pear mashes resulted in reduced product yields and were only sampled until fraction 19.

A headspace gas chromatograph (GC-2010 Plus, Shimadzu Scientific Instruments, Kyoto, Japan) equipped with a flame ionization detector (FID) and a Rtx-Volatiles column (Restek Corp., Bellefonte, USA) was used for volatile compound analysis in distillate fractions. All samples were adjusted to 40.0 % (v/v) ethanol prior to volatile compound quantification. The product fractions were quantified for typical fruit spirit volatile compounds [17,25,95,107,114] ethanol, methanol, acetaldehyde, 1-propanol, 2-butanol, ethyl acetate, isobutanol, isoamyl alcohol, 2-methyl-1-butanol, ethyl 2-methylbutanoate, 1-hexanol, trans-2-hexen-1-ol and hexyl acetate. As GC-FID is not a technique for absolute quantification [115], it is mandatory to perform calibration runs with standard solutions of fixed concentrations. For the calibration runs all analyzed substances were ordered from Merck KGaA (Darmstadt, Germany) in analytical standard grade with a purity of $\geq 99.9\%$ for ethanol, methanol, 1-propanol, $\geq 99.5\%$ for acetaldehyde, 2-butanol, ethyl acetate, $\geq 99.0\%$ for isobutanol, 2-methyl-1-butanol, ethyl 2-methylbutanoate, 1-hexanol, hexyl acetate, $\geq 98.0\%$ for isoamyl alcohol and $\geq 97.0\%$ for trans-2-hexen-1-ol. Each standard substance was diluted with distilled water to gain five defined concentrations. The five standard concentrations were prepared in a range that covered the concentrations, in which the analytes typically appear in fruit spirits. The peak area of all five standard concentrations was determined in chromatograms which can be used to establish a linear equation between both parameters. The fit of both parameters to the linear equation significantly correlated with accuracy of $R^2 \geq 0.99$ for each analyzed volatile compound. This linear equation, gained by five-point calibration, was thus used to quantify the concentration of an analyte in the fruit spirit sample by determination of its peak area in the chromatogram.

2.2.5. Data analysis

To identify whether fruit spirit distillations can be controlled by two variables, we evaluated the accuracy of replicated distillations by determining deviations between two replicated distillation runs in terms of distillation process parameters and volatile compound composition

in the product. The basis of data analysis within this study was the evaluation of deviations between duplicate data points. Median RSD analysis is often used to investigate the precision of analytical replicate data or process variability [116–118]. The calculation of median RSD values reflects the magnitude of reproducibility errors. In order to evaluate process replicability, the data of six process parameters (mash temperature, temperatures at three trays, internal reflux rate, product flow rate), which were logged every 10 seconds, were compared between the replicate distillation runs. A maximum of 36 data points was thus comparable for every minute of distillation run. Data of internal reflux and product flow were only considered after they started to run (flow rates >0.0 L/h). In order to evaluate product replicability in terms of their volatile compound composition, equally sampled product fractions were analyzed for 13 volatile concentrations. One distillation run with 20 sampled fractions thus allowed a comparison of a maximum of 260 data points.

Initially the relative standard deviation RSD was calculated for every set of two duplicate data points. In a second step we calculated the median RSD, which considered all RSD data evaluated within a single parameter, for instance one distillation parameter (e.g. mash temperature) or the concentration of one volatile compound (e.g. 1-propanol).

2.3. Results & Discussion

2.3.1. Distillation process parameters

The control of thermal energy input and cooling water flow rate to the partial condenser resulted in variations of the six monitored distillation parameters. Since the cooling water flow rate was set to a constant rate, the main impact on process variations were induced by alteration of the thermal energy input. All distillation processes showed that thermal energy regulation had a decisive influence on the development of process temperatures.

Figure 6 shows distillation parameters of processes A-C of the fermented wine mashes. Different heating profiles clearly influenced total distillation time which was 116.0 ± 2.0 minutes in distillation process A. Due to lower thermal energy input, distillation profiles B and C were finalized after 141.0 ± 3.0 minutes and 128.0 ± 1.0 minutes, respectively. Processes B and C showed a slower increase of internal reflux volumes but reached a maximum value of 42.0 ± 1.0 L/h within all distillation profiles.

Distillation processes D-F in *Figure 7* show the process data of fermented Williams pear mashes. The fastest distillation run was finalized after 98.0 ± 1.0 minutes in distillation profile D, which also had the highest initial thermal energy input. While product flow started after 65 ± 0 minutes in distillation profile D, this was shifted to 91.0 ± 1.0 minutes and 76 ± 0 minutes in distillation profiles E and F, respectively. Different thermal energy inputs during the distillation profiles also affected the internal reflux rates of the distillation processes. The highest reflux rates were 41.0 ± 0 L/h after 64 minutes in distillation profile F, while distillation profiles D and E showed a maximum value of 39.0 ± 0 L/h after 37.0 ± 1.0 minutes and $74.0 \pm$

1.0 minutes, respectively. Replicates of each distillation profile showed the highest standard deviations during the heating phase until the third tray reached thermal equilibrium.

Distillation processes G-H in *Figure 8* show the process data of fermented plum mashes. Different thermal energy inputs resulted in 13 ± 0 minutes longer distillation run of distillation profile H. A timely shift could also be determined during the distillation run. For instance, maximum temperature of $92 \pm 0^\circ\text{C}$ on tray one was reached 10 ± 0 minutes later in distillation process H. This also induced a 13-minute delay until initial reflux flow rates were detected. Replicates of each distillation profile showed the highest standard deviations during the heating phase and at the beginning of product volume flow.

All distillation processes commonly showed that with the start of product flow streams, the internal reflux flow rates reduced over time. This is due to the fact, that initially all the vapor mass condensed at the cool surface of the partial condenser. The partial condenser is heated up during the process, until a stream of vapor passes the partial condenser which is condensed in the product cooler and the product flow starts. As far as we know, no other study on fruit spirit distillation processes has ever directly evaluated reflux flow rates. García-Llobodanin et al. [28] showed the energy demand for cooling the partial condenser without providing information on reflux flow rate quantities. Balcerek et al. [87] evaluated effects of double- and single-stage fruit mash distillations without defining the magnitude of energy input or reflux ratios. They also stated to have varied the reflux rate by adjusting the cooling water flow rate without giving more specifics. Spaho et al. [107] compared alembic and column distillation techniques without providing any specifics on thermal energy input or reflux rates for pot or column still distillations. They mentioned, however, distillate flow rates of 5.3 L/h which provides information on the mass stream that exited the distillation column. The product flow rates of our study showed average values of 8.5 ± 1.8 L/h in distillation profiles A-H, which indicated that the product flow rate does differ by simply adjusting thermal energy input without changing the cool water flow of the partial condenser. As no more specifics are given in the study of Spaho et al. [107], it is not clear whether reduced energy inputs or increased reflux rates led to lower distillate flow rates compared to our study.

Liebmingner et al. [106] evaluated column distillation processes for three fruit mashes. This study is interesting as it provides insights into effects of limited process control. The data indicated strong variations in the temperature profiles between the three distillation processes. Despite using a similar distillation setup, the temperature sensor measured values ranging from 79°C to 92°C 20 minutes after beginning of distillate collection in the three distillations. Based on the vapor phase diagram of ethanol-water mixtures [96] this indicated deviating ethanol concentrations of 86% to 53% (w/w) in the vapor stream despite utilizing fruit mashes (plum, pear) with similar ethanol concentrations. This shows that the distillation process was not able to perform mass and heat transfer with similar efficiency, which affected the physical separation of ethanol and water. In addition, the collected tails fraction was increased by 82% which suggests that the separation of volatile compounds was also affected due to different relative volatility of the apparent ethanol or water concentration [6,96,102]. Since thermal energy input was not monitored, the authors assumed that the energy input of the oil-heating system varied which possibly led to uncontrolled heating patterns. The temperature sensor was placed at the

exiting pipe close to the product cooler and additional temperature control was not mentioned in this study. This indicated that the energy input could not be controlled nor monitored by temperature sensors positioned within the distillation column. Also, different dephlegmator cooling setups were chosen for the three distillation runs. The study did not describe the amount of cooling energy or the quantities of internal reflux rates. Since both parameters, thermal energy input and reflux rates, could not be controlled nor monitored, this resulted in largely deviating product flow rates ranging from 12.1 – 23.3 L/h. The lack of process regulation and monitoring technique led to an uncontrolled vapor mass transfer to exit the distillation column.

Several other studies also investigated the volatile compound composition in the distilled product without providing specifics for the crucial distillation process parameters that define physical principles of heat and mass transfer [119–122]. None of these studies have the potential to provide data that allow the evaluation of the physical separation principles on behalf of mass or heat transfer rates during the distillation process. This makes it difficult to evaluate beneficial or disadvantageous distillation process conditions.

Our study showed additional process data to be able to evaluate separation processes on behalf of physical principles. In dependency of distillation time the distillation profiles A-H provided a minimum of 2,927 comparable data points for distillation profile G and a maximum of 4,358 data points for distillation profile B. In total, the acquisition of process data from six process parameters within eight duplicate distillation profiles enabled the comparison of 28,600 duplicate data points. The median RSD (*Figure 9*) was determined at a range of <0.1% - 7.0%. This indicated that enabling control over two distillation parameters allows largely reproducible distillation processes with a replication error $\leq 7.0\%$.

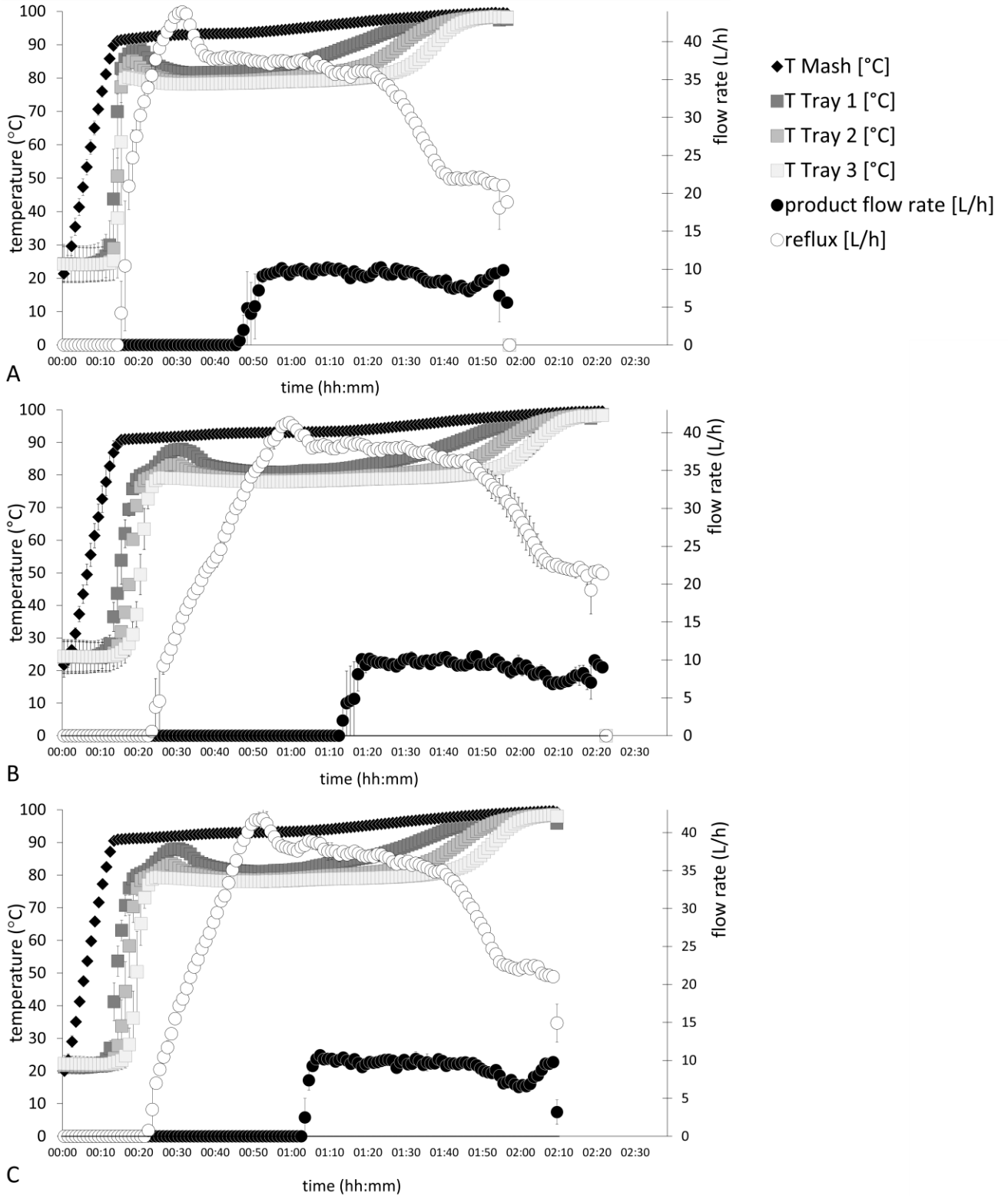


Figure 6. Monitored distillation process parameters of repeated wine mash distillation processes A-C. Each data point was averaged over 60 seconds for better visualization.

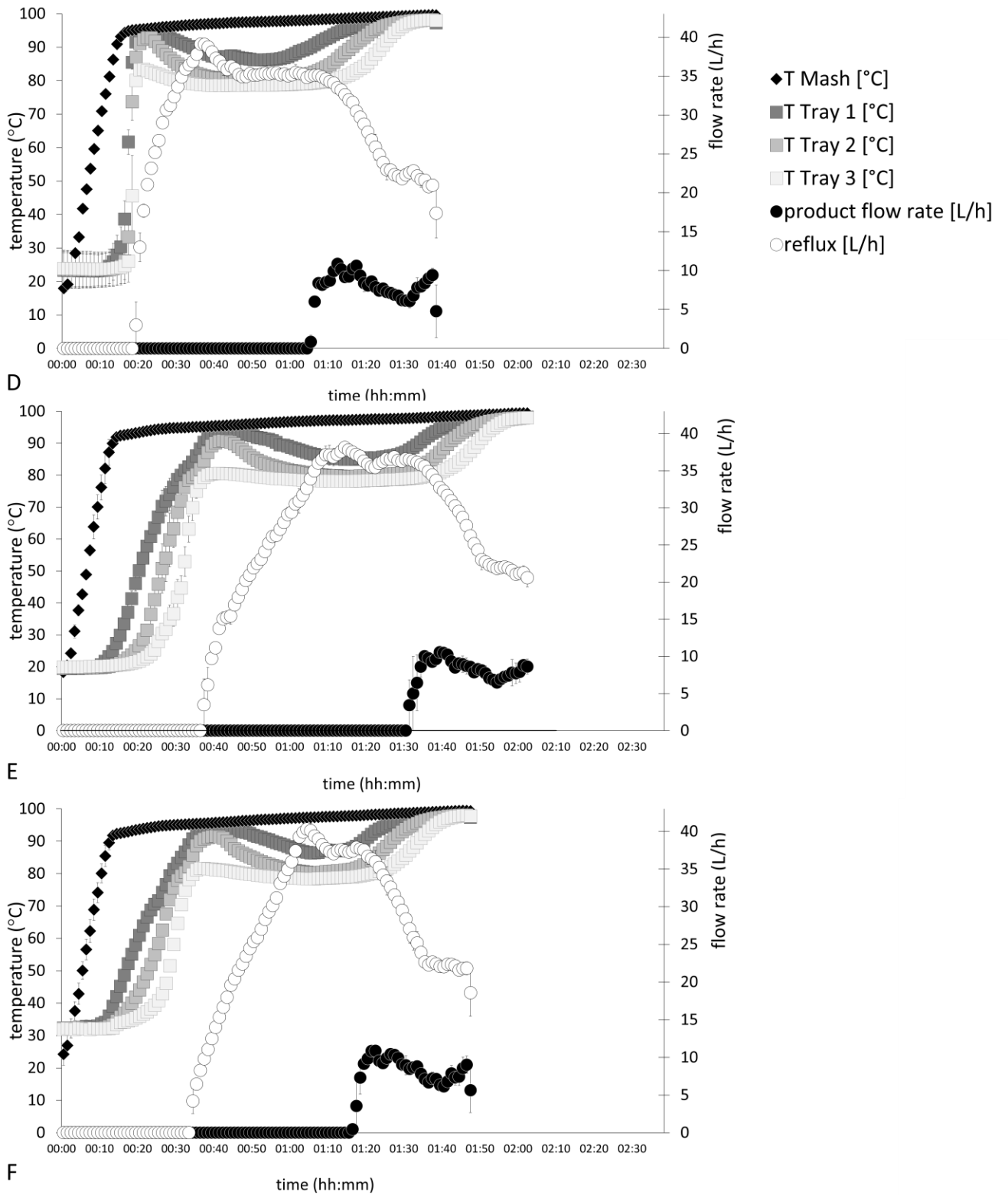


Figure 7. Monitored distillation process parameters of repeated Williams pear mash distillation processes D-F. Each data point was averaged over 60 seconds for better visualization.

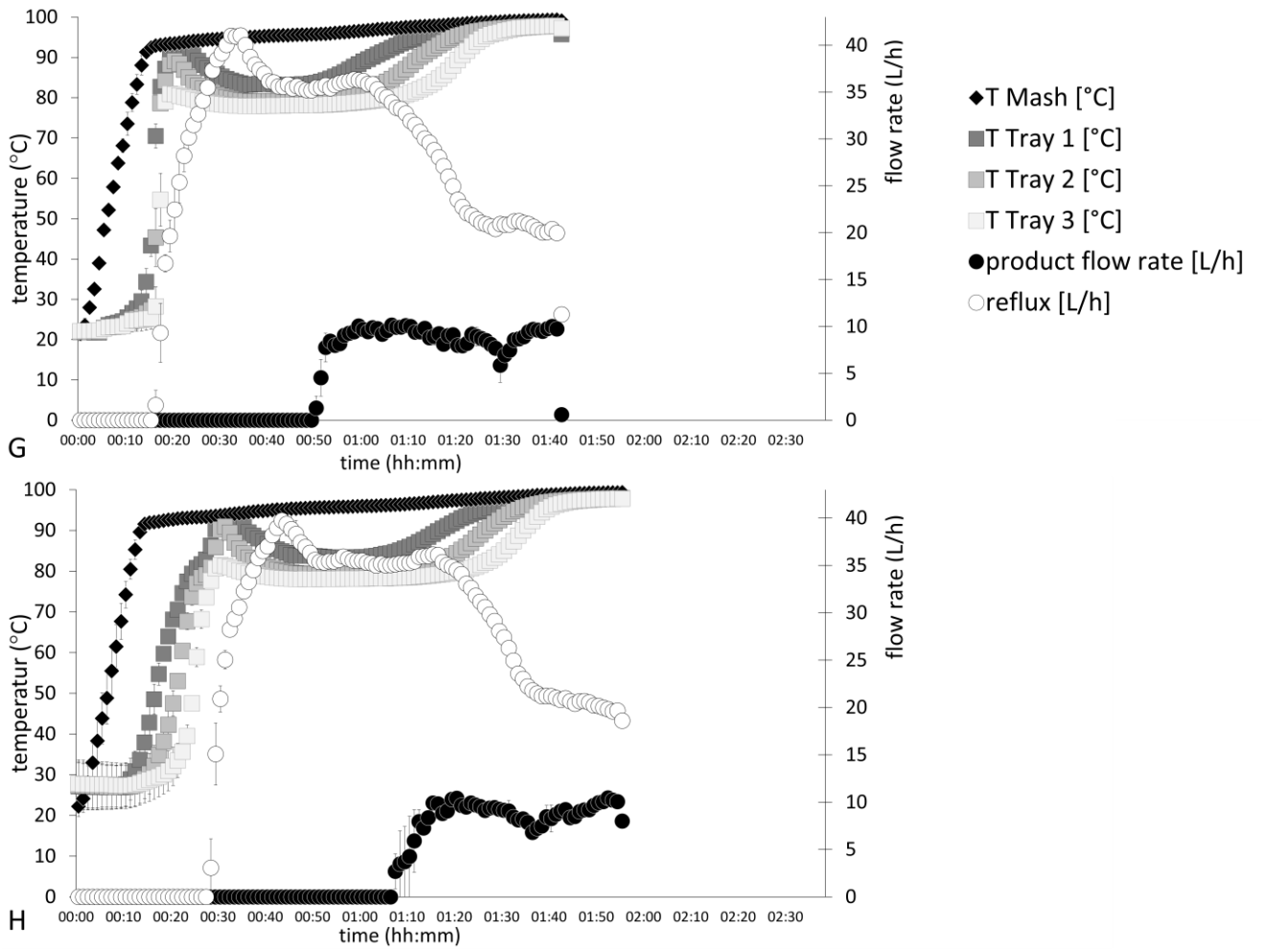


Figure 8. Monitored distillation process parameters of repeated plum mash distillation processes G-H. Each data point was averaged over 60 seconds for better visualization.

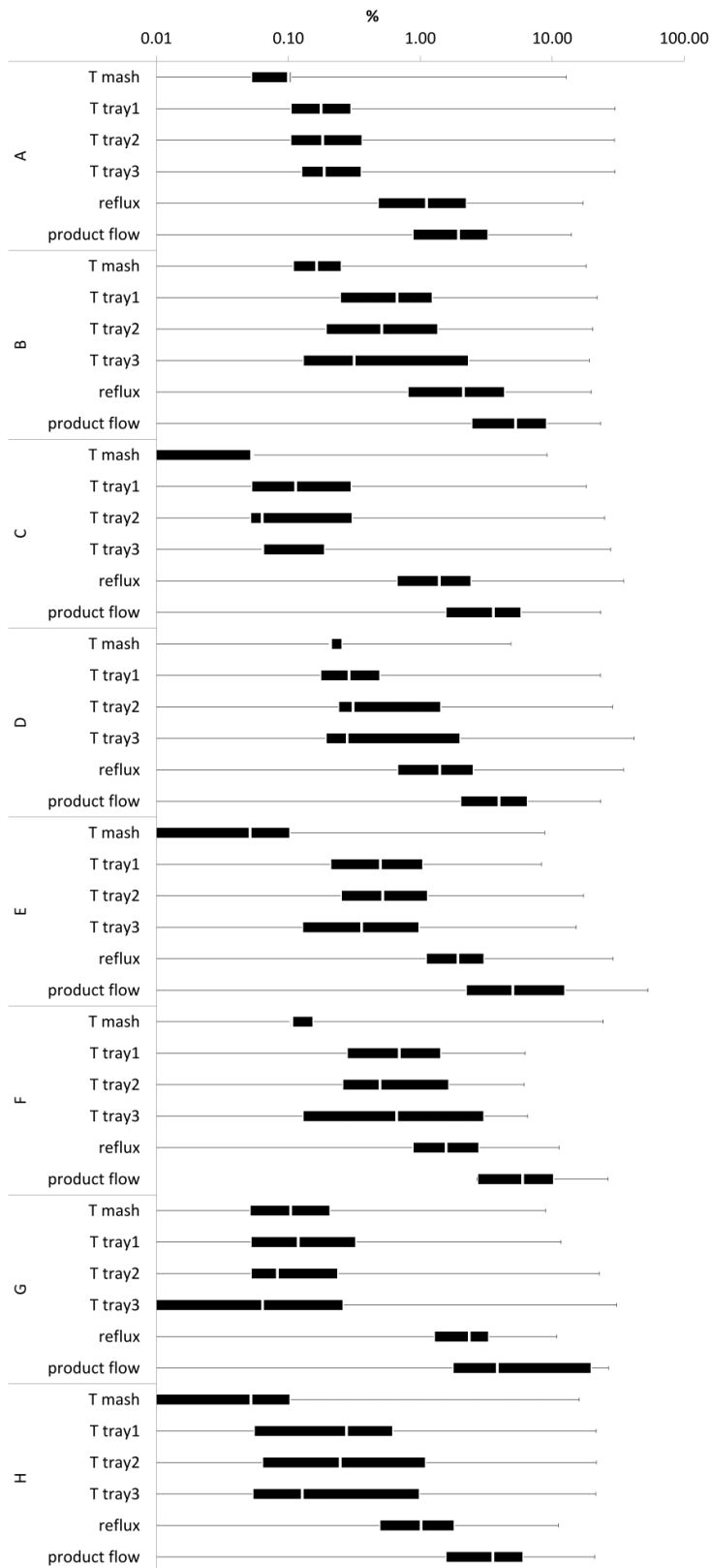


Figure 9. RSD values of monitored process parameters in duplicated distillation runs A-H. Each parameter considered data of the whole distillation run. Note logarithmical x-axis scaling.

2.3.2. Volatile compound composition of product fractions

The volatile compound compositions of wine, pear and plum distillate fractions are presented in *Figure 10 - Figure 12*. The figures also indicate the cut of heads to hearts fraction, which was consistently performed at 450 mL. All distillation profiles commonly showed that the concentrations of acetaldehyde, ethyl acetate and 2-butanol significantly decreased during the shift from heads to hearts fractions. Acetaldehyde and ethyl acetate are known to implement strong pungent characteristics and negatively influence product quality [123]. Due to their low boiling point, both substances are typically enriched in the hearts fraction of fruit spirit distillation processes [119,124]. In addition, this study indicated that 2-butanol is also enriched in the hearts fraction. Similar behavior of 2-butanol was also described by Spaho et al. [95]. This might be beneficial for the final product quality as high 2-butanol concentrations (>50.0 mg/100mL aa) are considered a marker for spoilage of the raw material or negative microbiological influences of the fermentation process [17]. The averaged 2-butanol concentrations of each distillation run ranged from 2.7 ± 0.7 mg/100 mL to 4.3 ± 0.3 mg/100 mL ethanol and was thus below the considered perceivable odor threshold of 5.0 mg/100 mL ethanol [125].

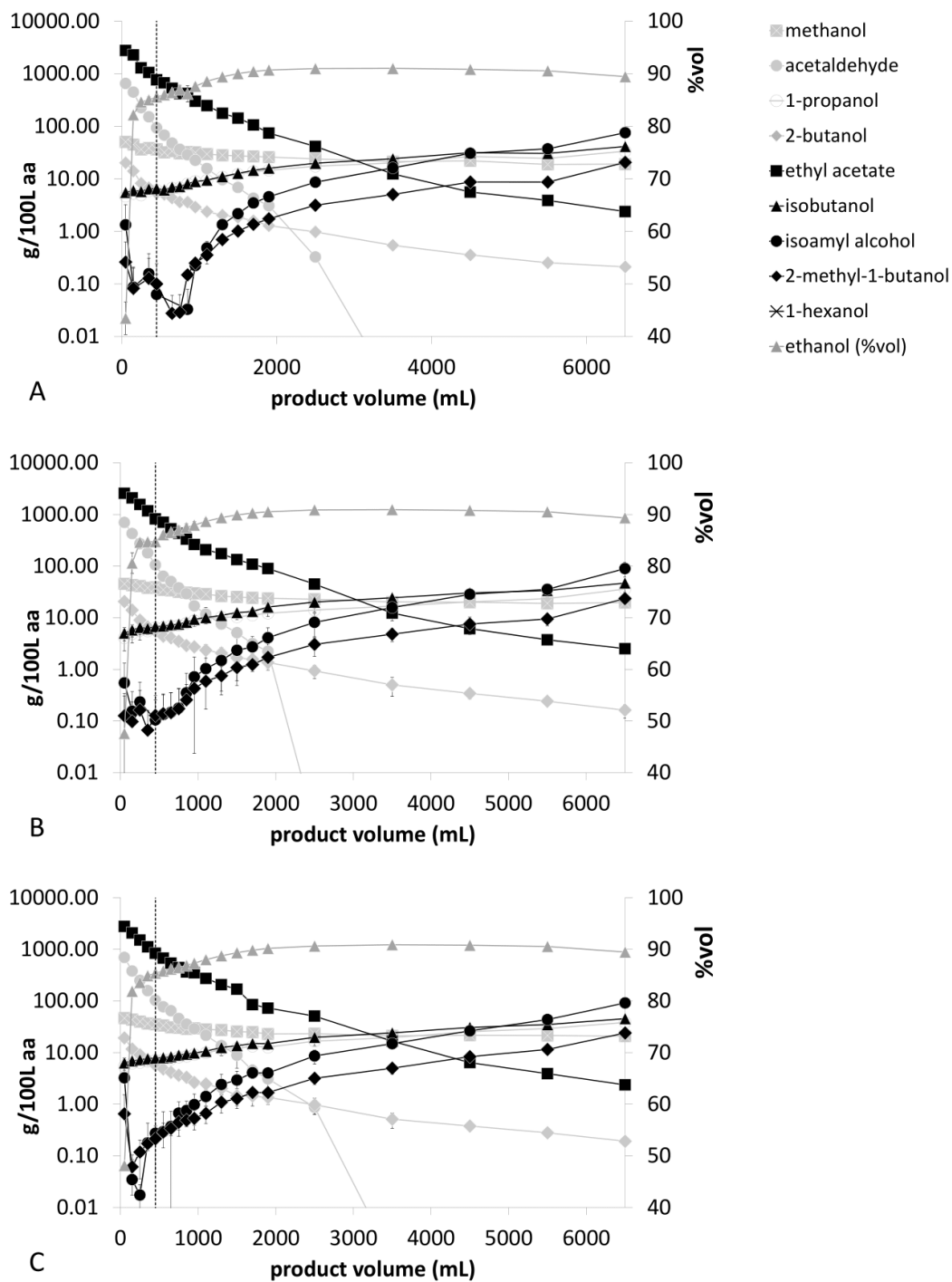


Figure 10. Volatile compound concentrations in distillate fractions produced by distillation profiles A-C performed in duplicates. Note left logarithmical y-axis scaling. aa = anhydrous alcohol

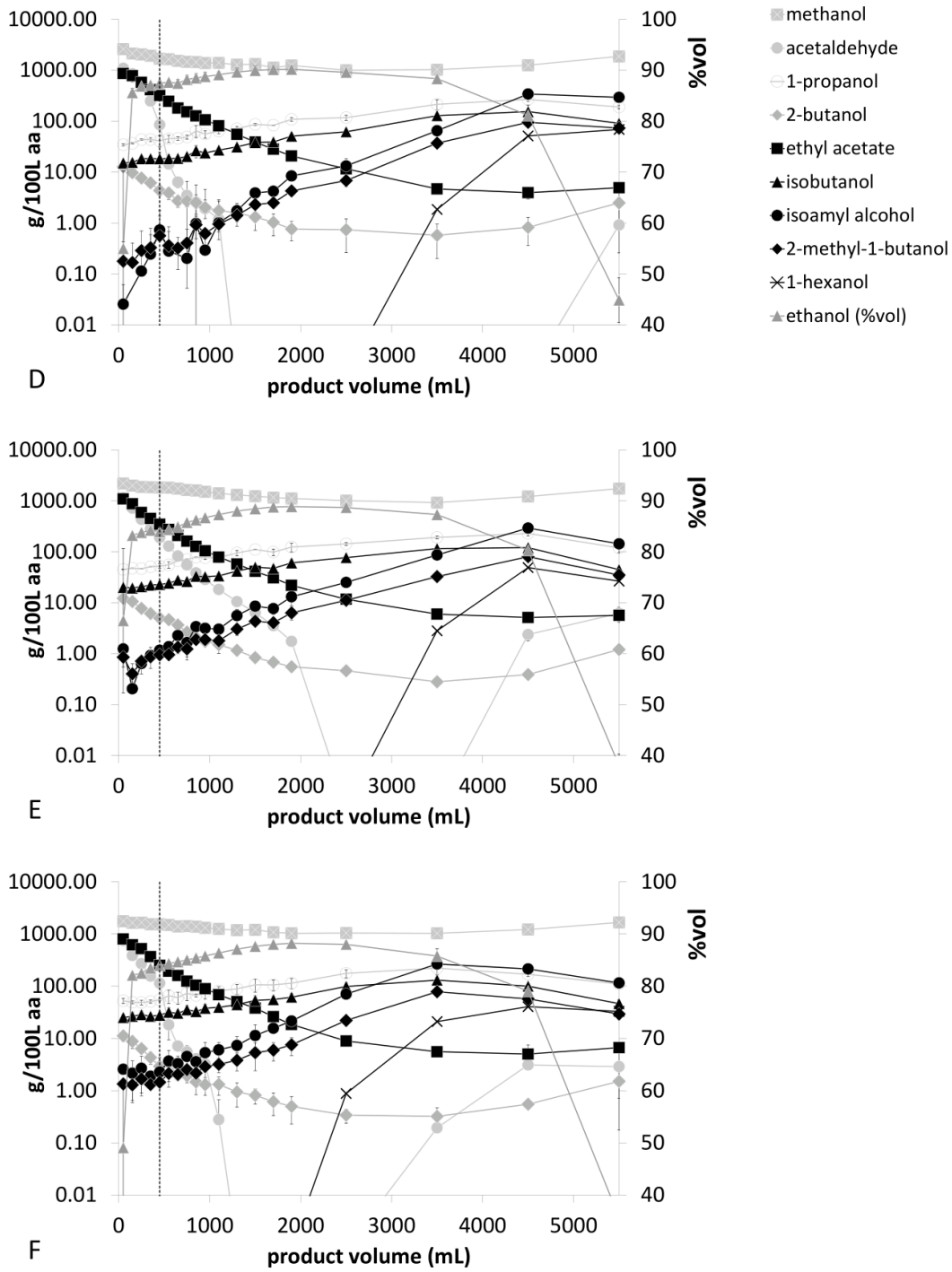


Figure 11. Volatile compound concentrations in distillate fractions produced by distillation profiles D-F performed in duplicates. Note left logarithmical y-axis scaling. aa = anhydrous alcohol

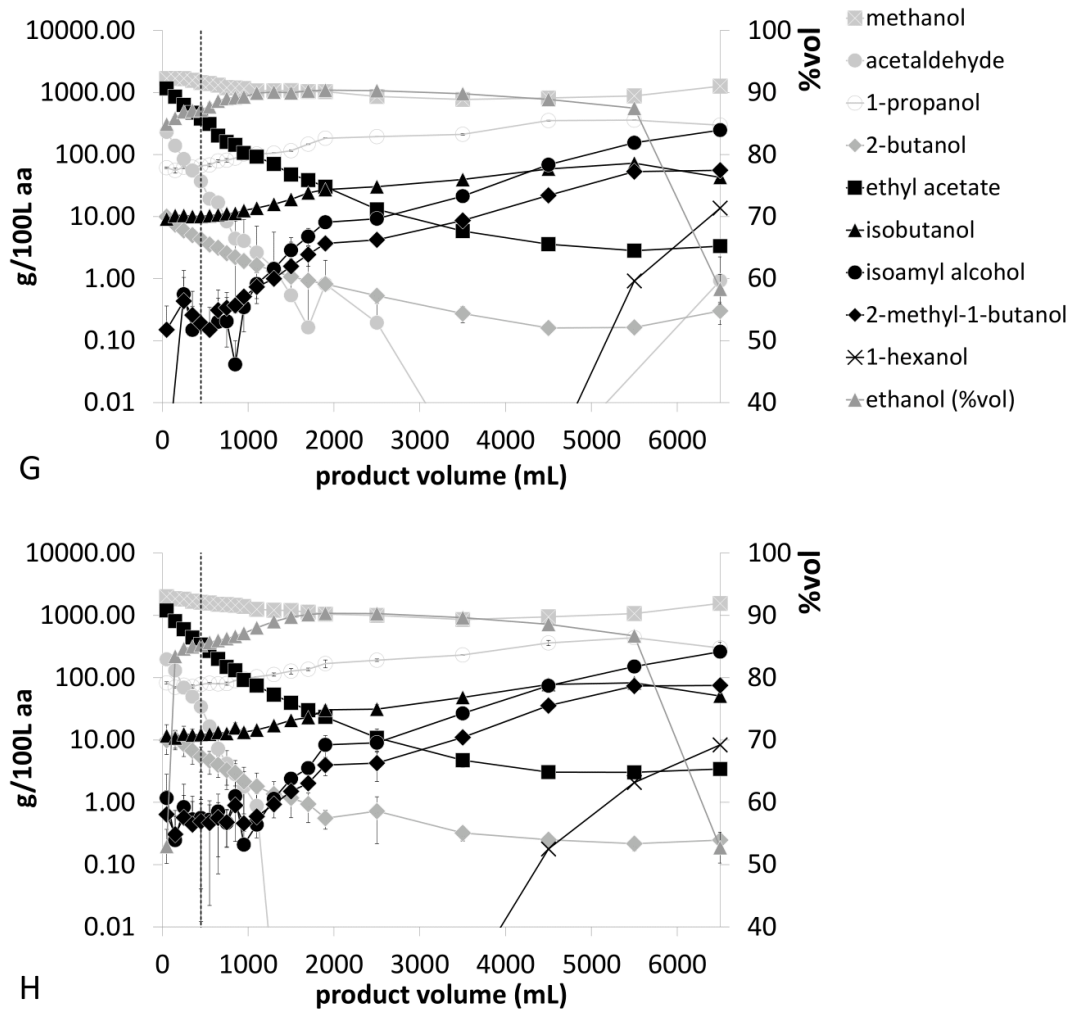


Figure 12. Volatile compound concentrations in distillate fractions produced by distillation profiles G-H performed in duplicates. Note left logarithmical y-axis scaling. aa = anhydrous alcohol

Higher alcohols 1-propanol, isobutanol, isoamyl alcohol and 2-methyl-1-butanol steadily increased during the distillation run. They are important congeners of the yielded product as optimal levels of higher alcohols impart fruity characters of the distillate. However, excessive concentrations of higher alcohols can result in a strong pungent and fusel-like smell and taste [126–129]. As the concentration of higher alcohols increases towards the end of the distillation run, a final tails cut of the distillate is separated from the value product.

The methanol concentrations indicated a typical behavior for fruit spirit distillation processes [124,130]. They showed slightly higher concentrations during the beginning and the end of the distillation run. However, the presented data state once more that an efficient separation of methanol from ethanol-rich solutions is not possible with simple fruit spirit distillation technique. Based on the European legal limits [131] of 200 mg/100mL ethanol for wine spirits, 1,200 mg / 100 mL ethanol for plum spirits and 1,350 mg/100 mL ethanol for Williams pear spirit, the data on wine spirit production never exceeded the limit. In contrast, all distillation

runs with Williams pears exceeded the legal methanol limit until 1,100 mL of distillate was produced, independently of the distillation profile. For plum spirit production, distillation profile G resulted in exceeded legal methanol limits until 750 mL of distillate was produced. Distillation profile H exceeded the legal limit until a product yield of 1,700 mL. This indicated that the degree of thermal energy input had an impact on the separation efficiency of methanol from ethanol-water solutions. Overall, it is essential to mix all hearts fractions of one distillation process together in order to ensure that the final product contains sufficiently low methanol concentrations.

All wine mash distillation profiles A-C showed relatively similar ethanol concentrations. The averaged ethanol concentrations were 85.8 ± 0.5 % (v/v), 85.9 ± 0.8 % (v/v) and 85.7 ± 0.3 % (v/v), respectively. This indicated that different distillation profiles did not affect the separation efficiency of ethanol in the rectification column. The replicates of wine distillations showed the largest median RSD for isoamyl alcohol and 2-methyl-1-butanol in distillation profile C. Here, median RSD values were 27.0% and 19.0%, respectively (*Figure 13*).

It should be considered that the RSD values for volatiles such as isoamyl alcohol and 2-methyl-1-butanol might be affected due to methodical and analytical limits when volatile concentrations reach a limit of <1.0 mg/100 mL. Small differences at low concentration values do result in relatively large standard deviations. In fact, when the mean value is close to zero, the coefficient of variation will approach infinity and is therefore sensitive to small changes. For instance, the isoamyl alcohol concentration in sampled fraction 11 of distillation profile A showed a value of 0.37 mg/100 mL ethanol in the first distillate run, while the duplicate sample showed a value of 0.60 mg/100 mL ethanol, resulting in a relatively large RSD of 34.0%. Both concentration values can be considered low while the RSD determination becomes less resilient to deviations. This might impair the evaluated RSD values of volatiles with especially low concentrations, without having a prominent effect on the sensory quality of the yielded product. All other volatiles of distillation profiles A-C showed a median RSD of $\leq 16.0\%$, indicating a high repetitiveness of the duplicate distillation runs.

The Williams pear distillation runs D-F indicated that the averaged ethanol concentrations decreased from $84.0 \pm 1.7\%$ (v/v) and $82.4 \pm 1.1\%$ (v/v) in distillation profiles D and E to $77.7 \pm 1.0\%$ (v/v) in distillation profile F. This is possibly due to different thermal energy input of profile F and a slower increase of the ethanol concentration during the distillation run. The largest median RSD of the replicates was apparent for 2-butanol with 30.0% in distillation profile F. This volatile substance again showed relatively low concentrations from 0.3 mg/100 mL ethanol to 12.7 mg/100 mL ethanol, which affects the methodical and analytical limits of volatile quantification. In addition, low concentrated volatiles isoamyl alcohol and 2-methyl-1-butanol showed again maximum median RSDs of 22.0% and 27.0%, respectively. 1-propanol also indicated a larger median RSD of 19.0% in distillation profile F. The largest discrepancy between 1-propanol concentrations of the duplicates of distillation profile F was 81 mg/100 mL ethanol within the sampled fraction at 3,500 mL. Since the odor threshold of 1-propanol is estimated at 83.0 mg/100 mL ethanol, this difference might not be detectible for the consumer [17]. All other volatiles showed median RSD values of $\leq 16.0\%$.

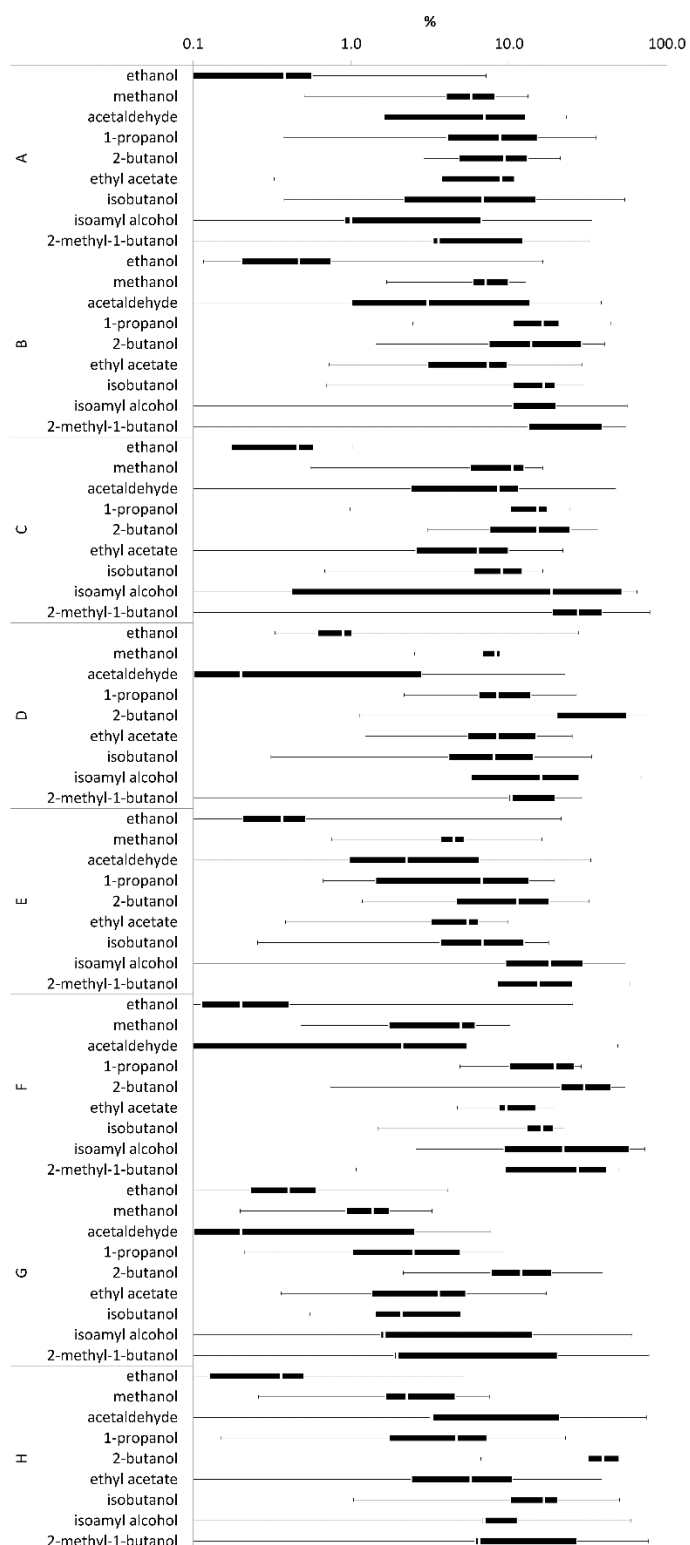


Figure 13. RSD values based on volatile compound concentrations in product fractions sampled during replicated distillation profiles A-H. Each box plot considered data of all sampled fractions. Note logarithmical x-axis scaling

For plum spirit distillations, the averaged ethanol concentrations decreased from 87.1 ± 0.5 % (v/v) in distillation profile G to 83.9 ± 0.5 % (v/v) in distillation profile H. A slower increase of

the ethanol concentration during the process might again be a result of different thermal energy inputs. The highest median RSD value was found for 2-butanol with 39.0% in distillation profile H. 2-butanol was again present in relatively low concentrations. All other volatiles showed a median RSD value of $\leq 17.0\%$.

Volatiles ethyl-2-methylbutanoate, trans-2-hexen-1-ol and hexyl acetate were not detected in any of the distillate fractions. The evaluation of 10 volatile compound concentrations in eight duplicate distillation runs enabled the comparison of a total of 1,540 duplicate data points, which resulted in a median RSD range of 0.2% to 39.0% (average $9.0 \pm 8.0\%$). This indicated that enabling control over two distillation parameters allows largely reproducible fruit spirit products with similar volatile compound concentrations considering an average median RSD deviation of about $9.0 \pm 8.0\%$. When excluding volatile concentrations of $\leq 1.0\text{mg}/100\text{mL}$ ethanol from this evaluation, the median RSD range changed to values from 0.2% to 23.0% (average $7.0 \pm 6.0\%$). This indicated that low-concentrated volatiles have a major impact on median RSD determination and should be evaluated carefully, since they will not affect the sensory profile of the product in a similar manner.

2.4. Conclusion

This study indicated that thermal energy input and internal reflux rates are crucial parameters that define physical heat and mass transfer rates during fruit spirit distillation processes. Gaining control over both parameters creates possibilities to perform reproducible distillation processes and to produce fruit spirit products with similar volatile compound compositions. The fruit spirit distillation industry should integrate technical sensors to enable control and monitoring of the distillation process. This could benefit to produce fruit spirit drinks of similar aroma qualities in a repeatable manner. Future scientific studies on fruit spirit distillation process should incorporate data on thermal energy input, reflux rates and temperature profiles within the distillation column in order to be able to evaluate the physical separation principles during distillation. This could enable comparability between different fruit spirit distillation studies.

Declarations

Funding This IGF Project of the FEI was supported via AiF within the program for promoting the Industrial Collective Research (IGF) of the German Ministry of Economic Affairs and Energy (BMWi), based on a resolution of the German Parliament, grant number AiF 4PN

Acknowledgments The authors are grateful for analytical and technical support by Julia Switulla, Simon Roj, Julia Pesl and Oliver Reber

Conflicts of Interest The authors declare no conflict of interest

3. A minimal-invasive method for the evaluation of liquid fractions in foams with a point level sensor

Rolf Staud¹, Daniel Heller^{2†}, Leon Knüpfer^{3†}, Sascha Heitkam^{3,4}, Daniel Einfalt², Katharina Jasch^{1,*} and Stephan Scholl¹

¹Technische Universität Braunschweig, Institute for Chemical and Thermal Process Engineering, Langer Kamp 7, D - 38106 Braunschweig, Germany

²University of Hohenheim, Institute of Food Science and Biotechnology, Yeast Genetics and Fermentation Technology, Garbenstraße 23, 70599 Stuttgart, Germany

³Helmholtz-Zentrum Dresden-Rossendorf, Institute of Fluid Dynamics, Bautzner Landstraße 400, 01328 Dresden, Germany

⁴Technische Universität Dresden, Institute of Process Engineering and Environmental Technology, 01062 Dresden, Germany

Corresponding Author: Dr.-Ing. Katharina Jasch (E-Mail: k.jasch@tu-braunschweig.de), Technische Universität Braunschweig, Institute for Chemical and Thermal Process Engineering, Langer Kamp 7, 38106 Braunschweig, Germany

Abstract

Liquid foams occur whether intentionally or unintentionally across different industrial sectors. The detection of foam and characterization of liquid content currently requires complex measurement methods such as electrical conductivity measurements. This paper presents a novel method for foam detection and characterization of its liquid fraction based on a capacitive level sensor. A correlation between the sensor output signal and defined liquid fractions of dry to wet foam indicated a high accuracy of this sensor technique. Regarding the sensor operation in different liquid solutions, a minimum screw-in depth is presented. The sensor allows minimal invasive inline measurements in equipment regardless of the wall material and of extreme process conditions, e.g., explosion hazard areas.

Keywords

Frequency sweep technology, Liquid foams, Minimal-invasive methods, Point level sensors

3.1. Introduction

Liquid foams have many practical applications in several industrial sectors. They are used for separation processes, e.g., in foam/froth flotation, in food and pharmaceuticals processes, e.g., in vacuum drying or chemical processes, e.g., for the acceleration of reactions also known as foam catalysis [132]. However, foams also have properties that may be undesirable in other industrial processes and result in operational issues, e.g., in distillation or desorption columns [46].

Due to their widespread occurrence, there is a great interest to evaluate foam formation, stability, and properties [43]. Besides many other properties of foams, their liquid fraction is of great relevance with respect to stability and potential countermeasures and thus of scientific and industrial interest. Liquid fraction represents the ratio of the volume of the liquid to the volume of foam. The liquid content influences most physical properties of foams. For example, the liquid fraction of foam is linked to the shear modulus [66], to the drainage, and to the stability of foams [133–135]. It is important in industrial processes, e.g., for determining the interfacial area available for mass transfer and mixing process [85].

The most commonly applied method to determine the liquid fraction of foams is the electrical conductivity of the foam. Several theoretical analyses and experimental studies have been performed to state approximate relations between foam conductivity and liquid fraction at different liquid fraction values [76–79]. The resulting mathematical and empirical relation can be used with some confidence [79]. However, there is a limitation in the application of the present measurement method in industrial processes. To perform foam conductivity measurements, two (or more) opposite electrodes have to be mounted at the sides of the foam holding vessel. The vessel itself has to be nonconductive so that only the conductivity of the foam is measured. However, in many industrial processes the equipment used is made of electrically conductive metal.

Other techniques to determine the liquid fraction are based on optical measurements following different approaches. They are either based on the determination of optical transmission [80] or of the surface fraction by imaging light reflected from the foam surface [81]. All optical methods require a transparent vessel/wall. In addition, some optical methods, e.g., the measurement of the transmission, requires a non-opaque foam/medium. These requirements limit the applicability in industrial processes.

Recently, a method based on ultrasound was proposed [82]. But its applicability still has to be assessed in industrial processes. Currently, the most precise methods used in scientific research for determination of the liquid fraction are based on X-ray radiography [83] or neutron imaging [84]. However, these methods are not applicable in industrial settings.

This study proposes a method to measure the liquid fraction in foams via capacitance measurements performed with frequency sweep technology (FST). The basic idea of this method is to use differences in the electrical permittivity of gases and liquids to determine the liquid fraction.

An electrode, which forms a capacitor with the surrounding medium, is introduced into foam. The capacitance (C_0) of the formed capacitor is dependent on the relative permittivity (ϵ_r) of the medium present in the surroundings (Eq. (1)). Since liquids generally have a higher permittivity than gases, the capacitance theoretically rises as the liquid fraction of the foam increases. Introducing an additional inductor, with an inductance L , a resonant circuit is created. Finally, the resonant frequency (f_0) of the created circuit is measured, which depends on the capacitance. Depending on the resonant frequency, the sensor signal (sweep range SR) is returned.

$$f_0 = \frac{1}{2\pi\sqrt{LC_0}} ; C_0(\epsilon_r) \quad (1)$$

By applying an additional pulse width modulation, the frequency sweep technology is also able to distinguish between liquid phase media with similar permittivity.

This study presents and assesses a novel and minimal-invasive way to determine the liquid fraction in foams utilizing FST sensors. A commercially available FST level sensor was modified to continuously measure and record the resonant frequency. The sensor was calibrated in a liquid fraction range of $1.2\% < \varphi < 16\%$ by means of additional electrical conductivity measurements. The study also investigated operational limitations based on immersion depth, material interference, and foam liquid characteristics (surfactants, solvents).

3.2. Experimental setups and methods

Investigations with the point level sensor were carried out in two measurement setups, one with conductivity measurement and one without. Based on the industrial use of the point level sensor, the immersion depth of the sensor in liquid within containers made from different materials was investigated. The point level sensor model LBFS-03G21.0 (Baumer Electric AG, Switzerland) based on FST was used. A digital interface recorded the sensor signal continuously over time. This enabled the investigations of the SR in addition to different solvents and in various material surroundings.

3.2.1. Variation of immersion depth and container materials

To evaluate the influence of the immersion depth (ImD) and the material of the wall on the sensor output signal, two beaker sizes and three different wall materials (PVC, glass, stainless steel 1.4407) were compared (*Figure 14*). To investigate the influence of the immersion depth (ImD), the round sensor tip was (a) not, (b) partially, (c)–(f) fully immersed in liquid surfactant solution ($1.35 \text{ g}_{\text{SDS}} \text{ L}_{\text{total}}^{-1}$) in the vicinity of these different materials. Sodium dodecyl sulfate (SDS) was used as the surfactant (Carl Roth GmbH & Co. KG, Germany). The immersion depth was determined by the sensor tip and varied by different liquid levels.

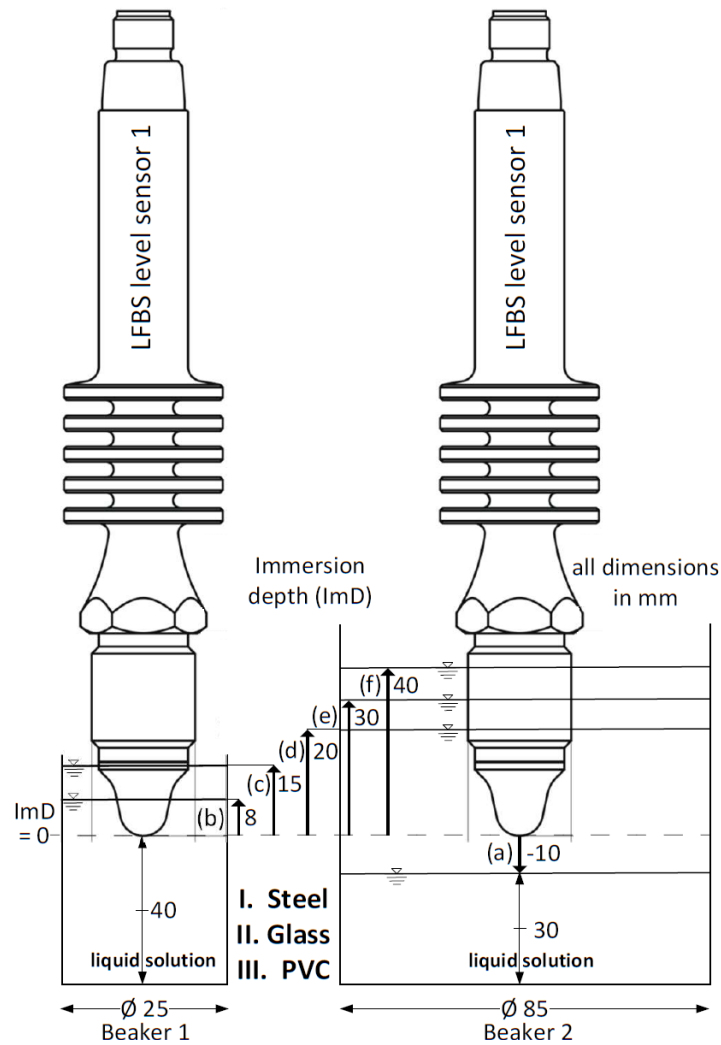


Figure 14. Measurement setups for various materials, immersion depth (ImD), and beaker diameters to characterize the SR of the liquid with the capacity point level sensor [136]

Besides the solution of SDS and water ($1.35 \text{ g}_{\text{SDS}} \text{ L}_{\text{total}}^{-1}$), beaker experiments were repeated with foamable mixtures. A mixture of chlorobenzene and ethylbenzene (CB/EB) with impurities of rust (FeO_2) particles was used. The mixture had an equimolar composition of $0.5 \text{ mol}_{\text{CB}} \text{ mol}_{\text{total}}^{-1}$ with a liquid density of $\rho_{\text{CB/EB}} = 0.9756 \text{ g cm}^{-3}$. In addition, SDS with a concentration of $1.35 \text{ g}_{\text{SDS}} \text{ L}_{\text{total}}^{-1}$ was dissolved in > 99 % monoethylene glycol (MEG; Carl Roth GmbH & Co. KG, Germany). As alternative aqueous surfactant solution of an anionic secondary alkylsulfonate, SAS 93[®] (WeylClean, WeylChem International GmbH, Wiesbaden, Germany) ($0.18 \text{ g}_{\text{SDS}} \text{ L}_{\text{total}}^{-1}$) in deionized water was employed.

3.2.2. Measurement setup with conductivity sensors and capacitive level sensor

To be able to explore the relationship between the output signal of the sensor and liquid fraction, it requires a defined foam with known bubble size and controllable liquid fraction. This can be achieved by the principle of forced drainage [137].

In addition, the actual liquid fraction in the foam has to be determined as a reference value. This was done using electrical conductivity measurements [79]. The measurement setup is depicted in *Figure 15*. A cylinder made of PMMA (Perspex[®]) with an inner diameter of $d_i = 100$ mm was used. Prior to each experiment, it was filled with $V = 1000$ mL solution made from deionized water and $1.35 \text{ g}_{\text{SDS}} \text{ L}_{\text{total}}^{-1}$. Foam was produced by pneumatically introducing air at the bottom of the column by means of a sparger with a flow rate of $dV_{\text{air}+\text{C}_6\text{F}_{14}}/dt = 1.7 \times 10^{-5} \text{ m}^3 \text{ s}^{-1}$ ($1000 \text{ sccm min}^{-1}$), resulting in a superficial gas velocity in the empty column of 0.22 cm s^{-1} . The effect of coarsening during the experiments was reduced by adding a small amount of perfluorohexane (C_6F_{14}) to the air before entering the cell [138].

To investigate the influence of bubble size on the sensor signal, different sparger geometries were applied, resulting in a variation of bubble sizes [139]. The largest bubble size was achieved using seven syringe needles with an inner diameter of $d_i = 0.8$ mm as sparger geometry. Smaller bubbles were generated by porous glass plates with varying pore diameter. The bubble radii resulting from different spargers were determined by taking a sample of foam from the column and squeezing it between two glass plates separated by a known distance h . Images of the bubbles between the plates were recorded using a camera. The diameter of individual bubbles $R_{i,eq}$ in the images was then calculated as described in Gaillard et al. [140]. In the last step, the Sauter mean radius was derived as Eq. (2):

$$R_{32} = \frac{\langle R_{i,eq}^3 \rangle}{\langle R_{i,eq}^2 \rangle}. \quad (2)$$

The liquid fraction in the foam was controlled by introducing a foaming solution at the top of the column using a porous cylinder, i.e., an additional drainage flow rate Q_{Dr} was imposed. This results in a constant liquid fraction distribution along the column height and cross section where the distance to the foam/solution interface is sufficiently large. Increasing Q_{Dr} using a peristaltic pump gives rise to increased liquid fraction in the bulk of the foam. However, the highest achievable liquid fraction is limited by the appearance of the convective instability. This occurs at higher drainage flow rates and results in the collective movement of bubbles and inhomogeneous liquid fraction distribution inside the experimental column, making a comparison between the sensor signal and electrical conductivity measurement unfeasible [141]. Therefore, the measurements were limited to points where no bubble motion caused by the convective instability was visible at the column wall.

The sensor was inserted horizontally in the column wall with the sensor tip placed in the foam. As will be shown later, the presence of a solid wall does influence the sensor signal. Therefore, the wall material and the immersion depth (ImD) had to be kept constant to $ImD = 20$ mm during different experiments. Electrical conductivity measurements were achieved using a pair

of wall-mounted electrodes and a custom-made measurement setup [82]. The liquid fraction φ was then determined by using the well-established Eq. (3).

$$\varphi = \frac{3 \sigma (1 + 11 \sigma)}{1 + 25 \sigma + 10 \sigma^2} \quad (3)$$

with $\sigma = \sigma_f \sigma_{sol}^{-1}$ where σ_f and σ_{sol} are the measured electrical conductivity of the foam and the foaming solution, respectively [79].

The measuring region of the conductivity measurements extends over the volume between two electrodes, above the measuring location of the level sensor. The distance between measurement region and liquid/foam interface, as well as the distance between measurement region and drainage injection point were chosen to be large enough to assume that no gradient in liquid fraction appears between the sensor and the electrode pair.

Before each experiment, it was ensured that the whole cell was filled with foam. Afterwards, the peristaltic pump started injecting liquid at the top. An adjustment time of at least 2 min was set to ensure that the liquid fraction distribution was homogeneous and in steady state before proceeding. Electrical conductivity measurement and the sensor measurement were then carried out in parallel. Independent experiments ensured that both techniques do not interfere with each other. This was done by continuously operating the sensor over the time of $t = 60$ s and starting the electrical conductivity measurement after $t = 30$ s in parallel. No measurable change in the SR of the sensor could be detected throughout the whole measurement time of all measurements.

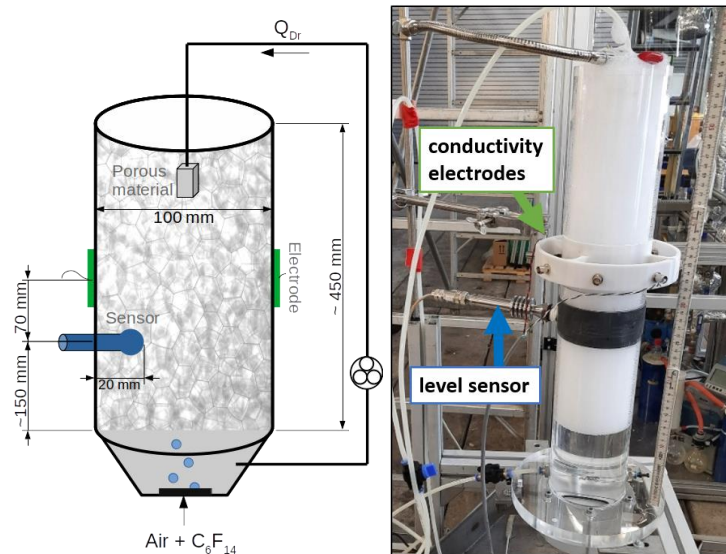


Figure 15. Schematic drawing and photo of the experimental setup used for correlating level sensor signals and liquid fractions of foams via conductivity measurements

3.3. Results and Discussion

In the results section, parameters which influence the coupling and usage of the sensor are presented first. In this context, the operational limitations of the sensor are discussed. Subsequently, foam-based experiments are shown based on the results on operational limits. The last section focuses on the correlation of the liquid fraction of foam with the sweep range.

3.3.1. Immersion Depth and Sensor Surroundings

The output signals of the sensor depend on various parameters regarding its insertion, the medium to be measured, as well as its temperature. To investigate the influence of immersion depth, vessel diameter, and vessel material, the temperature of the medium was kept constant to $T = 14\text{ }^{\circ}\text{C}$.

Figure 16 illustrates that the data of SR are depending on the depth of immersion. At low or even negative ImD ($ImD = -10\text{ mm to } 15\text{ mm}$), the SR depends on the level, which is not suitable for measuring the liquid fraction. Above $ImD = 20\text{ mm}$ it converges and measurements are reasonably possible. The wall effect is negligible if the criterion of $ImD > 20\text{ mm}$ is met. The wall material and beakers' diameters may play a role for partially immersed sensors. The lowest SR values were found for the stainless-steel beaker at all immersion points (exception $ImD = 8\text{ mm}$; $d_i = 25\text{ mm}$) due to the fact that the steel was not grounded and shielded the electrical signal. The capacitance (C_0) of the liquid compared to air turns out to be larger because the relative permittivity of the polar liquid water $\epsilon_{r,\text{water},20\text{ }^{\circ}\text{C}} = 80.2\text{ F m}^{-1}$ is known to be higher as that of metal, e.g., $\epsilon_{r,\text{metal},20\text{ }^{\circ}\text{C}} = 1\text{ F m}^{-1}$ [142,143].

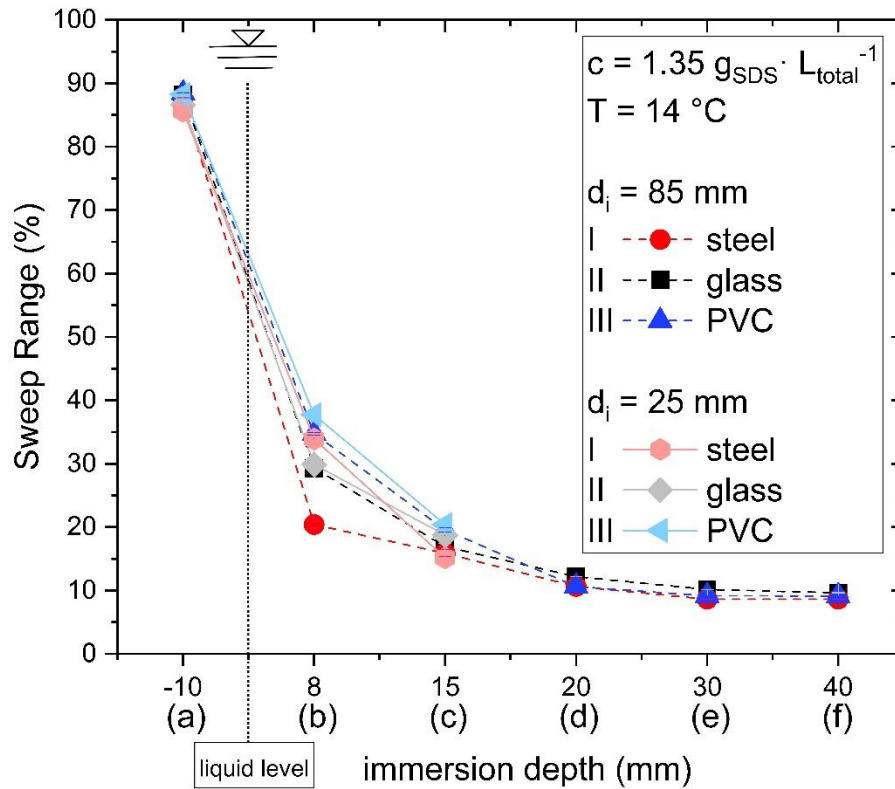


Figure 16. Experimental data of sweep range (SR) as a function of immersion depth (ImD) of the sensor in addition to varied beaker materials with different beaker diameters at 14 °C in a liquid SDS/water mixture

3.3.2. Surfactants and Solvents

To investigate the sensor's limitations based on foam liquid characteristics, its SR was investigated in different setups of liquid solutions. For the comparison of various surfactants and solvents (aqueous and organic), the sensor was inserted into different liquids and the SR was recorded. Applying the same introduced procedure, a beaker with a diameter of $d_i = 85$ mm was chosen, so that the material exerted minimal influence on the sensor.

First, the influence of the anionic surfactant SDS on the SR had to be investigated. The SR values shown in *Figure 17* were normalized to the SR of deionized water (9.7 %). The SR was normalized by dividing the measured SR of the liquid by the SR of the liquid solvent. At the SDS concentration of $c_{SDS} = 9.1 \text{ g}_{SDS} \text{ L}_{total}^{-1}$, the SR was 20 % higher than the SR of deionized water. This showed that the SR is dependent on the concentration of ions in the liquid. Concentration differences of ionic components in the foam therefore represent a limiting factor for the usage of the sensors for the detection of liquid fractions of foams.

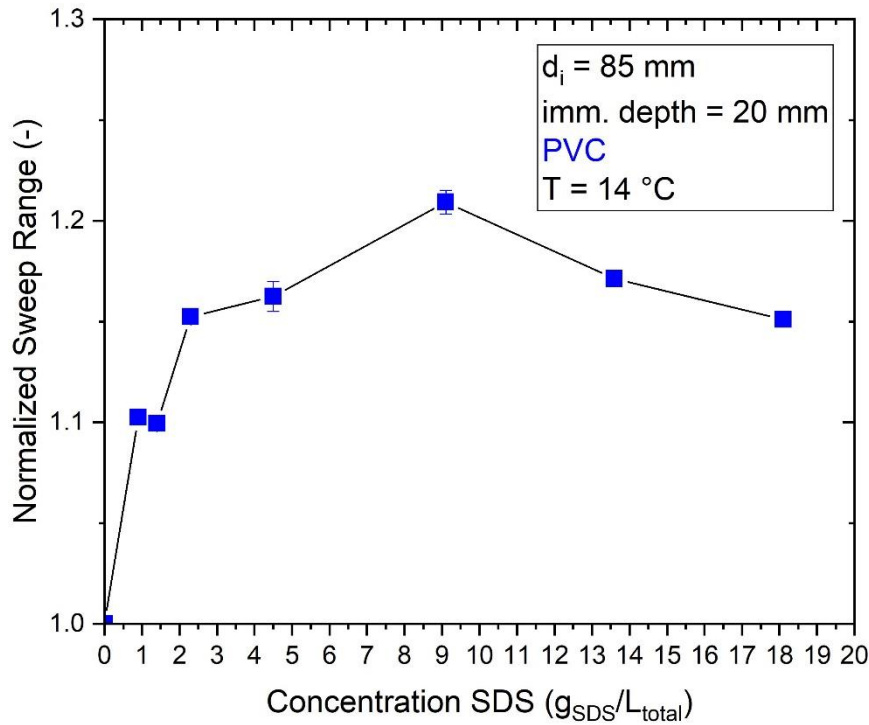


Figure 17. Influence of the anionic surfactant SDS on the normalized SR (nSR) of a full-immersed sensor tip, in PVC surroundings at 14 °C

Concentration differences of ionic components influence the sensor signal and, therefore, represent a limitation for the application range of the sensor. With respect to the characterization of the liquid content of foam, it must be ensured that the SDS concentration in the foam is constant. Therefore, subsequently performed experiments were based on liquids with SDS concentration of $c_{\text{SDS}} = 1.35 \text{ g}_{\text{SDS}} \text{ L}_{\text{total}}^{-1}$.

The results shown in *Figure 18* indicate that the sensor outputs medium-specific SR values. For instance, equal concentrations of secondary alkylsulfonate (SAS) dissolved in water or in monoethylene glycol (MEG) resulted in significantly different SR values. The reason lies in different relative permittivities ϵ_r and polarizability of the molecules at the same temperature. This demonstrates that the sensor signal is sensitive to different solvents.

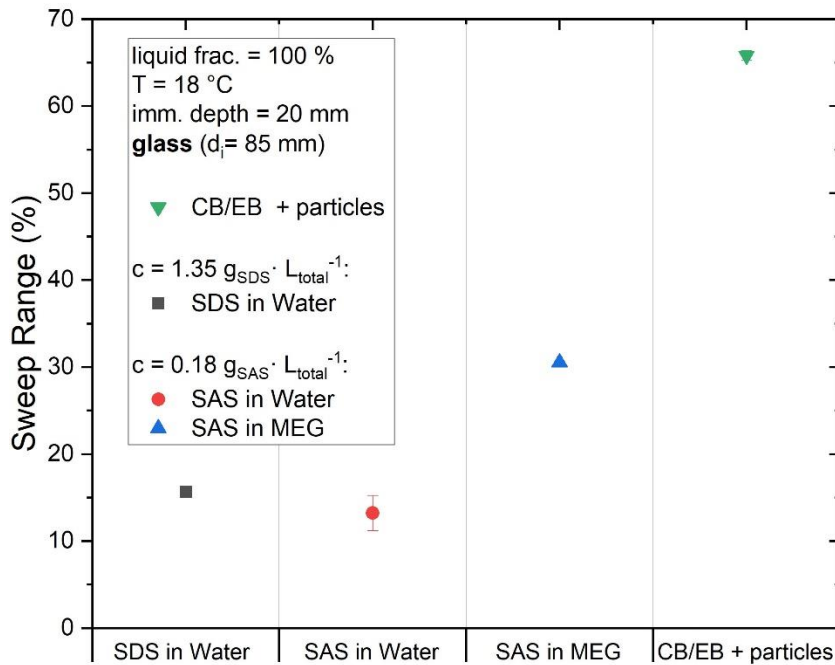


Figure 18. Experimental data of Sweep Range (SR) measured in various liquid mixtures at 18 °C

The solvent monoethylene glycol (MEG) has a lower polarity than deionized water. Therefore, the relative permittivity decreases, and the sensor outputs a lower capacitance and SR . In contrast to the aqueous mixtures ($SR < 30\%$), significantly higher SR values were measured for the polar and foamable mixture CB/EB with iron oxide particles ($SR = 65\%$). This difference illustrates the sensitivity of the capacitive measurement method of the point level sensor to different chemical components' properties.

With regard to the following investigations of liquid contents of foam in a PMMA column with the level sensor in a PVC ring, it was shown that the SR is sensitive to different wall materials. A sufficiently deep immersion depth of the whole sensor tip with at least $ImD_{min} = 20$ mm is necessary to measure a signal based only on the permittivity of the liquid. When inserting the sensor in pipes or container walls, the immersion depth can be adjusted by the screw-in depth of the thread.

3.3.3. Correlation of Water Content Fractions of Foam with SR

The experimental data for the SR was normalized by dividing the measured SR of foam through the one of the liquid. The normalized SR (nSR) as a function of the liquid fraction and bubble radius is depicted in *Figure 19*.

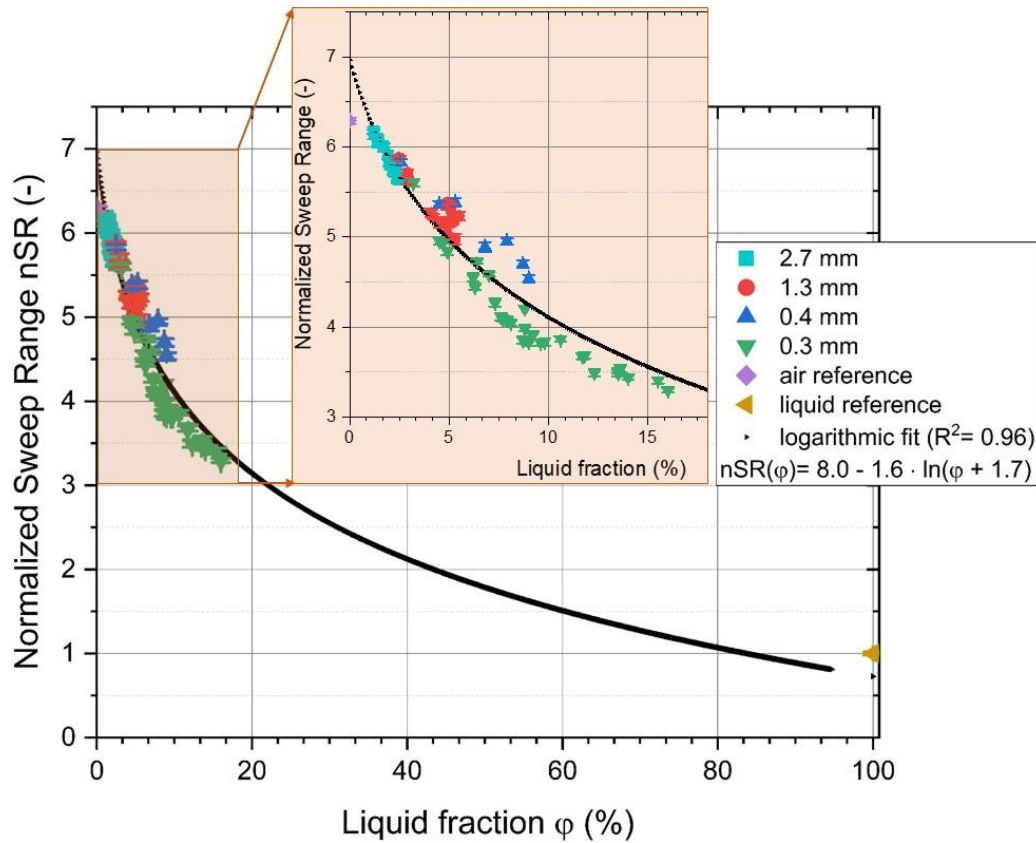


Figure 19. Experimental data of normalized Sweep Range (nSR) as a function of liquid fraction

All recorded data of the measurements in the foam ($n = 77$) and the measurement of the liquid and the air were fitted with the logarithmic Eq. (4) using parameters as specified in *Table 3*.

$$nSR(\varphi) = a - b \cdot \ln(\varphi + c) \quad (4)$$

Table 3. Parameters of the logarithmic fit regarding nSR as a function of liquid fraction (φ)

Parameter	Value
a	8.0276 ± 0.24798
b	1.57835 ± 0.07617
c	1.96291 ± 0.39237
R^2	0.96198

The measured values deviate up to 13 % from the fitted values. Overall, highest deviations were found in measurements with a bubble radius of 0.4 mm (*Figure 20*). These high deviations may be referred to issues in the setup. Foam with a bubble radius of 0.4 mm was especially prone to

destruction by the introduced foaming solution at the top of the column. It was made sure that the whole cell was filled with foam and in steady state before starting the experiments.

Measurements of foams with bubble radius of 0.3 or 1.3 mm in *Figure 20* showed deviations of $< 10\%$ and $< 8\%$, respectively. Least deviations were found in measurements of foams with a bubble radius of 2.7 mm. This indicates that there is no systematic dependency of the received *SR* on bubble radii. However, it is assumed that there is an upper limit to the detection by the sensor in terms of bubble radii.

In general, the majority of measured values ($n = 44$) showed an error of $\leq 4\%$ (*Figure 20*). An error of $\leq 8\%$ occurred in more than 90% of the measured values. It also has to be considered that the state-of-the-art method (electrical conductivity), which was used for determining the liquid fraction in the experiment, is referred to have a relative experimental error of about 5% in liquid fraction [79]. Due to using a relative method and no absolute method for calibration, the measured values were also subjected to the errors of the electrical conductivity method. Thus, the precision of this method for determining the liquid fraction of foams is comparable to methods like determination via surface fraction [81] or via electrical conductivity [79,134].

In summary, the experiments demonstrated that there is a clear correlation between the *SR* and the liquid fraction of foam with the measured *SR* being independent of the bubble radius. Additionally, this method comes with the benefit of being easily applicable in many industrial plants, regardless of the wall material and also being usable in explosion hazard areas.

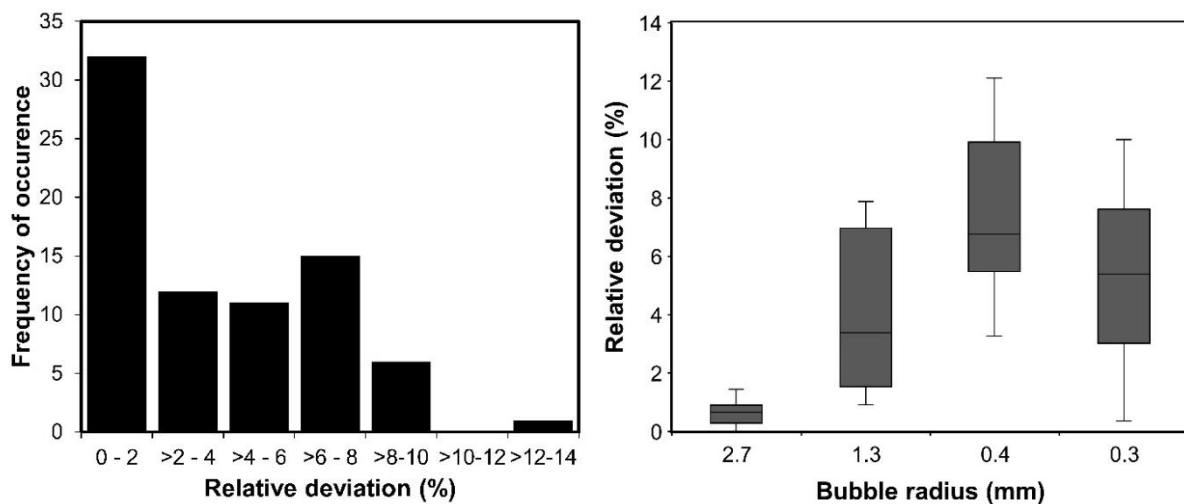


Figure 20. Representation of the frequency of deviations (left) and the dependence of the deviation on the bubble size (right)

3.4. Summary and Outlook

A capacitive point-level sensor was used to obtain information on the liquid fraction inside aqueous foams. Regarding the sensor operation, the minimum immersion depth was found to be 20 mm where the influence of the confining wall is negligible. The sensor signal depends on the components and composition of the liquid. Thus, the sensor signal needs to be normalized

by the signal for the pure liquid without bubbles. The sensor was then placed in a stable foam made from SDS. By comparing the sensor signal to the liquid fraction, determined by measuring the electrical conductivity of the foam in parallel, it was shown that it is possible to relate a change in the sensor signal to a change in liquid fraction. The obtained data in the liquid fraction range of $1.2 \% < \varphi < 16 \%$ could be well described by a shown single curve of logarithmic type. Furthermore, this relationship was found to be nearly independent of the bubble size by considering foams with bubble radii in the range of $0.3 \text{ mm} < r_{32} < 2.7 \text{ mm}$.

This method comes with the benefit of being easily applicable in many industrial plants independently of the apparatus, especially as the sensor can be applied to processes independent of the wall material and can be used in explosion hazard areas as well.

While the initial applicability of this novel method was successfully demonstrated in this study, several points are still to be elucidated. Especially the influence of solvents in the foaming solution has to be examined in more detail. The case when the sensor's tip is not continuously in contact with the foaming liquid (e.g., foams made of large bubbles in the centimeter range), could also be of interest for relevant technical applications such as evaporation-induced foams.

Acknowledgment

The authors gratefully acknowledge the financial support within the project ‘‘Physical management of disturbing foams’’ (AiF 4 PN), which was supported via AiF within the program for promoting the Industrial Collective Research (IGF) of the German Ministry of Economic Affairs and Climate Action (BMWK), based on a resolution of the German Parliament. We also thank the Research Association of the German Food Industry (FEI) for administration of the collaborative research network. Additionally, we would like to thank the German Research Foundation (DFG) for financial support under grant HE 7529/3-1. Open access funding enabled and organized by Projekt DEAL.

The authors have declared no conflict of interest.

Symbols used

c	[g L ⁻¹]	concentration
d	[mm]	diameter
h	[mm]	distance between two glass plates for determination of bubble radii
Q	[m ³ s ⁻¹]	volumetric liquid flow
R, r	[mm]	radius
T	[°C]	temperature
t	[s]	time
V	[cm ³]	volume
\dot{V}	[m ³ s ⁻¹]	volumetric gas flow

Greek letters

ε	[F m ⁻¹]	permittivity
ρ	[kg m ⁻³]	density
σ	[μ S cm ⁻¹]	electrical conductivity
φ	[-]	volumetric liquid fraction

Sub- and Superscripts

acrl	acrylic glass
cyl	cylinder
Dr	drainage
eq	equal diameter
f	foam
g	gas
i	inner
in	individual bubbles
min	minimum
rel	relative
sol	foaming solution
tot	total

Abbreviations

CB	chlorobenzene
CMC	critical micelle concentration
EB	ethylbenzene
FST	frequency sweep technology
ImD	immersion depth [mm]
nSR	normalized Sweep Range
SAS	secondary alkylsulfonate
SDS	sodium dodecyl sulfate
SR	Sweep Range

4. Foam-resilient distillation processes - Influence of pentosan and thermal energy input on foam accumulation in rye mash distillation

Daniel Heller^{a,*}, Daniel Einfalt^a

^aInstitute of Food Science and Biotechnology, Yeast Genetics and Fermentation Technology, University of Hohenheim, Garbenstraße 23, 70599 Stuttgart, Germany

* Corresponding author. Tel.: +49 (0) 711 459 24432;
E-Mail address: daniel.heller@uni-hohenheim.de
ORCID: 0000-0001-7580-3025

Abstract

Foaming of mashes during distillation is a common problem encountered in spirit drink production. It has a negative impact on the purity of the final product. This research article presents the key aspects of foam accumulation in rye mashes during distillation. Foam accumulation was influenced by substrate characteristics and process parameters. The experiments showed that pentosan levels and thermal energy input were the crucial parameters for foam accumulation in rye mashes. Foam accumulation was significantly enhanced by higher pentosan levels, due to the higher viscosity imparted by pentosan. Hence, degradation of pentosans prior to distillation presents a way to reduce foam accumulation. In terms of thermal energy input, foam accumulation was significantly lower when the thermal energy input was reduced from 400 W/L to 200 W/L. Substantial foaming only occurred in a narrow temperature range of 89.5 to 98.2°C. The results allowed for the first time to make recommendations to prevent problematic foam accumulation during distillation of rye mashes.

Keywords

foam, distillation, rye mash, pentosan, spirit drink production

4.1. Introduction

Excessive foam accumulation is a common cause for malfunctions and process failures in various technological processes. It occurs regularly in food and beverage industries and chemical processing (agitation, distillation) [43,53,144,145]. In spirit drink distillation

excessive foam accumulation can lead to increased maintenance costs and impaired product quality [15,47]. In extreme cases, it can even cause plant flooding resulting in the necessity of a partial or complete process shut down [146]. To be able to avoid such process interferences, it is important to gain excessive information on foam accumulation mechanisms during distillation.

The main reasons for impairing foam accumulations in industrial distillation processes are the utilization of substrates with high foam formation capacities, inadequate operational process management and technical faults [46]. It is likely that similar factors apply to batch distillation processes of spirit drinks.

In order to understand the mechanisms that promote foam accumulations it is important to investigate substrate properties supporting the formation of foam during distillation. Specific substrate properties with stabilizing effects on foam formation have already been investigated in various food products. It is known that the presence of proteins and polysaccharides play an important role on the physical stability and structure of food foams [37–41]. Therefore, we hypothesized that the presence of proteins and polysaccharides might also be important for foam accumulation in distillation processes.

The spirits industry utilizes various different fruits and cereals. All substrates have specific protein and polysaccharide contents and different foam formation capacities. So far, the literature only provides descriptive information on foam formation capacities of different fermented mashes. Enhanced foam formation capacities are known for cherry, wine lees and cereal mashes [15]. Within cereal substrates, rye mashes are especially prone to an excessive formation of foam [15]. Rye is known to contain higher concentrations (7 to 8 wt%) of the non-starch polysaccharide pentosan compared to other cereals with 1.4 to 4.1 wt% [147], which might influence foam formation properties. Pentosan mainly consist of arabinoxylan chains made out of 50 to 60% xylose and 30 to 35% arabinose [148]. In the bakery industry, pentosan is known to have a positive effect on dough network formation and loaf volume [149–152]. Such dough and bread structures are often characterized by their gas-holding capacities and, therefore, have similar properties as classical foam structures [153]. As pentosan supports the foam structure in doughs, it is possible that the presence of pentosan might also enhance the formation of foam during distillation.

Next to substrate properties, process management can drive foam formation. Scientific knowledge on foam accumulations related to operational management of distillation processes is still scarce. Simon et al. [51] investigated the dependency of reboiler vessel size and vapour flow rate on reboiler vessel swelling (foam accumulation). Further literature only provides descriptive information on process management strategies that reduce the risk of impairing foam accumulations. This includes recommendations to run batch distillations with a 25 to 50% reduced reboiler vessel filling to provide sufficient space for accumulating foams and to use a reduced thermal energy input at ‘critical foam-prominent temperature ranges’ (no further details given) [15]. However, in extreme cases plant flooding occurred despite the implemented process management strategies [15,51].

A common strategy for dealing with excessive foam accumulation is the application of chemical additives, which are usually based on silicone-oil. These additives effectively reduce or prevent undesired foam accumulations after addition of 2 to 4 g/hL mash [15,55]. However, these ‘antifoam additives’ are known to have negative environmental effects when released to aquatic systems, e.g. interfere with oxygen transfer rates in water bodies and metabolic activities of microorganisms, or impair biodegradation processes [58]. They also reduce catalytic activities in downstream processes [59]. As environmental regulations become more stringent, alternative foam control methods need to be employed. Therefore, it is important to understand foam accumulation mechanisms on substrate and process level to be able to prevent foam formation.

The aim of the study was to minimize foaming in spirits production with a substrate that is especially prone to foaming. Therefore, the present study investigated foam accumulations in rye mash distillation in regard to substrate and process parameters. It examined the relation of different pentosan concentrations as well as thermal energy input levels on foam accumulation during the process.

4.2. Material and methods

4.2.1. Mash preparation

Coarsely ground winter hybrid rye meal (RW S1 1363, HYBR 2012), grown and harvested in Lundsgaard, Germany, was provided by the Federal Plant Variety Office of Germany. Rye mash preparation was carried out according to *Figure 21*. Rye meal and water were mixed in a 1:4 mass ratio. Calcium hydroxide (Merck KGaA, Darmstadt, Germany) and sulphuric acid (Carl Roth GmbH & Co.KG, Karlsruhe, Germany) were used for pH adjustment. To investigate the influence of pentosan the pentosan degrading enzyme pentosanase EX-Tosan (C. Schliessmann Kellerei-Chemie GmbH & Co.KG, Schwäbisch Hall, Germany) was applied during mash preparation. Enzymatic liquefaction was performed with Distizym BA-TS (Erbslöh GmbH, Geisenheim, Germany) and added in concentrations of 0.066 mL/kg rye meal. Enzymatic saccharification was carried out with an enzyme mixture consisting of 0.27 mL Distizym AG-Alpha (Erbslöh GmbH, Geisenheim, Germany) and 0.1 g Tegaclast 220P (tegaferm Holding GmbH, Vienna, Austria) per kilogram rye meal.

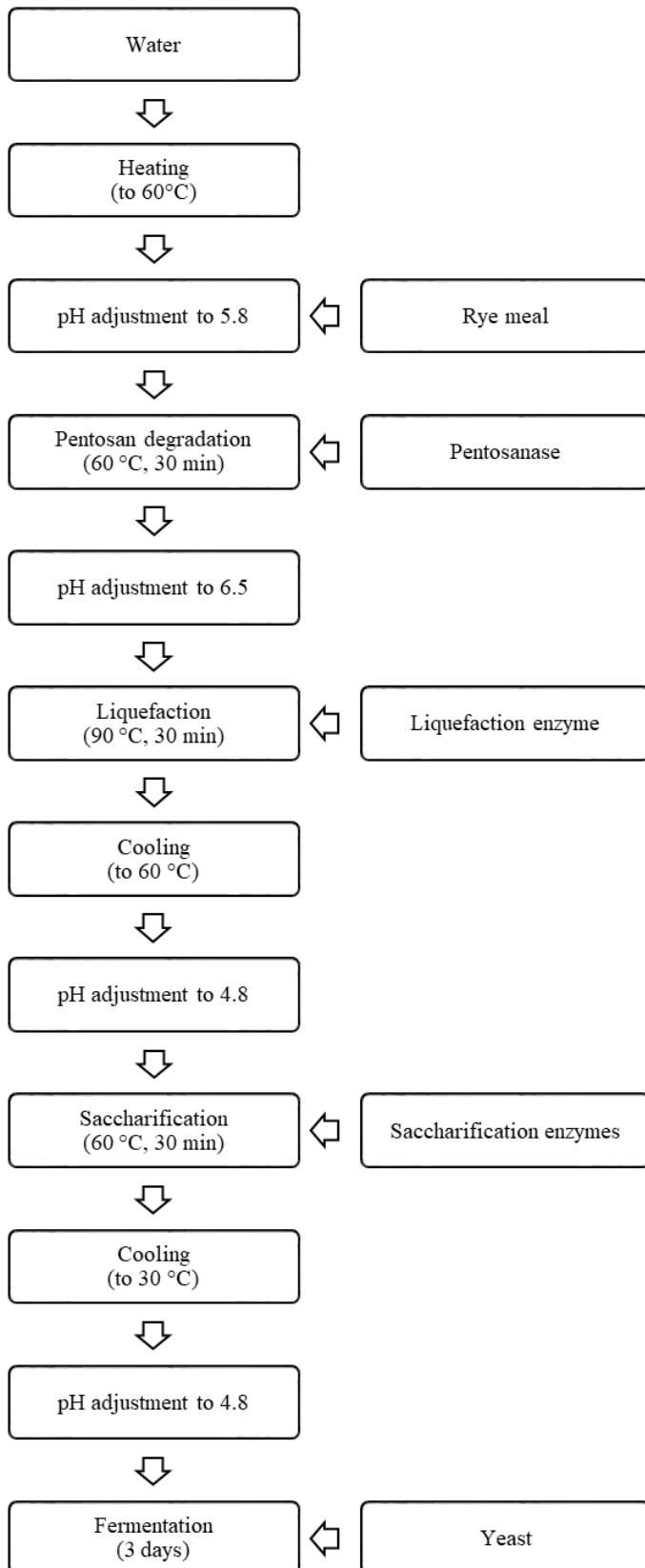


Figure 21. Flow chart of rye mash preparation

4.2.2. Substrate characterisation

Fermented rye mashes were characterized for dry matter (DM), ash, pentosan, protein and ethanol content, while rye meal was investigated for fermentable substances (FS). DM and ash were determined according to VDLUFA [110] and ICC [111], respectively. Quantification of pentosan was performed according to AOAC [154]. The method was modified as described by Jäger & Unger [155]. Protein (N x 5.83) content analysis was conducted using sample sizes of 100 mg and a nitrogen analyser (Dumatherm, Gerhardt GmbH & Co. KG, Königswinter, Germany) according to Duma's combustion method [156]. Ethanol content was determined via lab-scale steam distillation (Autodest 10, Leo Kübler GmbH, Karlsruhe, Germany) of 50 g mash samples [157]. The density of distillates was analysed via u-tube-oscillator (DMA 4500 M, Anton Paar GmbH, Ostfildern, Germany).

Determination of FS in rye meal was carried out according to Senn & Pieper [157]. They defined FS as 'the sum of glucose and maltose contents of the raw material, calculated as starch, that can be determined using HPLC after the raw material is completely digested and dispersed as well as liquified and saccharified by addition of technical enzymes'. The method was modified by additionally determining fructose contents and adding it to the FS calculation in Eq. (6).

$$FS (wt\%) = \frac{(\varphi_g (C_g + C_f) + \varphi_m C_m) V_S}{W_{rm}} \times 100, \quad (5)$$

where φ_g is the hydrolysis factor for glucose and fructose (0.899) and φ_m for maltose (0.947), C_g , C_f and C_m are concentrations of glucose, fructose and maltose (g/L), V_S is the sample's end volume (L) and W_{rm} is the initial mass of rye meal (g).

The HPLC system for sugar analysis was set up with a Rezex RPM-Monosaccharide Pb+2 Ion exclusion column (\emptyset 7.8 × 300 mm, Phenomenex, Aschaffenburg, Germany) and a refractive index detector (RID, Shodex RI-101, Thermo Fisher, Waltham, USA) with sulphuric acid (0.005 N) as eluent at a flow rate of 0.6 mL/min. Five-point standard calibration was used for fructose, glucose and maltose ($R^2 > 0.95$).

4.2.3. Pentosan degradation effects

To determine the influence of pentosan on rye mash properties, nine different pentosanase concentrations (0.0; 0.1; 0.2; 0.8; 1.0; 1.2; 1.6; 2.0; 4.0 mL/kg rye meal) were applied and investigated in triplicates for converted pentosan, mash viscosity and unspecific protein degradation. The same sample set was also used for studies on foam accumulation.

For the determination of converted pentosan the pentosan hydrolysis products xylose and arabinose were quantified via five-point standard calibrated ($R^2 > 0.95$) HPLC-RID analysis before pentosan degradation and after the saccharification step of the rye mash preparation. The

conversion of pentosan to xylose and arabinose was calculated by Eq. (6) including the hydrolysis factor of 0.88 (φ_x) for xylose and arabinose.

$$\text{pentosan conversion (\%)} = \frac{\varphi_x (C_x + C_a) - (C_{x0} + C_{a0})}{C_{p0}} \times 100, \quad (6)$$

where C_x and C_a are final concentrations of xylose and arabinose (g/L) after saccharification and C_{x0} , C_{a0} and C_{p0} are initial concentrations of xylose, arabinose and pentosan before pentosan degradation (g/L).

Effects of pentosan degradation on mash viscosity were determined using a rotational rheometer (MC1, Paar Physica, Ostfildern, Germany) equipped with a double gap measuring system. Viscosities were measured with rye mash supernatants centrifuged at 2000 rpm for one minute.

To exclude secondary activities of pentosanase in terms of additional unspecific protein degradation, an additional experiment was set up that added pentosanase in different concentrations of 0.0, 0.1, 0.2, 0.8, 1.6, 2.0 and 4.0 mL/kg to 10 wt% protein-solutions (Wheat Protein Isolate, Carl Roth GmbH, Karlsruhe, Germany) in citrate buffer. Protein blanks with each tested enzyme concentration were equally prepared. All samples and blanks were incubated for 1 h (60 °C; pH 5.8) and remaining protein concentrations were determined by Bradford test [112].

Additionally, SDS-PAGEs [158] of the rye mash samples with 0.0; 0.1; 0.2; 0.8; 1.6; 2.0; 4.0 mL/kg pentosanase addition were carried out to identify changes in the protein composition by analysis of their molecular masses with and without pentosan degradation.

4.2.4. Foam accumulation experiments

The first set of distillation experiments focused on foam accumulation in rye mash distillation in regard to the nine different pentosan-degraded rye mashes. All rye mashes were distilled with a constant energy input of 200 W/L. In the second set of experiments, the influence of thermal energy input level was evaluated by distilling an additional sample set of nine different pentosan-degraded rye mashes with an energy input of 400 W/L.

Distillation experiments were conducted using a small-scale distillation plant set up. The dimension of the experimental setup corresponded to the dimensions of a standard distillery plant with 150 L reboiler vessel size and rectification column in a scale of 1:10. Mashes were electrically heated (LabHeat, SAF Wärmetechnik GmbH, Mörlenbach, Germany) in a 250 mL two-necked round bottom flask (CN ST 29/32, SN ST 19/26, Lenz Laborglas GmbH & Co. KG, Germany). Accumulating foam heights were logged every 60 seconds in a 34 cm high, 32 mm wide glass tube (ST 29/32, Lenz Laborglas GmbH & Co. KG, Wertheim am Main, Germany) equipped with a metric scale. Mash temperature was measured simultaneously with a thermometer (testo 735 PT100, Testo SE & Co. KGaA, Titisee-Neustadt, Germany) inserted

into the side neck of the glass flask. The term ‘foam accumulation’ was defined for foam levels > 3 cm.

4.2.5. Statistical analysis

A total of 54 mashes were analyzed for substrate characteristics and foam accumulations. The sample set included triplicate analysis of nine different pentosan-degraded rye mashes, distilled with two different energy inputs. Results are given in mean values with standard deviation. Significant differences ($p \leq 0.05$) were evaluated by one-way ANOVA with Tukey HSD post-hoc tests and performed with SPSS software (Version 25, IBM, USA). Pearson’s correlation coefficients (r) were analyzed to identify the relation between pentosanase addition and pentosan conversion rate or mash viscosity.

4.3. Results and Discussion

4.3.1. Substrate characteristics

The substrate characteristics of the rye mash are shown in *Table 4*. The investigated rye meal had a FS content of 60.1 ± 0.1 wt% based on fresh matter (FM) ($n = 3$). The analysed substrate composition of the mashes was in accordance with the results of Hansen et al. [159], who found similar pentosan, protein and ash contents. The fermented mashes contained ethanol concentrations of 6.2 ± 0.6 % vol. This showed that $51.5 \pm 5.1\%$ of the FS was metabolized to ethanol, which indicated an efficient and complete fermentation.

Table 4. Substrate characteristics of rye mash

Properties	Values	Replicates
DM (%FM)	7.0 ± 0.1	54
Ash (%DM)	4.1 ± 0.4	54
Pentosan (%DM)	22.8 ± 0.8^a	6
Protein (%DM)	21.5 ± 0.1	54
Ethanol (% vol)	6.2 ± 0.6	54
Ethanol yield (mL/kg rye)	309.5 ± 30.6	54
pH value	4.1 ± 0.1	54

^a Value based on control mash (0.0 mL/kg pentosanase addition)

4.3.2. Pentosan conversion

Additions of pentosanase did result in increasing levels of the hydrolysis products arabinose and xylose. This indicated an efficient enzymatic conversion of pentosan. In comparison to the control mash, a significant increase of pentosan conversion was achieved with pentosanase concentrations ≥ 0.2 mL/kg. The Pearson correlation revealed a significant positive relationship between the pentosan conversion rate and the amount of added pentosanase ($r = 0.99$, $p \leq 0.05$). Pentosanase concentrations of 4.0 mL/kg resulted in the highest pentosan conversion rate of $66.8 \pm 6.3\%$. A conversion rate of $33.1 \pm 0.9\%$ was also observed in the control sample without added pentosanase. This could be due to unspecific secondary activities of liquefaction and saccharification enzymes on pentosan degradation during mash preparation.

4.3.3. Effects of pentosan conversion on mash viscosity

The addition of pentosanase resulted in a decrease of mash viscosity (*Figure 22*). The decrease in viscosity was proportional to the degree of pentosan conversion up 42 % of converted pentosan. Further degradation of pentosan did not result in a substantial decrease of viscosity, indicating a threshold of mash viscosity minimum. The reason for this behaviour could be the two pools of pentosan. First the soluble pool consisting mostly of arabinoxylans with the ability to form a highly viscous solution in water at a relatively low concentration [160], which are quickly degraded leading to a steep decline in viscosity. Second the insoluble pool associated with insoluble particles, which due to its insoluble, particulate state does not contribute to the viscosity of the mash. In any case, the mash viscosity could be reduced by a factor of 4 by pentosanase treatment.

4.3.4. Effects of pentosan conversion on foam accumulation

We then determined the foam forming capacity of the rye mashes at a constant energy input of 200 W/L (*Figure 22*). The control mash without added pentosanase showed maximal foam accumulation (26.2 ± 1.5 cm). With increasing pentosanase concentrations and thus concomitant reduction of viscosity the foam height was reduced. A strong decrease to 18.6 ± 1.2 cm and 5.3 ± 0.8 cm was observed when pentosanase was added in concentrations of 0.2 mL/kg and 0.8 mL/kg, respectively. Latter resulted in a significant reduction of the maximum foam accumulation level by 79.4 % compared to the control. A complete inhibition of foam formation was achieved with addition of 4.0 mL/kg pentosanase. These results indicate that pentosan concentrations have a major influence on foam accumulations. Further a clear correlation was observed between the viscosity of the mashes and the height of the foam ($r = 0.98$, $p \leq 0.05$). Similar linear correlations between foam forming ability and viscosity were also reported in other alcoholic beverages like (sparkling) wine and beer [161–164].

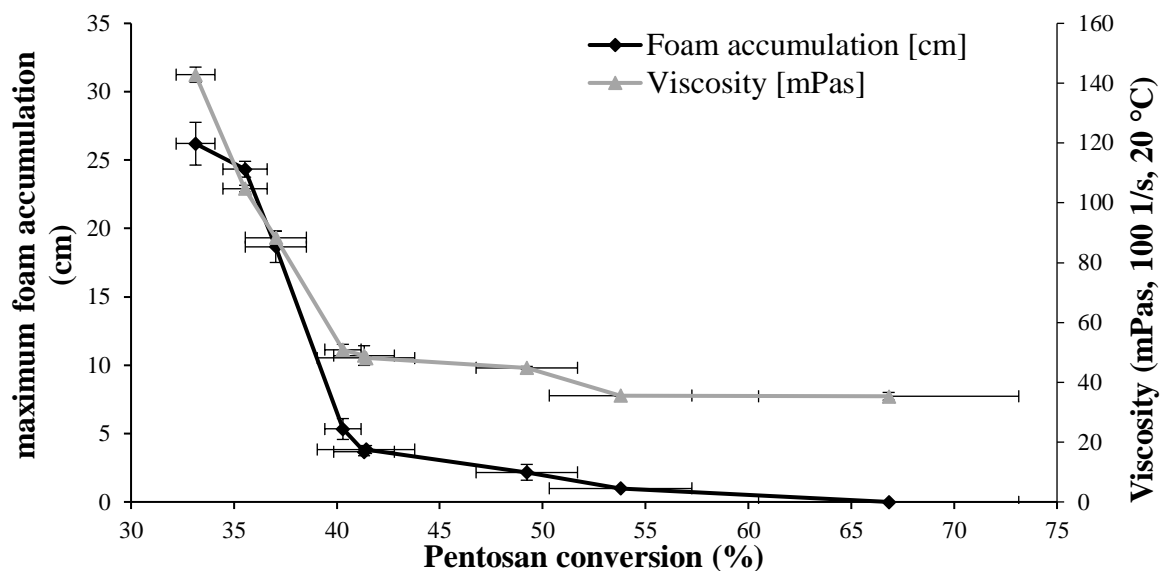


Figure 22. Maximum foam accumulation levels (primary y-axis) and viscosity (secondary y-axis) of nine rye mashes in relation to pentosan conversion (x-axis), added pentosanase from left to right: 0.0; 0.1; 0.2; 0.8; 1.0; 1.2; 1.6; 2.0; 4.0 mL/kg ($n = 3$)

Polysaccharides are known to contribute to structural and textural properties of foams. They have a significant impact on the interlamellar liquid and the air/water interface by acting as steric stabilizers, thickening or gelling agents [37,39,165]. An increase in the interlamellar liquid viscosity leads to reduced drainage of foam films and thus stabilised foams [163,165]. It is likely that degradation of the polysaccharide pentosan to its monosaccharides arabinose and xylose impairs such foam stabilizing properties resulting in reduced longevity and limited accumulation of foam bubbles. Our results on rye mash viscosity are in favour of this theory. A positive correlation between foam stability and the presence of arabinoxylans, like pentosan, was also noted in the study of [163]. Further, it was reported that arabinoxylans prevent the expansive destruction of gas bubbles under thermal conditions (95 °C) [153]. However, the investigation of Meuser et al. [166] indicated contradictory results. They reported only a minor foam reduction and physically stabilized foams after addition of pentosanase. The reason for this discrepancy could be that these experiments were performed at lower temperatures (between 5°C-35°C).

4.3.5. Unspecific protein degradation

We also considered the possibility that foam reduction by pentosanase could also be due to side activities of the enzyme. For instance, unspecific protease activity may lead to the degradation of proteins, which could also result in a reduction of viscosity and foaming ability. To rule out this possibility, Bradford tests of protein-solutions with different pentosanase addition and SDS-PAGEs of the rye mash proteins were performed. No significant changes in the protein concentrations and protein banding patterns were observed after addition of pentosanase to protein solutions and the rye mashes, respectively. Therefore, we assumed that unspecific secondary degradation effects of pentosanase can be excluded. We concluded that the

degradation of pentosan was the main cause for the reduction of mash viscosity and, in-terms, foam formation.

4.3.6. Effects of thermal energy input on foam accumulation

Energy input levels had a major effect on foaming. With an energy input of 400 W/L the maximum foam height of the experimental setup with 34 cm was exceeded within all experimental conditions, independently of pentosanase addition (*Figure 23*). With 200 W/L the maximum foam height was 26.2 ± 1.5 cm. The influence of thermal energy input on foam accumulation can be explained by a temperature dependent increase in the gas vaporisation rate resulting in enhanced foam bubble formation. It can be concluded that energy input levels have a more severe effect on foam accumulation during distillation than the pentosan concentration of the rye mashes.

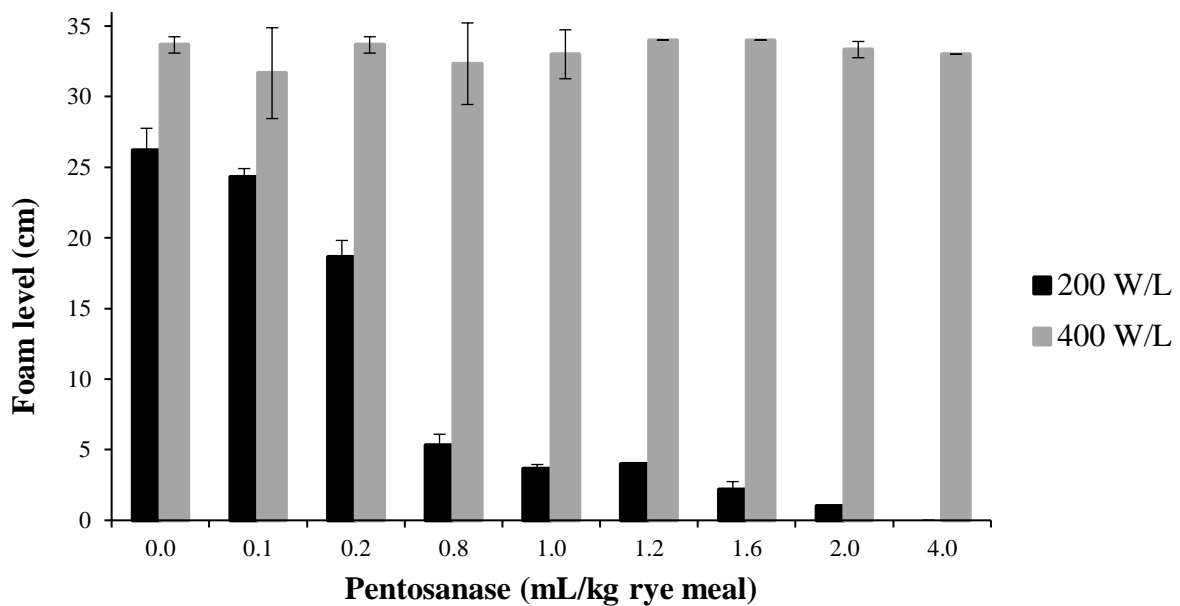


Figure 23. Maximum foam accumulation levels in rye mash distillation performed with different thermal energy inputs and different pentosanase concentrations ($n = 3$)

4.3.7. Critical temperature range

The temperature range in which foam formation occurs during the distillation of rye mashes has so far not been investigated. This study provides for the first time experimental data that defines the temperature range in which rye mash foaming occurred. A summary of heat-related foam formation of all distillation experiments is shown in *Figure 24*. The first mash foam formation appeared at a mash temperature of 63.2 °C (0.5 to 3 cm foam level height). Substantial foaming (> 3 cm) was observed at mash temperatures above 89.5 °C, while the highest level of foaming occurred between 91.2 °C and 94.5 °C. When mash temperatures

exceeded 95.2 °C the accumulated foams began to collapse and a steep decrease in foam accumulation was observed. At 98.2 °C no foam accumulation > 3 cm could be observed. This showed that increasing mash temperatures indeed triggered foam formation and induced foam collapse above a certain threshold temperature. The data set enables the definition of a foam critical temperature range during distillation. 90% of the foam accumulation occurs in the temperature range from 89.5 °C to 98.2 °C. This temperature range can be defined as the most critical in terms of excessive foam accumulations and possible process impairments.

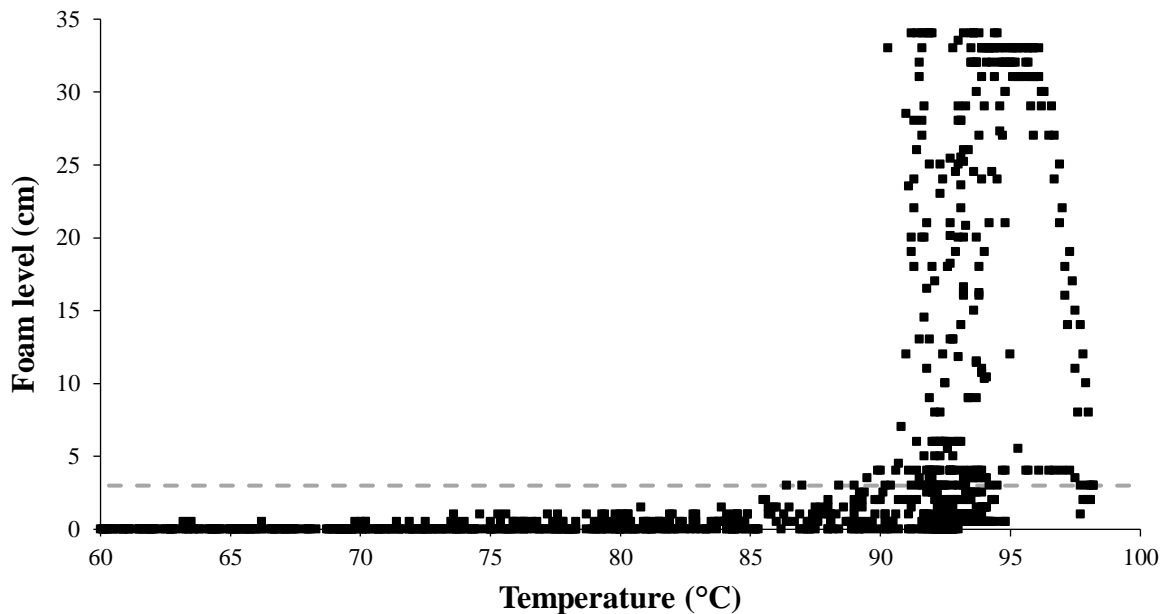


Figure 24. Foam accumulation levels and mash temperature during distillation of 54 rye mashes, grey line indicates 3 cm foam level

4.4. Conclusion

The investigation identified mechanisms of foam accumulations on substrate and process level. On substrate level, pentosan degradation had a major impact on mash viscosity and foam accumulation. A significant inhibition of foam accumulations can be achieved by addition of pentosan degrading enzymes during rye mash preparation.

On process level, foam accumulations were significantly dependent on energy input. Reduced energy inputs of 200 W/L have the potential to lower the risk of process impairing foam accumulations. The main foam accumulation occurred only in a narrow temperature range. The experimental data offer the opportunity to define foam-resilient distillation parameters. We propose the following procedure to minimize the risk of foaming. The distillation process can be initiated with high energy input (e.g. 400 W/L) until the critical mash temperature (89.5 °C for rye mash) is reached. Then the thermal energy input is reduced to 200 W/L. After reaching a mash temperature of 98.2 °C a higher energy input level can again be restored. Pentosanase treatment of the rye mash is highly recommended. In a next step, the obtained data can be used for a validation of foam-resilient processes in industrial distillation plants.

Declarations

Funding This work was supported by The German Federation of Industrial Research Associations (AiF) within the programme Industrial Collective Research for SMEs (IGF) [AiF 4 PN]

Declarations of interest The authors declare no conflict of interest.

Availability of data and material The data that support the findings of this study are available from the corresponding author, Daniel Heller, upon reasonable request.

Code availability Not applicable

5. Tackling foam-based process disruptions in spirit distillation by thermal energy input adaptations

Daniel Heller^{a,*}, Simon Roj^a, Julia Switulla^a, Ralf Kölling^a, Daniel Einfalt^a

^aInstitute of Food Science and Biotechnology, Yeast Genetics and Fermentation Technology, University of Hohenheim, Garbenstraße 23, 70599 Stuttgart, Germany

* Corresponding author. Tel.: +49 (0) 711 459 23512;

E-Mail address: daniel.heller@uni-hohenheim.de

ORCID: 0000-0001-7580-3025

Abstract

Process impairing foam formation occurs regularly in batch distillation devices of the spirit industry. It negatively influences process and product quality. Up to now, such foam-related problems have not been in the focus of scientific investigations. This study aimed at preventing impairing foam formations by adapting the thermal energy input in fruit and grain mash distillations in larger-scale batch distillations. The results showed that a reduction of the thermal energy input to $43 \pm 1 \text{ W} \cdot \text{L}^{-1}$ during the initial heating of the mash leads to less flooding of the distillation apparatus and to higher concentration of lower boiling compounds like methanol, acetaldehyde and ethyl acetate as well as ethanol in the first fractions of the distillates. A standard process time and less energy consumption could be achieved by increasing the energy input again after prior reduction. However, this led to a reduction of the ethanol concentration in the distillate fractions of up to 4.3 % vol, also most severe in the first fractions. A significant influence on analyzed volatile compounds in the distillate beside ethanol could not be detected. This is the first study that uses defined thermal energy input adaptations for foam management in larger-scale distillation devices. The results lead the way to a more efficient distillation process with less foam formation.

Keywords

Foam management; Distillation control; Spirit drink production; Process design; Energy efficiency

5.1. Introduction

In fermentation technology foam formations are generally considered as an undesired side effect [167,168]. Foam formation can lead to over foaming of fermentation vessels or disturbances during subsequent process steps of the fermented substrates [169]. With respect to distillation processes, the presence of excessive foams leads to carryover of foams onto separation trays, product contamination and increased cleaning demands. The effects are associated with reduced separation efficiency and process disruptions [46,47,49]. When it comes to column malfunctions in distillation industry, foaming plays a major role [48]. In spirit drink production, certain raw materials are referred to be especially prone to excessive foam formation, such as cherry, wine yeast, Bartlett pear and grain mashes [170]. Aside from this descriptive information on foam formation capacities of different mashes, Heller and Einfalt (2021) demonstrated in laboratory experiments that the polysaccharide pentosan found in rye has a major impact on foam formation in distillations of rye mashes. Additionally, it is well known that beside polysaccharides proteins play a crucial role in the physical stability of food foams [37–41]. However, in spirit drink production comprehensive researches on substrate-based factors influencing foam formations in distillations are still missing.

To reduce foam formation during distillation several measures have been applied. For instance, manufacturers introduced adaptations to their distillation devices such as increased pot still headspace volume and foam retention installations [170]. This, however, increases manufacturing costs. Such adaptations already have a long history. For example, the elongated swan necks in Scottish pot-stills in whisky distilleries were originally invented to prevent the transfer of rising foams into the product stream [49]. Unfortunately, larger distillation devices have a higher surface area, which is associated with higher process costs due to additional surface area heat radiation.

In addition to these aspects, operators of distillation plants take their own actions to prevent undesired foam formations. Chemical defoamers based on silicone or mineral oil, also called antifoam agents, are widely used for this purpose [47]. The negative aspect of defoamers is their disposal with the stillage without special treatment. They end up in the environment, where they can cause undesired ecological effects [58].

Detailed information on process-related solutions for proper foam management in distillation are scarce and for the most part based on heuristic recommendations. Heller and Einfalt [171] showed that 90% of foam formation took place at mash temperatures ≥ 89.5 °C. Pieper et al. [15] recommended ‘reduced thermal energy input’ in order to diminish excessive foam formation. They found it beneficial to ‘slow down the heating process in the foam-critical temperature range’. However, no additional information is given to define the thermal energy input magnitude or foam critical temperature range. Therefore, handling of foams is still dependent on operator experience. Extensive research is required to support new and experienced distillation plant operators in handling foam formations and in assessing the impact of anti-foam measures on their distillate.

Therefore, it would be desirable to define parameters that enable a foam-resilient distillation process with low additional costs for manufacturers and operators. To close this knowledge gap, this study investigated the effects of different heating profiles on foam formation in larger-scale distillation processes based on fruit and grain mashes. The study also evaluated effects on process time, energy consumption and volatile compound composition in the resulting product.

5.2. Materials and methods

5.2.1. Distillation system

A steam heated 120 L batch copper distillation device equipped with a rectification column (Carl GmbH, Eislingen, Germany) on top was used for the distillation experiments (*Figure 25*). The attached rectification column was equipped with three sieve trays, a partial condenser at the top, and a foam retention installation at the bottom. The distillation device also contained four foam-detecting sensors (cleverlevel, Baumer GmbH, Frauenfeld, Switzerland) installed in the reboiler at different heights positioned, 5 cm, 10 cm, 15 cm and 20 cm above the mash surface. Excessive foam formation, which reached the foam retention installation or the trays was logged manually. The distillation device was additionally equipped with eight temperature sensors (PT100) positioned in the reboiler, at different heights of the rectification column, in the vapor line, and in the product condenser. Further technical sensors (Coriolis Micro Motion H Series, Emerson Electric Co., Ferguson, USA) measured product volume flow and reflux volume flow of the partial condenser. Cooling water flow in the product condenser and the partial condenser were measured via SM6120 flowmeters (lfm electronic GmbH, Essen, Germany).

The distillation device was regulated and monitored via an automated process control system (DPC500, Carl GmbH, Eislingen, Germany). It enabled the regulation and control of the thermal energy input via an electro-pneumatic steam valve (SP400, Spirax-Sarco Engineering plc, Cheltenham, UK). Besides thermal energy input, the process control system also regulated the cooling water volume flows. All technical sensors were monitored and data were recorded every 10 s via the process control system. The measured data were averaged over 60 s.

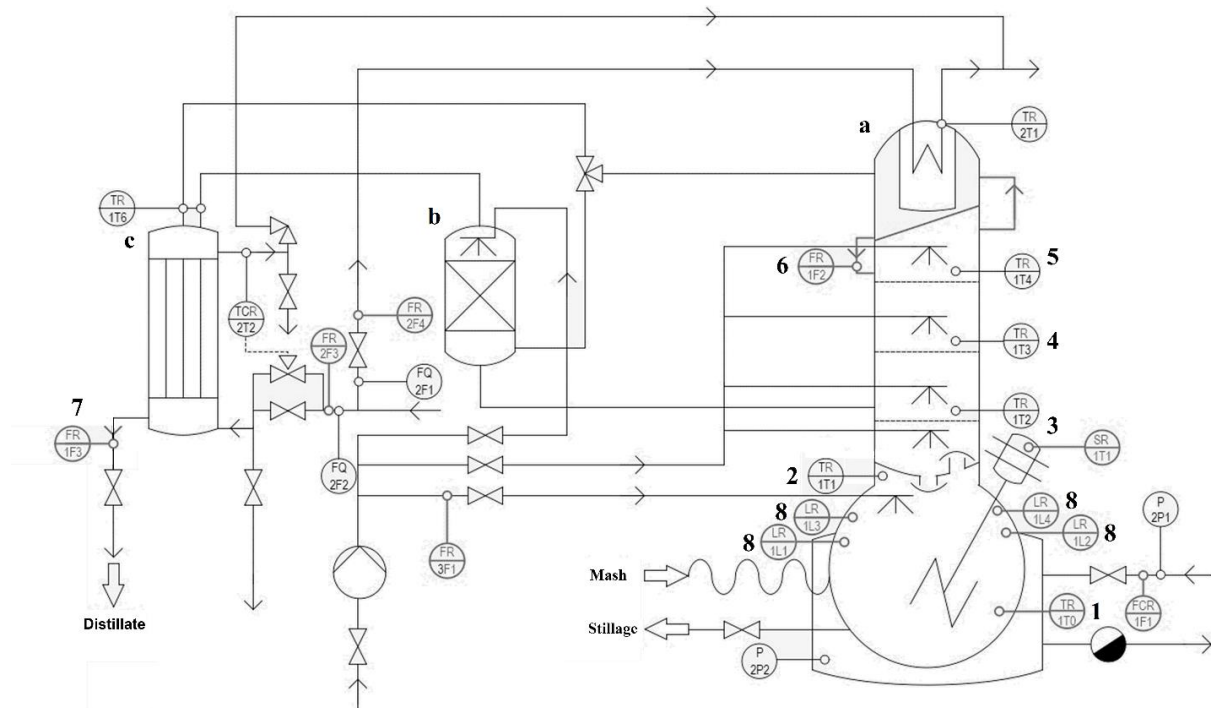


Figure 25. Instrumentation diagram of the batch distillation system equipped with rectification column (a), copper catalyser (b) and product condenser (c). 1: Temperature sensor ‘Mash’; 2: Temperature sensor ‘Headspace’; 3: Temperature sensor ‘Tray 1’; 4: Temperature sensor ‘Tray 2’; 5: Temperature sensor ‘Tray 3’; 6: Flow sensor ‘Reflux’; 7: Flow sensor ‘Product’; 8: Level sensors ‘Foam height’

5.2.2. Experimental setup

Two test series were performed in order to investigate the effects of modified heating profiles on foam formation (*Figure 26* and *Table 5*). The basis was a common heating profile (Dürr et al. 2010), which was modified at two points (adaptation points) in the test series and served as control.

The common heating profile started off with an initial thermal energy input of 450 W L^{-1} (\dot{Q}_1). At a defined mash temperature of $90 \text{ }^\circ\text{C}$ ($T_{\text{Mash}} = \text{first adaption point}$) the thermal energy input was reduced to 134 W L^{-1} (\dot{Q}_2). When the top/third tray of the rectification column reached a temperature of $75 \text{ }^\circ\text{C}$ ($T_{\text{Tray3}} = \text{second adaption point}$) a steady increase of thermal energy input ($\dot{Q}_3(t)$ and q , respectively) was applied. The thermal energy input was increased until the first product ran out of the distillation device. Subsequently, the distillation device automatically regulated the thermal energy input to maintain a constant product flow of 10 L/h . Cooling water flow of the partial condenser was kept constant at $2 \text{ L}\cdot\text{min}^{-1}$. The distillation process was terminated, as soon as the ethanol concentration of the product dropped below 25 \% vol .

The first test series employed reduced thermal energy input levels to inhibit foam formation. Thus, the control heating profile was modified at the first adaption point. In three experiments (HP1.1-HP1.3) the adaption point T_{Mash} was set to a mash temperature of $75 \text{ }^\circ\text{C}$ and the thermal energy input (\dot{Q}_2) was reduced to 95 , 59 and 43 W L^{-1} , respectively. In a subsequent experiment

(HP1.4) a reduced thermal energy input of 43 W L^{-1} (\dot{Q}_2) at the original T_{Mash} was applied. Because of customs restrictions concerning the duration of distillation runs, the increase in thermal energy input (q) were higher in HP1.3 and HP1.4.

The second test series aimed at counteracting process prolongations induced by the thermal energy reduction in the first test series. It was based on the most promising heating profile of the first test series and introduced changes at the second adaption point. When T_{Tray3} was reached the thermal energy input was raised by a certain amount ($\dot{Q}_3(0)$), then the thermal energy input (q) was increased over time as before. Distillation experiments in the second test series started with HP2.2. Subsequent distillation experiments were performed with HP2.1 or HP2.3 due to observed foam formation in HP2.2.

Distillation experiments of the first test series were performed with 100 L rye mashes in single determination. Distillation experiments of the second test series were performed with 100 L rye mashes and 100 L Bartlett pear mashes each in duplicates.

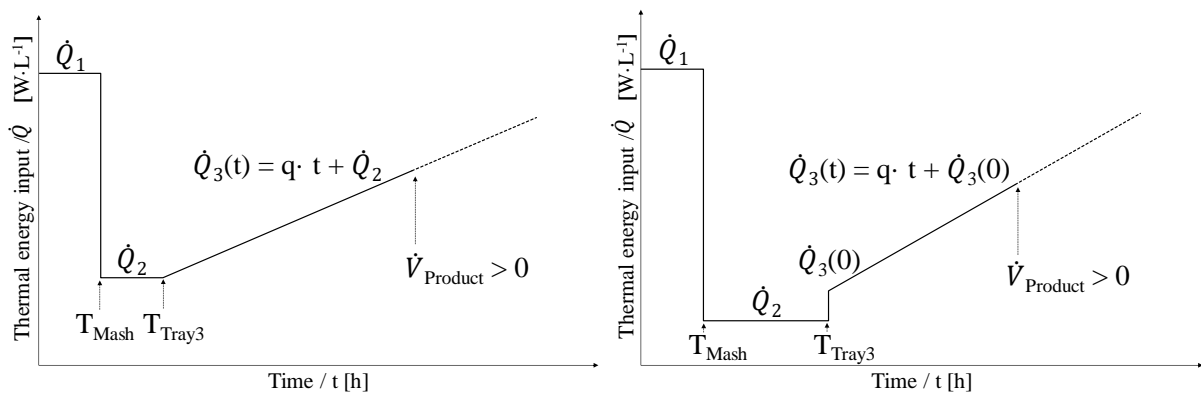


Figure 26. Heating profile of experiments in the first (left) and second (right) test series

Table 5. Process parameters for experiments in the test series

Test series Nr.	Heating profile	T _{Mash} [°C]	T _{Tray3} [°C]	\dot{Q}_1 [W·L ⁻¹]	\dot{Q}_2 [W·L ⁻¹]	$\dot{Q}_3(0)$ [W·L ⁻¹]	q [W·L ⁻¹ ·h ⁻¹]
1 & 2	Control	90	75	450 ± 1	134 ± 1	134 ± 1	46 ± 2
1	HP1.1	75	75	450 ± 1	95 ± 1	-	46 ± 2
1	HP1.2	75	75	450 ± 1	59 ± 1	-	46 ± 2
1	HP1.3	75	75	450 ± 1	43 ± 1	-	90 ± 2
1	HP1.4	90	75	450 ± 1	43 ± 1	-	90 ± 2
2	HP2.1	90	75	450 ± 1	43 ± 1	59 ± 1	80 ± 2
2	HP2.2	90	75	450 ± 1	43 ± 1	59 ± 1	121 ± 2
2	HP2.3	90	75	450 ± 1	43 ± 1	59 ± 1	161 ± 2

5.2.3. Sampling

The produced distillates were collected in 20 fractions for subsequent analysis. The first ten fractions contained 100 mL, while fractions 11 - 15 contained 200 mL and fractions 16 - 19 contained 1 L each. The final fraction contained the rest of the produced distillate. Distillations of Bartlett pears yielded less distillate. Bartlett pear distillates were therefore fractioned until fraction 18, while fraction 19 contained the rest of the produced distillate (< 1L).

5.2.4. Raw materials and mash preparation

Winter rye was purchased from Hahn-Mühle (Ostfildern, Germany) and Bartlett pears imported from South Tyrol were received from Kaiser Destillerie-Obstweinkellerei (Salach, Germany).

Bartlett pears were shred via fruit mill (Helmut Rink GmbH, Amtzell, Germany) and transferred to a 1000 L stainless steel tank. The pH value was adjusted to pH 3.0. The mash batch was simultaneously liquefied with 10 mL/hL pectin lyase (IUB 4.2.2.10, Schliessmann, Schwäbisch Hall, Germany) and fermented with 20 g/hL selected yeast strains (AROMA plus, Schliessmann, Schwäbisch Hall, Germany) over a period of three weeks.

Winter rye was mixed with water at a ratio of 1:4 (w/w), liquefied using 1.4 mL/hL of Distizym BA-TS (Erbslöh GmbH, Geisenheim, Germany) at 90 °C (30 min), and subsequently saccharified at 60 °C (30 min) with 5.4 mL/hL mL of Distizym AG-Alpha (Erbslöh GmbH, Geisenheim, Germany) and 2 g/hL of enzyme tegaclast (Tegaferm, Baumgarten, Austria).

Subsequently rye mash batches were cooled to ≤ 30 °C and pitched with 20 g/hL yeasts (Kornbrand-Premium, Schliessmann, Schwäbisch Hall, Germany). The mash batches were fermented for three to four days in 1000 L stainless steel tanks at pH 3.8.

In order to quantify only the effects of the changed heating profiles on the process and the distillate composition, it was necessary to exclude influences by differing mash characteristics. Therefore, each test series was performed with the same mash batch.

5.2.5. Substrate characteristics

In order to exclude temporal changes of substrate characteristics in mash batches between distillations, all drawn mashes were sampled before distillation and analyzed for specific substrate characteristics in triplicates. Samples were stored at -20 °C prior to analysis.

Substrate characteristics included quantification of ethanol concentration, performed according to Senn and Pieper [157]. Protein concentration was analyzed using the method by Bradford [112]. Total carbohydrates were quantified via phenol-sulfuric acid method [172]. pH and conductivity were measured via multimeter (HQ40D, Hach, Loveland, USA). Viscosity determination was performed after particle extraction (> 0.45 mm) with a rotary rheometer (MCR 92, Anton Paar, Ostfildern, Germany) equipped with a concentric cylinder system based on method DIN 53019 [173]. Viscosity determination was performed at shear rates from 0.1 to 1000 s^{-1} at 20 °C. In addition, dry matter (DM) and ash content of the mashes were determined according to Sluiter et al. [174].

5.2.6. Distillate product analysis

All distillate fractions were analyzed for ethanol concentration via standardized density determination by a u-tube oscillator (DMA 4100 M, Anton Paar GmbH, Ostfildern, Germany). Ten volatile compounds (*Table 6*) were analyzed using a GC-FID (GC-2010, Shimadzu, Kyōto, Japan) equipped with a headspace autosampler (HS20, Shimadzu, Kyōto, Japan) and a Rtx-Volatiles column (Restek Corp., Bellefonte, PA, USA). A five-point calibration of all analyzed substances was performed ($R^2 \geq 0.99$). All samples were water-diluted to 40 % vol ethanol prior to GC analysis.

Table 6. Analyzed volatile compounds in the fractionated distillates.

Nr.	Substance
1	Methanol
2	Acetaldehyde
3	1-Propanol
4	Ethyl acetate
5	3-Methyl-1-butanol
6	2-Methyl-1-butanol
7	1-Butanol
8	Acetaldehyde diethyl acetal
9	2-Methyl-1-propanol
10	1-Hexanol

5.2.7. Statistical analysis

Pearson correlation was applied to ascertain significant correlations of thermal energy input with volatile compounds concentrations of the distillates ($p \leq 0.05$). One-way analysis of variance (ANOVA) was performed to determine significant changes in substrate characteristics of mash batches between distillation experiments. All statistical analyses were performed using SPSS Statistics (V.25, IBM, Chicago, USA).

5.3. Results and discussion

5.3.1. Substrate characteristics

Analysis of mash samples taken prior to distillation showed no significant differences between mashes within a mash batch. This shows that the mashes were not significantly altered during storage between the distillation experiments. The determined substrate characteristics showed deviations of up to 6.25% (*Table 7*, viscosity curves not shown). We attribute these deviations to the non-homogeneous nature of the substrate, as well as to the limits of accuracy of the measurements. No alteration in ethanol content and viscosity indicated a completed liquefaction and fermentation of the mash batches prior to the distillations. Therefore, it can be assumed that differences in distillation occurred exclusively due to changes in the process conditions. The obtained results of the substrate measurements were in accordance with data from the literature [159,170].

Table 7. Mean values and standard deviations of substrate characteristics of each mash batch.

Properties	Unit	Rye (Batch 1) (n=5x3)	Rye (Batch 2) (n=6x3)	Bartlett pear (n=6x3)
pH	-	3.7 ± 0.1 ^a	3.5 ± 0.1 ^b	3.3 ± 0.0 ^c
Conductivity	mS·cm ⁻¹	2.0 ± 0.0 ^a	2.3 ± 0.1 ^b	2.5 ± 0.1 ^c
Ethanol concentration	% vol	6.1 ± 0.2 ^a	6.5 ± 0.2 ^a	4.2 ± 0.2 ^b
Total protein	g·L ⁻¹	0.44 ± 0.02 ^a	0.54 ± 0.01 ^b	0.6 ± 0.02 ^c
Total carbohydrates	g·L ⁻¹	18.1 ± 0.8 ^a	19.3 ± 0.2 ^b	16.4 ± 0.6 ^c
DM	%FM	6.7 ± 0.2 ^a	7.1 ± 0.1 ^b	5.6 ± 0.2 ^c
Ash	%DM	4.8 ± 0.3	4.8 ± 0.2	4.5 ± 0.1

FM = Fresh matter

Different lowercase letters within the same row indicate significant differences ($p \leq 0.05$)

5.3.2. Effects of different heating profiles (first test series)

5.3.2.1. Process and Foaming

Distillation with the control heating profile resulted in excessive foam formation > 20 cm and led to over foaming onto the first tray of the column (*Figure 27a*). Distillations performed with heating profiles HP1.1 and HP1.2 did not result in reduced foam formation (data not shown). Both experiments showed foam formation > 20 cm. Further, both heating profiles also led to excessive foam formation, which reached the first tray. In addition, both heating profiles resulted in increased process time compared to the control of 39% and 70%, respectively and in increased energy consumption of 6.8 - 10.9%. In HP1.3 a reduction of the thermal energy input (\dot{Q}_2) to $43 \pm 1 \text{ W}\cdot\text{L}^{-1}$ was applied. This resulted in reduced foam formation (*Figure 27b*), where the foam height fluctuated within 10 to 20 cm. However, this heating profile showed an 86% extension of the process time and resulted in an increased energy consumption of 14.6%.

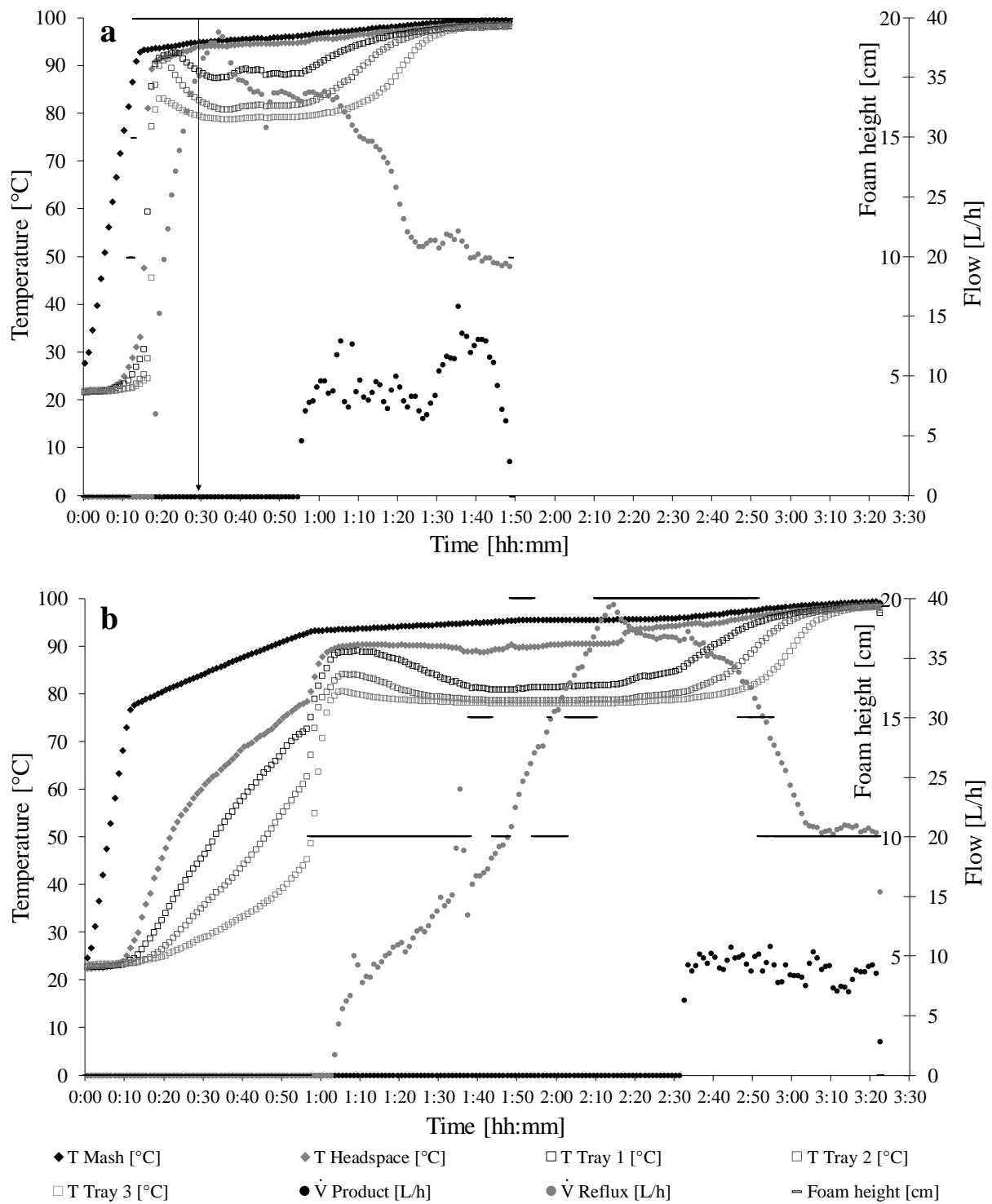


Figure 27. Distillation performance of control (a) and heating profile HP1.3 (b). Vertical, black arrow indicates excessive foam formation to reach the first trays

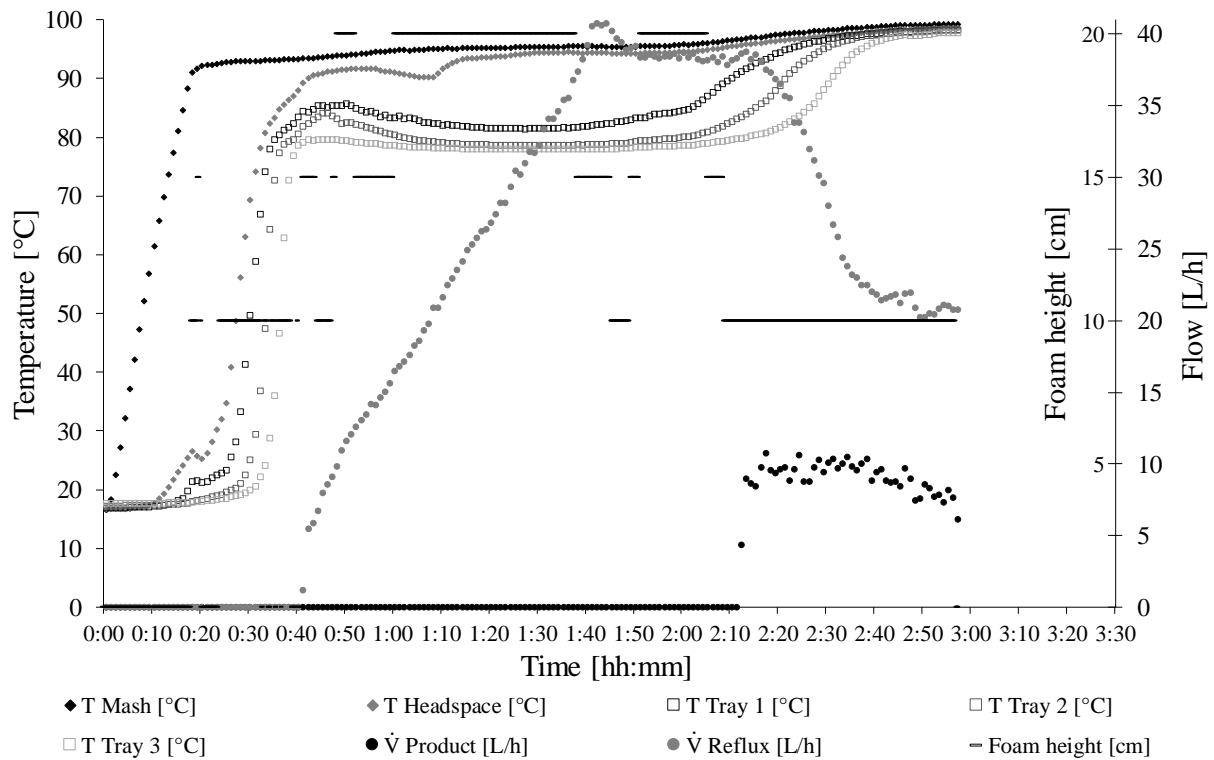


Figure 28. Distillation process with reduced thermal energy input at 90 °C mash temperature; HP1.4

To counteract the extension of the process time, the first adaption point T_{Mash} was shifted from 75 °C mash temperature to 90 °C in heating profile HP1.4 (Figure 28). This reduced the process time extension from 86% (HP1.3) to 63%, while maintaining a similar foaming behavior as in heating profile HP1.3. However, HP1.4 showed a higher energy consumption of 19.5% compared to the control. Excessive foam formation and over foaming onto the trays did not occur.

The experiments of the first test series demonstrated that foam formation can be controlled by reduced thermal energy input during the initial boiling of the mash in larger scale distillation devices. This result confirms the previously mentioned heuristic recommendation of Pieper et al. (1977) and the results obtained in laboratory scale experiments of Heller and Einfalt (2021). The heating profile HP1.4 showed the best results regarding foam formations. However, HP1.4 had the drawback of an increased process time (63%) and higher energy consumption (19.5%) compared to a common heating profile. Nevertheless, HP1.4 should be applied, if mashes with high foam formation potential are to be distilled. Otherwise, the usage of a common heating profile may result in over foaming of the mashes leading to a process stop, a time demanding cleaning of the distillation system and a restart of the process. This could cause an even longer process time and a higher energy demand compared to HP1.4.

5.3.2.2. Distillate composition

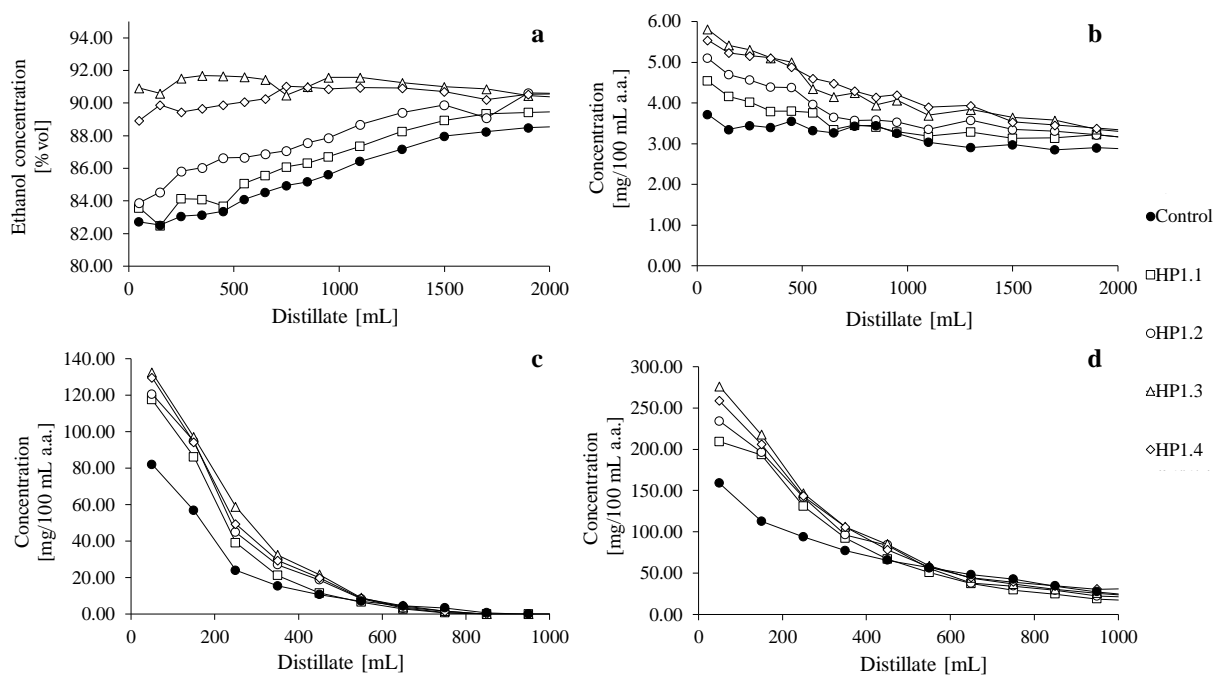


Figure 29. Concentration of Ethanol (a), Methanol (b), Acetaldehyde (c) and Ethyl acetate (d) in the first fractions with control and modified heating profiles with reduced thermal energy input (HP1.1, HP1.2, HP1.3, HP1.4)

A reduction of the thermal energy input (\dot{Q}_2) was negatively correlated with the ethanol, methanol, acetaldehyde and ethyl acetate concentrations in the first fractions of the distillates, i.e. the lower the thermal energy input, the higher the concentrations of the compounds in the first fractions (Figure 29). Significant correlations of thermal energy input and ethanol (fraction 1 - 13), methanol (fraction 1 - 14), acetaldehyde (fraction (1 - 5) and ethyl acetate (fraction 1 - 4) were found ($r = -1.000 - -0.951$; $p = 0.000 - 0.049$), respectively. The concentrations of methanol, acetaldehyde and ethyl acetate in the first fractions were 36.0%, 38.1% and 42.4% higher in HP1.3 compared to the control. The shift of the adaption point from 75 °C to 90 °C mash temperature (HP1.3 and HP1.4) resulted in a maximal difference of 11.3% for ethanol, methanol, acetaldehyde and ethyl acetate. The concentrations of all analyzed volatile compounds and their distilling behavior were in accordance with previous reports [175–178].

The reason for the increase of ethanol, methanol, acetaldehyde and ethyl acetate concentrations in the first fractions of the distillates in the distillation experiments with a reduced thermal energy input appears to be a higher internal reflux in the column. High internal reflux before and around the time when the first distillate fractions are collected allows for a higher enrichment of lower boiling compounds like methanol, acetaldehyde and ethyl acetate in the first fractions [36,88,179,180]. As shown in *Figure 27*, a decrease in thermal energy input increased the total volume of the reflux before the first distillate fraction were collected. The total reflux in the distillation experiment with HP1.3 was 33.8 L. The control distillation experiment showed a total reflux of 19.9 L. HP1.4 showed a total internal column reflux similar

to HP1.3 (37.8 L) (*Figure 28*). Because the internal reflux converges over time to a similar level of $20 \text{ L}\cdot\text{h}^{-1}$ in the different experiments, the volatile compounds no longer differed in their concentration after fraction 14.

In addition to the internal reflux, other factors, like the carryover of mash onto the first tray by excessive foaming in HP1.1 and HP1.2 could in part explain the observed differences. In essence, a separation step is lost due to carryover of liquid onto the first tray, which results in reduced rectification performance of the column [179].

All in all, the experiments show that a decrease of the thermal energy input in the heating phase of the mash affects only the composition of the first distillate fractions, the later fractions seem to be largely unaffected. Because the head fractions are normally discarded and not consumed, there is no drawback in using one of the modified heating profiles with respect to the final distillate composition. No significant changes in the concentrations of the other analyzed substances could be detected in the final distillate (not shown).

5.3.3. Effects of different heating profiles (second test series)

5.3.3.1. Process and Foaming

In the second test series we considered an increase in thermal energy input, when T_{Tray3} was reached, to counteract process prolongations induced by prior thermal energy reduction.

Rye mash distillations with the control heating profile resulted in foam formations $> 20 \text{ cm}$ (*Figure 30a*). In both distillations the excessive foam formations reached the first tray. In contrast to the first test series, the excessive foam formations now even reached the second tray. In the two duplicate experiments, the time when over foaming occurred differed by 1.5 min. Because of this temporal shift, only one profile is shown.

Distillations with HP2.2 (data not shown) reduced foam formation and showed no overflow onto the trays. Yet, HP2.2 showed foam formations $> 20 \text{ cm}$ and reached the foam retention device. To further reduce foam formation, subsequent distillations were performed with HP2.1. In distillations with HP2.1 foam formation was limited to the still pot and did not reach the foam retention device. Initially the foam height varied between 15 and 20 cm (*Figure 30b*). Both heating profiles (HP2.1 and HP2.2) showed a significantly reduced extension of the process time and energy consumption compared to HP1.4. HP2.1 extended the process duration by $5.9\% \pm 0.5\%$ and reduced the energy consumption by $1.9\% \pm 0.2\%$ compared to the control. HP2.2 showed no increase in the process duration ($< 1\%$) and reduced the energy consumption by $5.7\% \pm 0.1\%$.

Thus, the experiments show that the delay in process time introduced by a prolonged heating phase can be compensated by a higher thermal energy input in the later phase leading to a similar process time as in the control experiment.

The same experiments were performed with a different feedstock. Bartlett pear distillations with the control heating profile showed high initial foam formation of > 20 cm, which was limited to the still pot (*Figure 31a*). The initial foam collapsed and leveled off at 10 cm foam height. Distillations with the heating profile HP2.2 showed no foam formation throughout the process (data not shown). Distillation with HP2.3 showed foam formation of < 20 cm only in one of the duplicates (*Figure 31b*). The two heating profiles resulted in an extension of the process time of $23\% \pm 1\%$ (HP2.2) and $10\% \pm 1\%$ (HP2.3). However, HP2.2 and HP2.3 reduced the energy consumption by $5.5\% \pm 0.1\%$ and $12.1\% \pm 0.1\%$, respectively.

The results show that different mash types require specific heating profiles for inhibiting or reducing foam formation. Also, it became apparent that foam reduction is possible without excessive extension of process time as shown with HP2.3 in Bartlett pear and HP2.2 in rye mash distillations. Additionally, the altered heating profiles had the benefit of a lower energy consumption compared to the common heating profile. We therefore concluded, that the application of the altered heating profiles has no major drawbacks in terms of process efficiency, but also limit the risk of over foaming compared to a common heating profile.

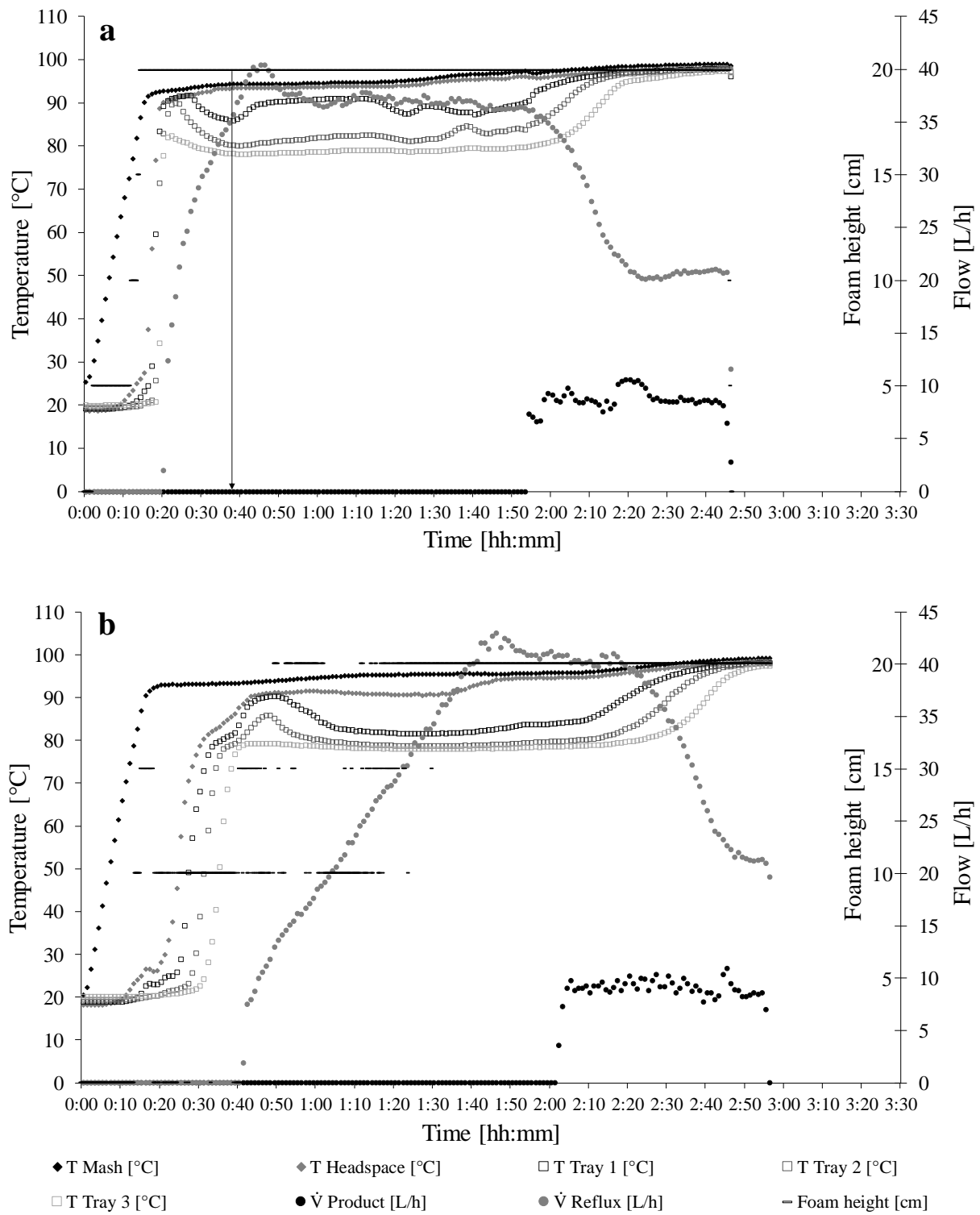


Figure 30. Distillation process of rye mash with control (a) and HP2.1 (b). Vertical, black arrow indicates overflow of foam onto trays

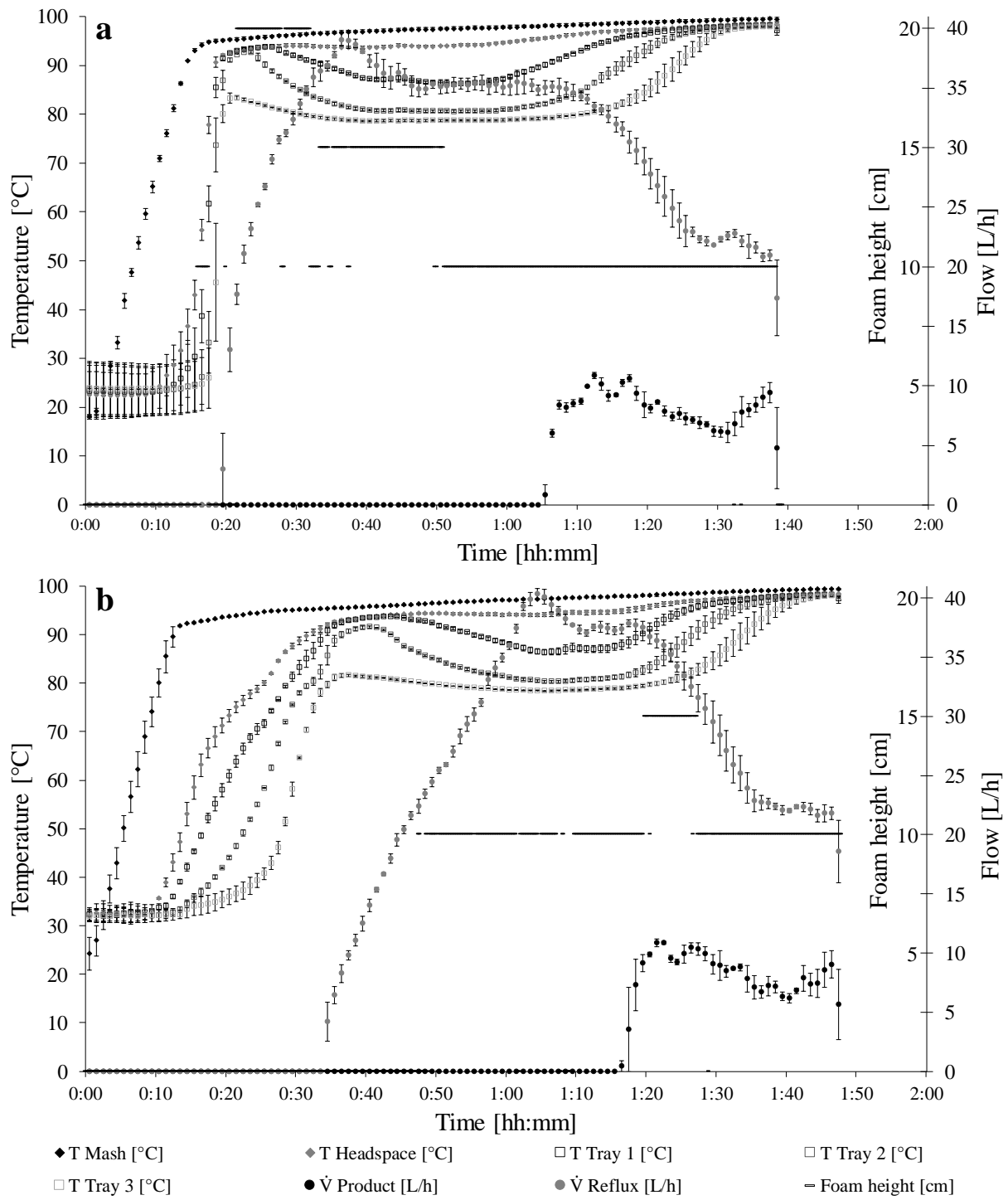


Figure 31. Distillation process of Bartlett pear mash with control (a) and HP2.3 (b)

5.3.3.2. Distillate composition

Statistical analysis of the data revealed a significant negative correlation of the ethanol concentration with a higher thermal energy input after the second adaption point in rye mash as well as in Bartlett pear distillation (Figure 32). In distillations performed with rye mashes significant correlations were found up to fraction 6 ($r = -0.940 - -0.848$; $p = 0.005 - 0.033$). In distillations with Bartlett pear mash a higher thermal energy input after the second adaption point was significant negatively correlated with the ethanol concentration up to fraction 16 ($r = -0.967 - -0.844$; $p = 0.002 - 0.035$). The highest ethanol concentration reduction of 4.3 %vol was found in the second distillate fraction of Bartlett pear distillation with HP2.3. The reduction of ethanol concentration in the drinkable fractions was 1.5 %vol - 3.15 %vol. No significant correlations with other analyzed volatile compounds' concentrations were found.

As previously we attributed differences of the ethanol concentration by different heating profiles to the internal column reflux and excessive foam formation, which reached onto trays. In distillation experiments with rye mashes the control had the highest total reflux of 55.3 ± 2.3 L before the first fractions. HP2.2 had the lowest total reflux of 36.0 ± 1.3 L. We assume that the ethanol concentration in the control distillation would have been even higher, if not for foam formations, which reached onto the trays. This probably counteracted the effects of the higher internal reflux. In distillation with Bartlett pear the control showed a total reflux 25.0 ± 1.2 L before the first fraction. In the same time HP2.3 showed a total internal column reflux of 20.8 ± 0.9 L. Therefore, these results were also in consistence with the results of the previous experiments.

In terms of distillate composition and ethanol recovery the altered heating profiles have the drawback of a reduced ethanol recovery compared to a common heating profile. However, the reduction in ethanol concentration was most severe in the first fraction of the distillates, which are normally discarded as heads. Considering the previous stated benefits of the altered heating profiles in terms of process and foaming the slight reduction in ethanol recovery is economically bearable.

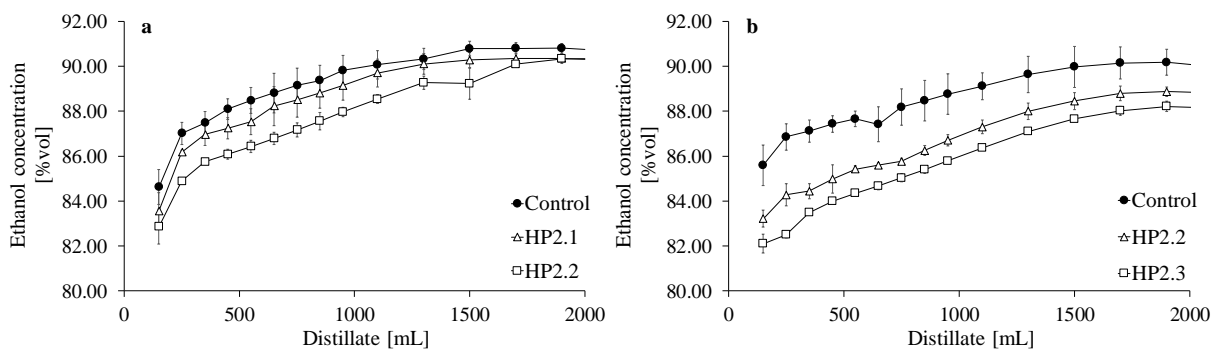


Figure 32. Ethanol recovery of rye mash (a) and Bartlett pear mash (b) distillation with heating profiles control, HP2.2 and HP2.1 or HP2.3.

5.4. Conclusion

Here, we demonstrate that foaming of fruit or grain mashes during distillation can be reduced or even prevented by reducing the thermal energy input in the initial heating phase of the mash. The altered heating profiles affected only the composition of the first fractions of the distillate. Since these fractions are discarded as a head cut, significant effects on the drinkable middle run are not expected. A major drawback of our regimen was the extension of the process time. But we could show that this can be compensated by a higher thermal energy input in the later phase of distillation leading to process times similar to the control experiments. Additionally, by using altered heating profiles the energy consumption of the distillation process could be reduced by up to 12.1%. The changes in the concentration of ethanol and the volatile compounds could be attributed to differences in the internal column reflux. Thus, a dynamic control of the partial condenser's cooling capacity should be considered to manipulate the ethanol and by-product concentrations in a desired way.

If problems with foaming occur in mashes during distillation, we recommend reducing the thermal energy input to $43 \pm 1 \text{ W}\cdot\text{L}^{-1}$, when the mash temperature reaches $90 \text{ }^\circ\text{C}$. After initial boiling, the thermal energy input can be raised to $59 \pm 1 \text{ W}\cdot\text{L}^{-1}$ with a steady increase over time with 80 ± 2 to $161 \pm 2 \text{ W}\cdot\text{L}^{-1}\cdot\text{h}^{-1}$ depending on the used feedstock.

Declarations

Declarations of interest The authors declare they have no financial interests.

Funding This IGF Project of the FEI is/was supported via AiF within the programme for promoting the Industrial Collective Research (IGF) of the German Ministry of Economic Affairs and Energy (BMWi), based on a resolution of the German Parliament. [AiF 4 PN]

Data Availability The data that support the findings of this study are available from the corresponding author, Daniel Heller, upon reasonable request.

Code Availability Not applicable

6. Resonant Ultrasonic Defoaming in aqueous evaporation / boiling processes at different size scales

Julian Thünnesen^{1*}, Christoph Gerstenberg², Daniel Heller³, Hannes Leuner⁴, Dr. Daniel Einfalt³, Dr.-Ing. Christopher McHardy², Prof. Dr.-Ing. Bernhard Gattermig^{1,5,6}, Prof. Dr.-Ing. habil. Cornelia Rauh², Prof. Dr.-Ing. habil. Jens-Uwe Repke⁴, Prof. Dr.-Ing. habil. Antonio Delgado^{1,6}

¹Institute of Fluid Mechanics, Friedrich-Alexander-Universität Erlangen-Nürnberg, Erlangen, Cauerstraße 4, D-91058 Erlangen Germany

²Department of Food Biotechnology and Food Process Engineering, Technische Universität Berlin, Königin-Luise-Str. 22, D-14195 Berlin, Germany

³Institute of Food Science and Biotechnology, Yeast Genetics and Fermentation Technology, University of Hohenheim, Garbenstraße 23, D-70599 Stuttgart, Germany

⁴Department of Process Dynamics and Operation, Technische Universität Berlin, Straße des 17. Juni 135, D-10623 Berlin, Germany

⁵University of Applied Sciences Weihenstephan-Triesdorf, Weidenbach, Am Hofgarten 4 D-85354 Freising, Germany

⁶LSTME, German Engineering Research and Development Center Busan, 46742 Busan, Republic of Korea

*Email corresponding author: J. Thünnesen < julian.thuennesen@fau.de >

Abstract

Unwanted foam bears the risk of affecting different thermal industrial processes negatively, by reduced process efficiency, contamination and total shut down. Mechanical defoaming methods are difficult to implement, while chemical anti-foaming agents are challenging in correct dosing. Ultrasonic defoaming actuators destroy foams purely mechanically from airborne, but their energy consumption per area is still excessive at 10 W cm^{-2} . Results show that a frequency sweep between 40-168 kHz and a water-borne sonication needs power densities of around 0.1 W cm^{-2} for lab-scale experiment to a copper column still. At this power level, ultrasound enforces the foam drainage and thus reducing the foam height and the process time of the column still by 20 %. The chosen frequency range indicates a resonant behavior of small liquid loaded lamella and Plateau-channels.

Keywords

column still, defoaming, resonance frequency, thermal processes, ultrasound

6.1. Introduction

Unwanted foam formation can affect various industrial processes and equipment negatively. Often a reduction in throughput, malfunctions in the production process, and even a total shut down of the production are the results of foaming [181], which lowers the efficiency of the production process and increases operational costs [171,182–185].

Foam formation requires the occurrence of surface-active components together with a penetration of gas through liquid either by injection or due to evaporation [185]. Especially distillation processes are reportedly affected by foam formation in processes of the chemical and food industry and require further investigations and development of foam management solutions [171,181,186].

In the past, various foam management solutions were developed to overcome the issue of unwanted foam generation in industrial plants in order to prevent the increasing operational costs [181]. The most sustainable long-term solution is a change of the equipment design to prevent foam formation. But is also the most difficult and extensive one to implement. The most popular solution is the use of anti-foam agents as they can be applied to a wide range of different processes and are typically very effective [181]. Here, anti-foaming agents are either continuously added to the product to inhibit foam formation or discontinuous added when foam formation is detected. The use of anti-foam may cause an undesirable contamination of the processes, which can lead to performance losses, lower product quality, and are therefore not allowed in numerous food processes [171,187].

Alternative mechanical defoaming solutions have been proposed such as centrifugal anti-foam pumps, rotary sieves [60,188–190], defoaming by sheeting the foam onto a spinning curved disk [191], defoaming with a water distribution system [192] and defoaming tanks [193]. Another mechanical way of defoaming is the use of ultrasonic devices. Several studies carried out with air-borne ultrasound device at frequencies between 10-40 kHz in the last century [145,167,194,195]. Significant defoaming occurred at acoustical intensity levels from 145-148 dB [194]. However, these intensity levels require ultrasonic transducers with large displacements of around 123 μm and diameters of around 300 mm [145,196–198] and cause aerosols by creating atomization and violent cavitation [199]. The mechanisms of ultrasonic defoaming are still unclear, although theoretical explanations are done by several authors [190,195,200]. One hypothetical mechanism is the introduction of vibration by using resonant behaviors of foam. Here, induced surface waves along the lamella might enhance the drainage and then a lamella rupture [195]. However, the link between resonant element and applied frequency is still not clear, because of the complex structure of the foam. Free bubbles in liquid usually undergo resonance at ultrasonic frequencies and convert acoustical energy into motion [201–203]. Especially larger bubbles become resonant at ultrasonic frequencies as the void

fraction in the liquid increases [204]. More recent publications in ultrasonic foam measurements showed a resonant behavior at frequencies above 80 kHz, which seems to be linked to the lamella and channel vibration modes [205,206].

This work follows this model and applies higher amplitudes to enhance the foam drainage by these resonant vibrations, while avoiding excessive amplitudes creating aerosols like air-borne actuators. The applied frequency-sweep between 40-168 kHz is above the previously studied frequency range. Furthermore, the approach to insonify the foam from the liquid bulk to resonate the liquid loaded foam structure of thermally induced foams is not yet to the authors' knowledge investigated.

6.2. Material and Methods

6.2.1. Fluids

Unhopped beer wort, fermented rye mash and SAS 93/H₂O (0.13 %mas) were used for the studies, and their density, viscosity and surface tension were measured beforehand and are displayed in *Table 8*. Beer wort was prepared by mixing malt concentrate (Pilsener Malz, Weyermann GmbH, Bamberg, Germany) and distilled water in a mass ratio of 10:6. Rye mash was obtained from the Institute of Food Science and Biotechnology, Yeast Genetics and Fermentation Technology, University of Hohenheim, Stuttgart, Germany. The recipe is published in Heller and Einfalt [171]. For better foamability, the addition of pentosan-degradable enzymes was avoided. A reference mixture of SAS 93 (WeylClean®, WeylChem International GmbH, Wiesbaden/Germany) was mixed with water in a mass ratio of 4:3000.

The dynamic viscosity, density and surface tension was measured at 60 °C in triplicate using the same methods and devices done in Morelle et al. [207].

Table 8. Density, viscosity, and surface tension given for beer wort, rye mash, SAS-solution (0.1 %). Rye mash displays shear thinning rheological properties, thus the viscosity value for rye mash is given at the maximum shear rate. * Measurements at 20 °C, ** Reference values of water have been used.

	Density [g cm ⁻³]	Viscosity [mPa s]	Surface tension [mN m ⁻¹]
beer wort	1.0208 ± 3.23*10 ⁻⁴	0.074221 ± 2.05*10 ⁻³	26.279 ± 0.175
SAS-solution	0,9989* ± 4.2*10 ⁻⁴	1.0**	30,945* ± 0,983
rye mash	0.989 ± 1.92*10 ⁻⁴	18.333333 ± 1.37	37.416 ± 0.801

6.2.2. Ultrasound frequency

For energy-efficient foam destruction, the applied ultrasonic frequency ought to match the resonant frequency of the foam structure. Due to the low natural frequencies of the bubbles of a few Hertz, the ultrasonic waves rather excite the lamella and Plateau channels. A frequency equation presented by Pierre et al. [205], which assumes similar resonance was used to calculate the frequency range of the transducers:

$$\omega_0^2 = \frac{12N\sigma(1-\phi)}{x^2\rho\bar{R}^3} \quad (7)$$

Herein, N is the number of adjacent films per bubble, σ the surface tension, ϕ is the liquid content in the foam, x is the area ratio of the linear-parallel part to the total area of a lamella, and \bar{R} is the arithmetic mean bubble radius. In the calculations $R = 0.5$ mm, $N = 13.7$ [208,209], $\sigma = 35$ mNm⁻¹ and ρ for water 998 kgm⁻³ were assumed.

The assumed range of the liquid content of spherical and polyhedral foams was between $0.26 > \phi > 0.1$. The area ratio x was calculated from Princen's [210] empirical formula:

$$x(\phi) = 1 - \frac{3.2}{\sqrt{7.7 + \frac{1-\phi}{\phi}}} \quad (8)$$

The calculations suggested a use of frequencies between 28 kHz and 106 kHz for foams between $0.26 > \phi > 0.1$ (see *Table 9*). Foams usually have a statistically vertical gradient of liquid content, which is decreases from bottom to top. Therefore, a waterborne sonication is reasonable approach where the water content of the foam is highest and the bubble diameter is smallest.

Table 9. Calculated resonant frequency of aqueous foams with a mean bubble radius of 1 mm for liquid fractions between those of spherical and polyhedral bubbles

ϕ [-]	0.05	0.1	0.15	0.2	0.25	0.26
f_R [kHz]	10.56	12.76	17.61	28.62	73.53	106.45

6.2.3. Ultrasound systems

For the demanded frequencies, several 40 kHz Langevin transducers (Hesentec, Rank E) and their harmonics up to 168 kHz were in use. Comparative measurements of the electrical impedance analyzer and hydrophone measurements showed the highest amplitudes at about 40, 42, 57, 85, 101 and 168 kHz (see *Figure 33*). A linear frequency sweep with a period of 500 ms was performed over the frequency range 40-168 kHz to hit broad spectrum of resonant lamellae in polydisperse foams. A frequency generator produced a sinusoidal excitation signal and the sweep, which was amplified by a 51 dBV voltage amplifier. A parasitic electrical series resistor compensated for the lack of electrical matching between the amplifier and transducer. Further information about the ultrasound system used are explained in Thünnesen et al. [211].

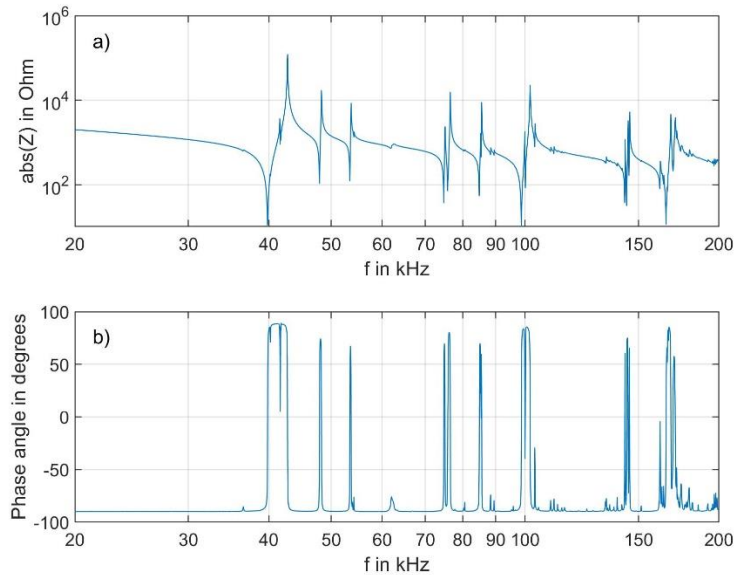


Figure 33. Measured electrical impedance Z (a) and phase angle (b) in frequency range between 20 kHz and 200 kHz. Local minima and maxima in a) indicate the transducers mechanical resonance and antiresonance, respectively

A firm clamping behind the transducer and ultrasonic coupling gel ensured the transmission of the vibrations over the wall into the beaker and into the distillation column, respectively. In the Lab-scale experiment, the transducers were tightened and bonded via a thread.

6.2.4. Mini-scale setup

In this setup, 200 ml beer wort boiled in a 400 ml beaker (VWR International GmbH, Darmstadt, Germany) with a diameter of 80 mm on a lab heating plate and ultrasonic actuator was positioned at a height of 60 mm which was at the same level of the liquid (see *Figure 34*). The beaker was covered to enhance the thermal foamability of the wort and to create a more stable foam height.

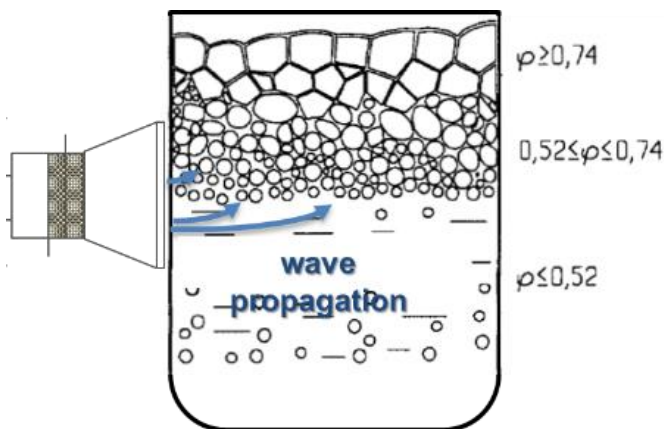


Figure 34. Schematic setup of beaker test showing wave propagation through liquid bulk

6.2.5. Lab-scale setup

This experimental setup consisted of a 100x100 mm rectangular glass vessel with a height of 200 mm (see *Figure 35*). In the aluminum bottom, 4x100 W heating elements with thermocouples were embedded. One side was made of stainless steel, to which the transducer was attached at a height of 100 mm. For the experiments, 1.25 l of the respective liquid was boiled, which placed the transducer below the liquid level. Thermal sensors in the liquid, the headspace and on the heating elements recorded the temperatures.



Figure 35. Lab-scale setup with ultrasound actuator clamped on metal wall

For each specific heat input, a reference foam height without ultrasound, and the foam height after each 4 min US sweep at different powers are noted. The power levels were chosen equidistantly between 0 and 40 W, in which the ultrasound-induced pressure amplitude did not fall below the gas saturation pressure or vapor pressure of the liquid to provoke an opposite foam formation due to the ultrasound. The heating power levels started at the minimum power for foaming and increased by 50 W L⁻¹ each time.

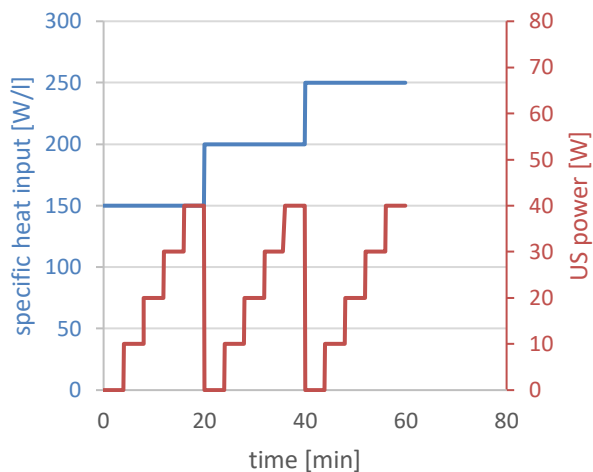


Figure 36. Schematic sequence of the test series by alternating heat input and ultrasound powers. Referencing foam heights and foam heights during sonication were measured within each heating step

6.2.6. Column still

The used copper column still (Carl GmbH, Eislingen, Germany) consisted of a 120 L still, 3 trays and a foam retention unit in between. The retention unit is a bottom with two outlets, which prevents the trays from partially flooding by horizontally distributing the foam over the cross-sectional area and by redirecting the foam back into the still. As the foam overflows the retention unit, the distilling process is negatively affected, thus the ultrasound actuators are clamped directly next to the retention unit in order to destroy any foam reaching this height (see *Figure 37*).

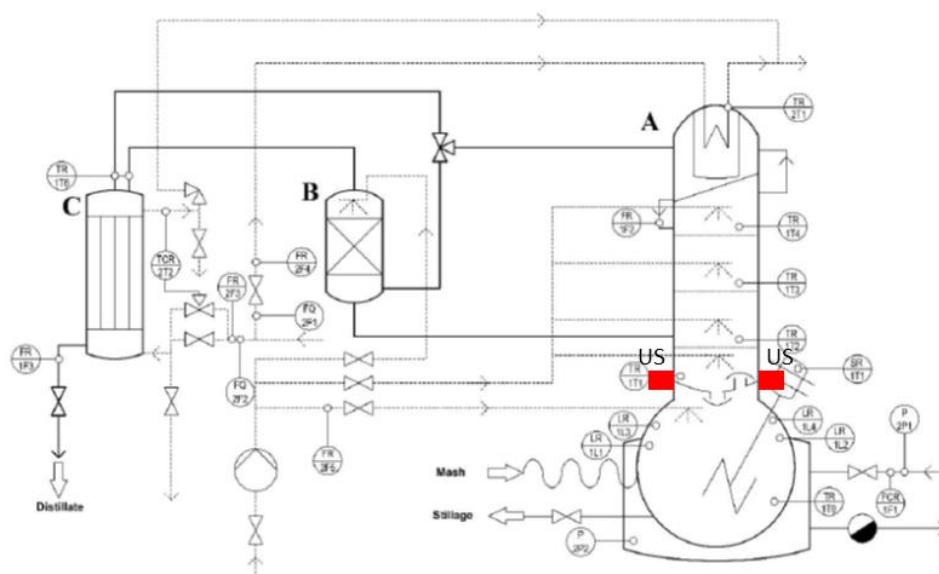


Figure 37. Sketch of the batch copper still with sieve tray column and dephlegmator (A), copper catalyst (B) and product cooler (C), ultrasonic actuators (US) and all installed sensors

A standard heating profile for distillation was used to create critical foam formation inside the column still, including three chronological periods with each different set specific heat inputs \dot{Q}_1 , \dot{Q}_2 , \dot{Q}_3 [52]. In the first heating period, a constant specific heat input of $\dot{Q}_1 = 450 \pm 1 \text{ W L}^{-1}$ raised the mash temperature to $T_{\text{mash}} = 90 \text{ }^\circ\text{C}$, where most foaming occurs [15]. After reaching this temperature, the specific heat input was decreased to $\dot{Q}_2 = 134 \pm 1 \text{ W L}^{-1}$, until the temperature of third tray were constant at $75 \text{ }^\circ\text{C}$ for 5 min. In the final period, the specific heat input is set to $\dot{Q}_3 = q * t + \dot{Q}_2$ with a heating rate of $q = 46 \pm 2 \text{ W L}^{-1}\text{h}^{-1}$ until the flow of distilled ethanol kept constant of 10 L h^{-1} .

6.2.7. Determination of foam height and lamella length

The foam heights were measured optically in the lab-scale setup via a measuring scale on the glass wall. The reading accuracy was $\pm 2 \text{ mm}$. The foam height was averaged over three measuring points equidistant to each other (25 mm) on the opposite glass wall of the actuator. For the beaker, serial images were taken with a camera (acA2500-60 uc, Basler GmbH, Ahrensburg, Germany) with a frame size of 1080x1920 px and a frame rate of 30 fps and measured by hand on screen. The conversion coefficient in the image was $K = 0.302 \text{ mm px}^{-1}$. With an uncertainty of $\pm 2 \text{ px}$ for distinguishing objects on an image, the uncertainty of foam height was 0.604 mm. The measurement of the lamella length also carried out by hand with the same uncertainties.

6.3. Results

6.3.1. Defoaming beer wort in beaker tests

In the beaker tests, constant foam formation occurred at a temperature in the liquid of $\vartheta_l = 99.9 \pm 0.1 \text{ }^\circ\text{C}$ and in the air at $\vartheta_g = 99.3 \pm 0.2 \text{ }^\circ\text{C}$. The water-borne ultrasound reduced this foam almost completely within 4 s during continuous boiling, as the liquid flowed out of the foam and the top bubbles shrank without bursting (see *Figure 38* and supplemental movie data). It suggests that the fluid surrounding the bubbles drains completely out of the foam and the steam filled bubbles condensate into the liquid. Furthermore, the effect was reversible, as the foam rose to its original height between 33-37 mm immediately after the ultrasound was switched off. Random cooling of the air, which could lead to condensation of the vapor in the foam and thus to foam decay, could not be detected outside the measurement tolerances mentioned above. Since this effect occurred uniformly over the entire diameter of the cup, it indicates that the waves have reached the entire base area of the foam via the liquid. Moreover, the subsequent foam appearing during sonication had a purely polyhedral structure, with the arithmetic median length of the wall bounded Plateau borders increasing from the original 1.59 to 3.9 mm. The applied electrical power was limited in a range between 5 and 15 W. If the power was too low, the foam decay was equal to the foam formation during boiling, which lead to a constant foam height of around 10 mm. Above a power level of 15 W, additionally

provoked foaming at the beginning of sonication disturbed the defoaming, since the acoustical pressure amplitude fell under the vapor pressure inside the liquid. However, sonication from the air with the same actuator could not produce any effect, despite a power level of 40 W.

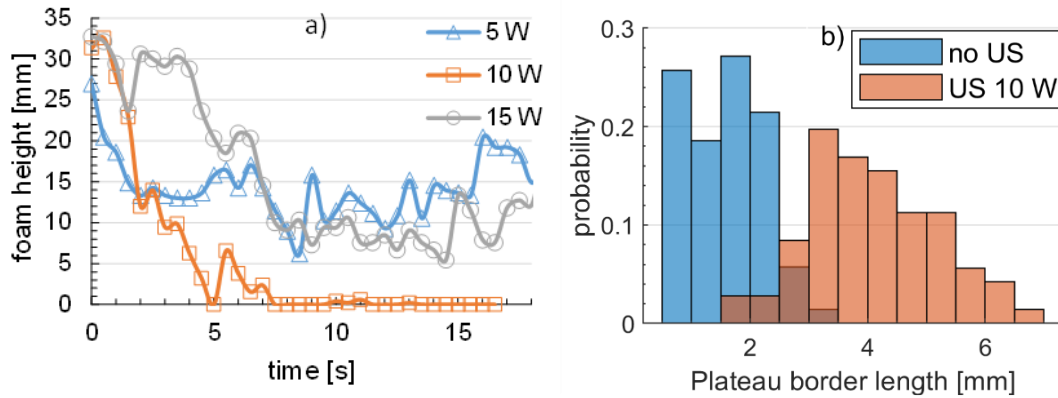


Figure 38. Temporal foam decay of boiling wort in waterborne ultrasound with a frequency sweep 40-168 kHz, at modified power a); and lengths of wall bounded Plateau borders before and 6 s after the start of sonication at 10 W, $n=50$ lamella.

6.3.2. Defoaming at different specific heat input and foam heights at lab-scale

6.3.2.1. Stages of foam formation

In the experiments, an increase in the specific heat input led to an increase in the foam height due to a higher vaporization rate. *Figure 39* shows the mean equilibrium foam height after 4 min at different specific heat input levels. First foam appeared with rye mash at 150 W L^{-1} . With beer wort and SAS, foaming just happened at input levels higher than 200 W L^{-1} . A lid on the setup maintained a steam atmosphere above the foam with a constant temperature. For beer wort and SAS, the temperatures were close to the boiling temperatures of water at $\vartheta_l=99.8 \text{ }^\circ\text{C}$ and $\vartheta_g=99.3 \pm 0.2 \text{ }^\circ\text{C}$, and $\vartheta_l=91.5 \text{ }^\circ\text{C}$ for rye mash. For rye mash, the lower boiling temperature is due to alcohol content. Previous studies with comparable mash showed a critical range of foaming at these temperatures [171].

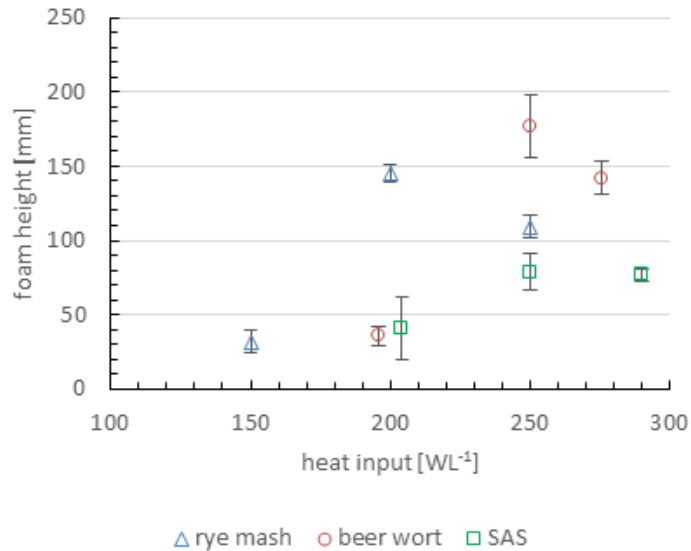


Figure 39. Mean equilibrium foam heights, averaged over 4 min without insonication at different heat inputs, $n = 3$

At the lowest specific heat input, the foam initially spread horizontally over the liquid surface. Only when applying the second largest specific heat input, the foam rose vertically, and the highest foam heights were reached. At the third heating level, foam heights slightly decreased again in the setup, caused by circulations inside the foam layers [141]. The lower circulations did not affect a stable upper layer in the SAS foam, so the height drop was not as large as with beer wort and rye mash. In addition, a temperature $\vartheta_l = 98.0 \text{ }^\circ\text{C}$ was measured for the rye mash, which was at the upper limit of the critical temperature range for foam formation, where the foamability decreases again [171].

6.3.2.2. Influence of ultrasound power

At large foam heights during the lab-scale measurements, the foam layer separated into a coarse-pored, foam at the bottom and finer-pored foam at the top. The characteristic of the bottom foam layer is dynamic movement caused by steady upraising bubbles and film rupture. In contrast, the top layer remained stationary floating on the bottom foam layer. The bottom layer foam decayed faster with increasing actuator power, causing the upper foam to move downward without forced decay and the total foam layer to sink (see *Figure 40*).

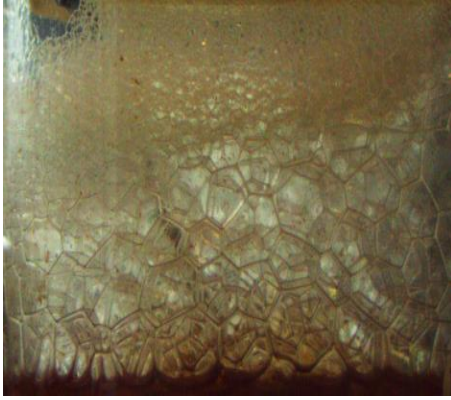


Figure 40. Separation of foam of beer wort in a fine-pored foam on the top and a coarse-pored foam layer at the bottom at incident heat input 250 WL^{-1}

Figure 41 shows that increasing the ultrasonic power led to a uniformly increasing reduction in foam height. The biggest effects of ultrasound were observed in both the beer wort (Figure 41, a) and the rye mash (Figure 41, b) at foam heights of 40 mm in each case, at which the non-sonicated foam layer was lowered by 80%.

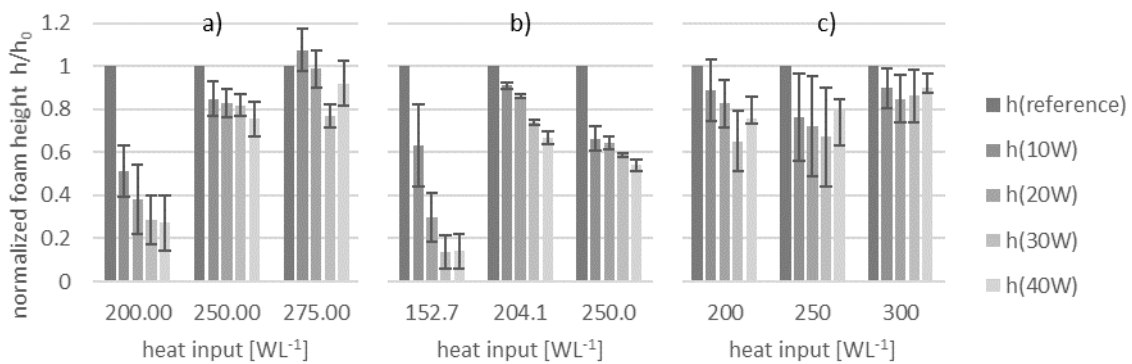


Figure 41. Mean equilibrium foam heights normalized to individual reference foam height for beer wort a), rye mash b) and SAS c)

The results suggest that the foam decay due to ultrasound induced drainage, is not dominant in the upper layer, because the high intrinsic absorptivity of the foam allows only a limited penetration depth of the ultrasound on the one hand, but also the drainage itself is more inhibited by the smaller bubbles and higher curvature of the plateau borders. In addition, as the liquid flows downward through the foam, surface-active agents, such as proteins, accumulate and stabilize the lamella [137,212]. As the lamella and channels shrink, capillary pressure increases and thus the potential of ultrasound induced drainage is reduced [213]. At the same time, the resonant frequency decreases with the liquid content under the applied ultrasound frequency into the audible frequency range. Under these conditions, only the films with a negligible amount of liquid still vibrate compared to the plateau channels with greatly reduced displacement [205].

6.3.3. Implementation to a column still

Figure 42 shows the temperature curves during a distilling process inside the mash, in the column head space and at the first and second tray. Without foaming only a vapor mixture of ethanol and water with boiling points at 78 °C and 100 °C reaches the trays. The foam carries an additional amount of water and with the higher boiling point of water, the mixture's temperature is raised. As the foam reaches the head space and is in contact with the temperature sensor, the headspace temperature suddenly raises and is close to the mash temperature (Figure 42b)). The foam carries more water into the column and thus temperature raises in the upper two trays with a small delay. The occurrence of foam was qualitatively confirmed by a inspection window. As the sonication started, it immediately suppresses the foaming, which can be seen in the drop of the temperature in the headspace. With a little time delay, the temperature of the first and second tray also dropped, because less water vapor is in contact with the temperature sensor and the ethanol content is increased instead. In the reference process without sonication the foam entered the first tray which resulted in constantly higher temperatures throughout the entire process compared to the defoamed process. With defoaming the process time could be reduced by 20 % in comparison to the reference process without defoaming.

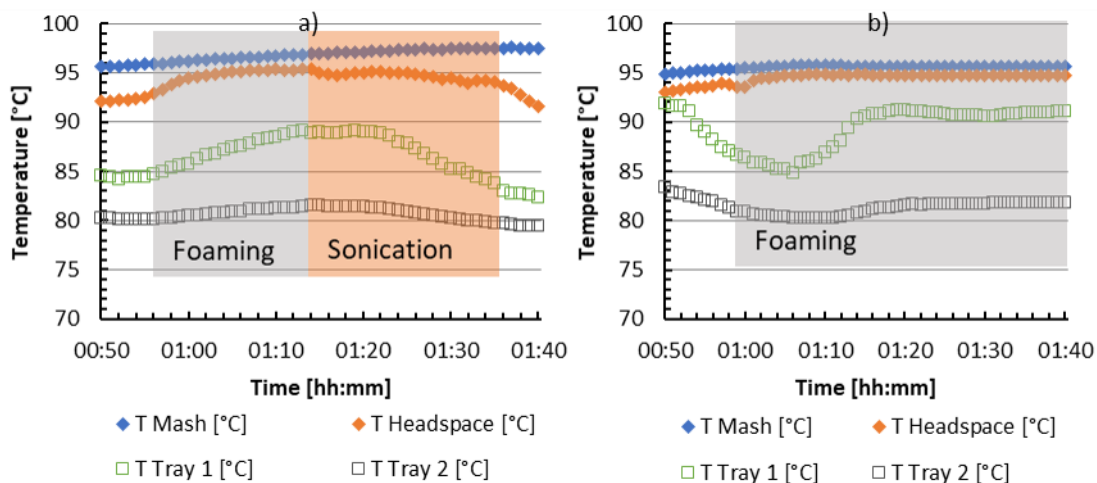


Figure 42. Comparison between process with ultrasonic foam suppression and a reference process without defoamers. A temperature difference $< 2^{\circ}\text{C}$ between temperature of headspace and of mash indicates flooding of the headspace with foam and reaching the sensors. Sonication suppresses the foam formation leading to a decrease of the temperature in the headspace and in the first and second tray again

6.3.4. Discussion of ultrasonic effects

In the beaker experiment, an immediate foam decay within seconds was only shown when ultrasound waves propagated through the liquid phase. This is partially due to the relatively small displacement amplitudes of the actuator used. The literature suggests pressure amplitudes of about 135 dB in air for similar foam destruction [198]. To achieve these values, 200 W actuators with diameters of 300 mm and max displacements of about 123 μm are required [145,195,197,198]. However, comparing to these actuators from literature, the water-borne insonication of an actuator with an electrical power of 10 W was sufficient to reduce the foam

height in a comparable amount of time in the beaker. One reason is the low transmittance of the actuator in air, which is subject to the high difference in the respective acoustic impedances of aluminum and air. If one assumes that the input power of the actuator equally distributes over the cross-sectional area of each setup, then the power density is of the same order of magnitude at different length scales (see *Table 10*).

Table 10. Summary of applied actuator power inputs and ratio of power to cross-section area

Setup	Cross-section [mm]	Applied actuator power [W]	Power density [W mm ⁻²]
Beaker	80	10	19,9*10 ⁻⁴
Lab-scale	100x100	10-40	10-40*10 ⁻⁴
Column still	300	60	8,49*10 ⁻⁴

However, the mechanism of foam destruction also seems to differ with the direction of incoming sound wave and at the frequencies being applied in the literature between 26- 40 kHz to the frequencies of 40-168 kHz being applied in this work. At higher frequencies, it is possible to match the resonant frequency of the foam linked to the film and Plateau channel vibrations and thus avoid the need of the actuator's high displacement amplitudes. These vibrations cause capillary waves, non-linear liquid flow towards the antinodes due to centrifugal forces, dimples and vortices [214–219]. Dimples usually move to the border by asymmetric tension gradients and carry fluid out of the lamella [220]. The antinodes are usually between the lamella center and rim which an opposite thickening, unless the Plateau borders move at frequencies $\leq f_R$ [205], thus enhancing the drainage and resulting in a less stable foam, on the one hand.

On the other hand, film thinning happens by the Marangoni effect of second order at the nodes if the diffusion time for re-adsorption $\tau_D = \frac{h^2}{D}$ lasts longer than the period time of applied frequencies of 5-23 μ s. If one assumes a diffusion coefficient $D = 14 \cdot 10^{10} \text{ m}^2\text{s}^{-1}$ for equivalent proteins and a diffusion height equal to a lamella thickness of 1 μ m, the re-adsorption is partially done during a period of the studied frequencies for the case of mash and beer wort [221,222]. The lamella elongation increases locally the surface tension and a lamella thinning, which promotes to go under the critical lamella thickness to rupture. To meet this condition, the largest capillary wave's length linked to the applied frequency must be at least equal the radius of the film assuming an axisymmetric vibration mode as in Gaulon et al. [215]. Calculated by the wave number of capillary waves on the film $k = \frac{f}{2\pi} \sqrt{\rho e / (2\sigma)}$ [205] with film thickness $e = 1 \mu\text{m}$ and earlier measured density and surface tension values, the wavelengths $\lambda = 1/k$ are with $< 1.3 \text{ mm}$ at the lower limit of the length distribution of Plateau borders measured during insonication (*Figure 38b*). The self-adaption of the lamella without an immobile rim might also result in a geometrical one during insonication.

Another difference is the direction of the incoming ultrasound. In air-borne sonication the foam volume decreases to a specific extent without decreasing the liquid hold-up [223]. The remaining foams become wetter and thus more resistant to further destruction due to an increased reflection coefficient of the lamella at liquid-air interface [200]. In contrast, the water-borne sonication enforces the drainage into the bulk liquid [224]. Liquid from the upper layers must replace the drained liquid in the lower part of the foam. The characteristics of the foam decay in the beaker (see support information) and high-speed pictures of resonant lamella [183] seem to agree with this hypothesis.

Additionally, the insonication of the liquid bulk might also alter the surfactants' concentration carried by rising bubbles into the foam. During bubble oscillation, the liquid-air interface compresses and expands at high rate. During the compression period, the surfactants and proteins desorb into the bulk liquid. At expansion, the absorption is limited by the diffusion time of the surfactant through the thickness of the laminar flow layer around the bubble. This leads to a reduced equilibrium surfactant concentration at the oscillating interfaces with increasing frequencies from around 40-1 MHz [225–227]. As a result, the coalescence of rising bubbles forced by Bjerknes-forces increases, while the feed of surfactants into the foam decreases. Thus, bigger bubbles raise and create a coarser and more unstable foam from the beginning [227].

However, we also showed that the range of this effect was limited because of a limited penetration depth into the foam layers. Most sound/foam interactions are thought to occur at the foam/liquid interface, as the attenuation within the foam is 10^7 to 10^{10} higher compared to the attenuation of water and air [197]. Especially sound attenuation is at its maximum at the resonance frequency [201,205,217]. An increase of the ultrasound power can compensate this effect to a limited extent, due to the high-pressure amplitudes of the sound waves which decrease the pressure below the vapor pressure and promote additional evaporation [228]. Thus, a trade-off between maximum foam/sound interactions and high attenuation versus low interaction and high penetration depth must be found. Moreover, the lab-scale measurements showed that already dried structures of the foam are more resistant to destruction. As the lamella thins to a certain thickness, the capillary pressure and Marangoni effect become dominant thus reduce drainage to a minimum and stabilized the lamella [60,213]. This means that in industrial processes a preventive use of the sonication is best suited to keep the foam height at minimum.

6.4. Conclusion

Ultrasonic waves with a frequency sweep of 40-168 kHz significantly lower the equilibrium heights of foams of boiling liquids such as beer wort and rye mash within time scales between seconds and a few minutes. The frequencies were tuned to the theoretically hypothesized resonant frequency of the foam, assuming that it is governed by the resonant behavior of the lamellar/channel structure and not the bubbles themselves. The coarsening of the foams and the decay characteristics suggest that the induced vibrations of the lamella and channels generate surface waves and squeeze out the fluid, enhancing the drainage of wet foams. The propagation

of sound waves through the liquid bulk increases the insonified surface of the foam, while the actuator itself may be attached to the sidewall of the system. However, the method is limited by the depth of sound penetration into the foam, making it dependent on the post-flow of the liquid and subsequent collapse. In the case of already high foam ceilings of >40 mm, the upper foam layer is relatively dry and inaccessible to sonication, making it necessary to use this method already at an early stage of foam formation. In the case of the surfactant foam with SAS, the final collapse failed to occur despite a forced drainage, which is in accordance to literature [224]. For a distillation process of rye mash in a column still, the sonication reduced the foam as soon as it was active and achieved a time saving of 20 %.

To treat the dry areas on the top of foams, airborne ultrasound would again be a possibility, but at audible frequencies, as the resonant frequency of the foam decreases with advanced drainage and coalescence.

Further work should investigate a combination of a broadband ultrasonic sensor and an actuator to investigate the relationship between the applied frequency and the instantaneous foam resonance frequency in detail. In addition, further considerations are needed in this area to improve the sound input to the foam layer by using different actuator designs.

Supporting Information

Supporting Information for this article can be found under DOI:
<https://doi.org/10.1002/ceat.202200068>

Acknowledgment

The authors gratefully acknowledge the financial support within the IGF project “Physical management of disturbing foams” (AiF 5 PN), which is supported via AiF within the program for promoting the Industrial Collective Research (IGF) of the German Ministry of Economic Affairs and Energy (BMWi), based on a resolution of the German Parliament. Open access funding enabled and organized by Projekt DEAL.

Symbols used

f_R	[s ⁻¹]	resonance frequency
N	[-]	number of adjacent lamellae per bubble
\bar{R}	[m]	arithmetic mean bubble radius

Greek letters

ϑ	[°C]	temperature
ρ	[kg m ⁻³]	mass density
σ	[N m ⁻¹]	surface tension
ϕ	[-]	liquid content
x	[-]	area ratio of the linear-parallel lamella to the total area of a lamella
ω_0	[s ⁻¹]	angular resonance frequency

7. Concluding remarks

In this work, a holistic approach to foam management, that prevents foam-related process disruptions by inhibition, reduction, and destruction of foams, is developed.

First, the problem of ‘lack of reproducibility’ of distillation processes in the spirits sector was solved by digitizing a distillations plant. This was an important step since otherwise foam management actions could not have been definitely linked to changes in foam formation or the product. By an expansion of the MSR technology, important process parameters such as the thermal energy input and the reflux rate in the rectification column could be precisely control. This allowed distillations to be carried out reproducible and with equivalent results in terms of the obtained distillate. Secondly, a suitable method to reliably determine foam structures or liquid contents, respectively, in distillation plants was established to be able to measure the effects of foam management measures on the foam.

On this basis, the work first investigated substrate-specific physical properties and their effects on foam formation, as well as the optimal choice of process parameters for foam inhibition on a laboratory scale. These laboratory scale experiments were secondly complemented by findings regarding the effects of thermal energy input on foam formation, on process separation effectiveness, and on product composition in industrial-scale distillation systems. Furthermore, validated parameters for foam destruction by acoustic actors were elaborated. The findings enable the design of a foam-resilient distillation process in the sector of spirits production.

The proposed foam management includes the inhibition of foam by selective reduction of foam-promoting substances, foam minimizing heating profiles, and an ultrasound-based method to destroy foam accumulation (Figure 43). Each of these measures was examined individually. However, a combined use was so far not implemented and should be investigated in the future. Nevertheless, important findings were made on foam dynamics under boiling conditions in distillation plants of the spirits industry. Due to its practical related design, it is of particular relevance concerning foam control and foam management under boiling conditions in industrial distillation systems of the spirit industry. The obtained results from all distillation experiments in the real system are summarized in the following.

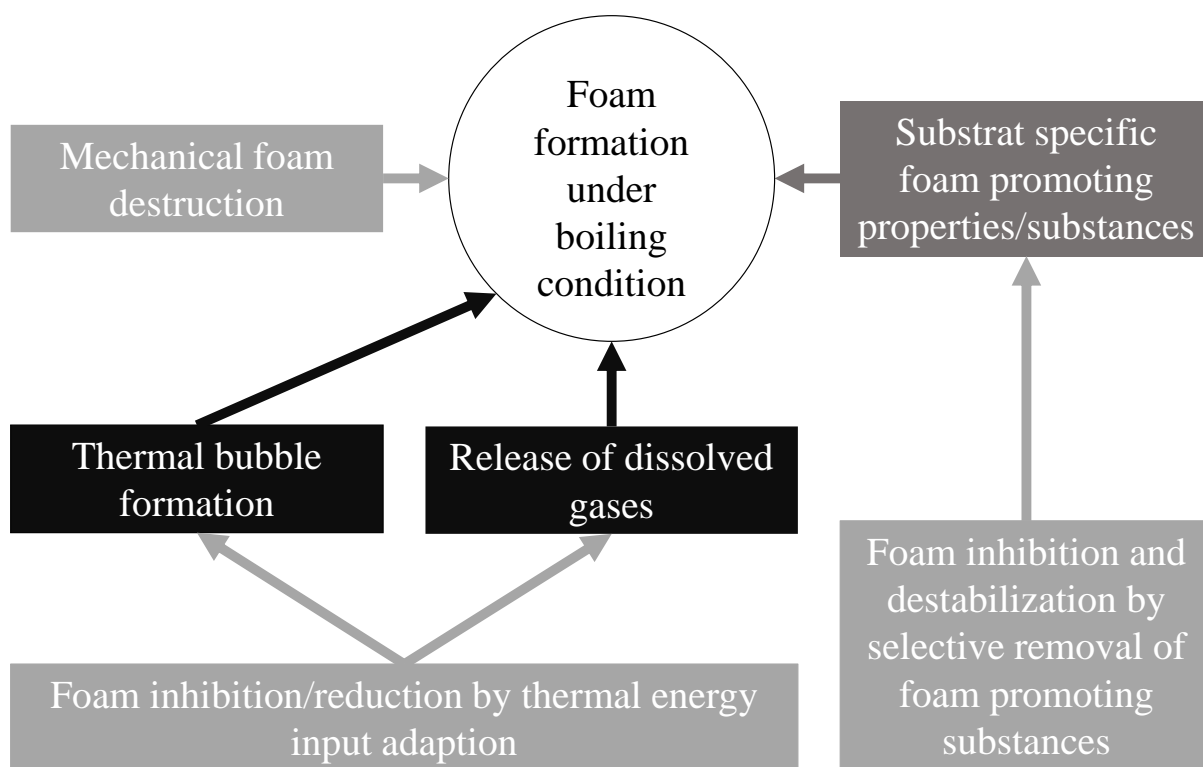


Figure 43. Overview of foam formation under boiling conditions, its causes (black), promoting factors (dark grey), and foam management methods (light grey) with their place of action

7.1. Reproducibility: operating conditions and foam formation

An important step in all research on distillation equipment in the spirits industry is to ensure reproducible distillation processes. Hereby observed effects can be linked to experimental variables. Despite its importance, this was a novelty in spirit distillation research. As García-Llobodanin et al. [28] pointed out, previous research had not addressed this issue.

The advancing digitalization offers new possibilities to create a reproducible distillation in the spirits sector. Based on this line of thought, a distillation plant was digitized and equipped with extensive sensor and control technology to reliably and reproducibly generate and determine different operating conditions and foam formation.

The sensor and control technology introduced into a traditional copper batch column still consisted of a total of 22 sensor and control devices. The sensor technology introduced was used to determine heat and mass flow in the distillation plant. The introduced control technology allowed precise control of the thermal energy input and internal reflux rates. As these are mainly responsible for the heat and mass transfer rates in the plant, their control was crucial for the reproducibility of distillation processes. A comparison of 28,600 data points of duplicated distillations showed a median RSD of <math><0.1\% - 7\%</math>, proving the largely reproducibility of distillations processes with the digitalized batch column still. Further, it was proven that the distillations also led to similar product quality and similar volatile compound concentrations (median RSD $9.0 \pm 8.0\%$), respectively.

In addition to measuring heat and mass transfer, the introduced sensor equipment was used to investigate foam formations. To reliably measure and characterize foam formations, a minimally invasive method based on capacitive point-level sensors was developed. Capacitive sensors were modified and calibrated using an electrical conductivity measurement to reliably determine the liquid content of foams. The development of the method made it possible to determine the liquid fraction in foams in industrial plants such as a distillation column. In contrast to previously used methods for measuring the liquid fraction, this method is easily applied and can also be used in ATEX environments or conductive vessels.

The findings were subsequently used to develop a foam management system in distillation plants. However, the solutions can also be applied in other industries.

Digitization of industrial plants can lead to higher reproducibility and comparability in all industrial processes since manual interactions and influences can be excluded. In the future, all research on the distillation of spirits should be carried out using a digitized system to exclude manual influences and quantify the influences of the ambient conditions on the obtained data. On the one hand, this would significantly improve research and, at the same time, enable easier comparison of research data between different research projects.

The developed method to characterize foams regarding their liquid content can be applied in other industrial plants, which are also affected by impairing foam formations. Here, too, the results obtained can contribute to the development of a coordinated foam management system. An application as a part of the process control in processes where foams with certain characteristics are desired is also conceivable.

7.2. Substrate-based factors influencing foam formation

To not only fight the symptoms or foam formation, respectively, but the cause, the study addressed the characterization of substrates concerning their foam dynamics. The aim was to discover foam-promoting properties and/or components in substrates. Results could be used, on the one hand, to predict foam formations and on the other hand as a basis for a preventive solution to foam formations.

Results showed that in the distillation of mashes, the substrate-specific property viscosity in particular correlated with foam formation. A reduction in viscosity due to the degradation of viscosity-determining compounds (e.g. pentosan) significantly reduces process-impairing foam accumulation. The most likely reason is increased drainage of the liquid phase resulting in reduced foam stability and a subsequently reduced foam formation. In addition to inhibiting foam formation, reducing the viscosity of mashes also has procedural advantages, e.g. in terms of pumpability. Furthermore, no change in the distillate is to be expected due to the reduction in viscosity before distillation. Therefore, a reduction in mash viscosity is recommended to largely inhibit foam formation during distillation. A similar approach is applicable for other processes with foam problems, as long as the viscosity reduction or the degradation of associated compounds, respectively, does not affect the final product.

7.3. Passive process parameters

As the second element of the foam management system, favorable, foam-inhibiting, or minimalizing passive process parameters were determined both at laboratory scale and on the digitized distillation system. First investigations were carried out on a laboratory scale. Here, initial findings on foam-critical temperature ranges were shown. In particular, a temperature range from 89.5 °C to 98.2 °C was found to be critical for foam formation. The laboratory scale also showed that in general, a reduction in the thermal energy input reduces foam formations.

By experimental distillations on the digitized distillation system, favorable operating conditions for a minimal foam formation were set based on the lab-scale findings. Distillation experiments with variable thermal energy input led to the conclusion that an initial reduction of the energy input to 43 ± 1 W/L at a mash temperature of 89.5 °C can prevent the formation of critical foam formation. To counteract an extension of the processing time, the thermal energy input can be increased again later, depending on the substrate-specific foam formation. These results led to the development of foam-minimizing heating profiles. These heating profiles could be used across substrates and reliably inhibited or minimized foam formation.

The investigations of passive process parameters included the study of volatile compounds in the distillates in addition to the determination of operational conditions and foam formations. Changes in the first fractions of the distillates occurred due to changes in the thermal energy input. Since the first fractions are generally discarded, this side effect is negligible. The wide application of the heating profiles in the industry is therefore possible without having to fear changes in the product quality.

Changing passive process parameters is a simple and cost-effective solution to overcome foam formations in industrial plants. Adjusting the temperature or the energy input is a possible solution for many thermal processes. For example, foam-prone processes with a set temperature could be modified so that the process temperature is outside the foam critical range. In a process such as distillation, where a temperature range must be traversed, adjusting the heating profile can be used to reduce foam formation.

7.4. Active foam management

As the last element for a foam management system, active measures for foam destruction were considered. The measures involve the destruction of foam accumulations using ultrasonic waves. Ultrasound with a frequency sweep of 40-168 kHz, which was the hypothesized resonant frequency of the foam, significantly reduced boiling-induced foam formations on a laboratory scale. The observed destruction of the foam was attributed to increased drainage from the liquid phase due to the introduced vibration of the lamella. However, the experiments showed that this method has two limitations. First, the experiments showed that dry foams are resistant to the effects of ultrasound, due to higher capillary pressure and a more prominent

Marangoni effect counteracting the ultrasound-induced drainage. Second, foam destruction by ultrasound has a limited area of effect, because of a limited penetration depth of the ultrasonic waves into the foam. Ultrasound should therefore be applied primarily to a narrow plant section to ensure that the introduced ultrasound covers the cross-section. In the experiments on the column still, the ultrasound was introduced at the lower end of the column at the level of the foam retention device. The applied ultrasound led to immediate destruction of the rising foam formations and prevented the overflowing of foam on upper trays. An application in a broader section, i.e. the heating vessel, is possible if an ultrasonic sonotrode with more power and/or several ultrasonic sonotrodes to increase the area of effect are available. This would allow ultrasound to be used in a preventive way rather than for foam destruction for already high foam formations. However, this would also entail increased energy consumption and/or higher investment costs. Due to this, methods based on substrate and passive process parameters modification are to be preferred. But, active foam destruction by the introduction of ultrasound showed potential and should be further investigated, as active destruction of foam is nonetheless part of a holistic foam management system. Alternatively, foam destruction by sprinkling of liquid onto the foam or by thermal actors during foam formation under boiling conditions should be investigated.

7.5. Economic relevance of the results

Equipment and plant manufacturers are potential users of the results. They can optimize their products to minimize foam formation and, if necessary, provide plant extensions for foam control, e.g. an ultrasonic sonotrode system. Engineering companies working in these business areas will also benefit. They can design new processes for foam-prone systems based on the findings of this work.

Admittedly, it is mainly operators of distillation plants who primarily benefit from the results of this work. On the one hand, these are producers of spirits in the food sector. On the other hand, by transfer of the results manufacturers of bioethanol by distillation in the area of renewable energy and to a limited extent also operators of distillations plants in the chemical industry benefit.

As initially mentioned, there are currently about 17,800 operators of distillation plants for spirit production. The majority are part of small and medium-sized enterprises. Although they are most affected by the foam problem, they do not have the infrastructural and human resources to solve the foam problem through extensive research themselves. However, this work provides a remedy.

The results offer them the possibility to select, combine and implement the most economical foam management measure for their respective foam problem. This leads to a more energy- and resource-efficient operation of the distillation plant even under foam risky conditions.

Summary

Foam formation occurs for various substrates during distillation processes. Their intensity depends on the substrate properties and processing parameters. A concrete prediction of the foam potential can only be approximated due to the physical, chemical, and biochemical complexity of the influencing factors. Foam formations affect both the design and the operation of distillation plants, due to various undesirable negative effects of foams on the process and the product.

In this work, foam formations under boiling conditions in distillation plants of the spirit industry were investigated and different foam control methods for a holistic foam management system were developed. All foam control measures were studied individually and optimized for minimizing foam formation in distillation processes. It was intended to make the distillation process more foam-resilient, and less subjected to foam-induced process disruption.

To investigate foam formation in distillation processes lab-scale experiments and experiments on a column still were carried out. Because up to now there is a lack of reproducibility in distillation processes of spirit drinks, this problem had to be overcome first. In this work, it was possible to largely reproduce spirit distillation processes by digitizing the distillation system. The digitalization included the installation of several sensors and devices for the measurement and control of energy and mass flows. In particular, the precise control of thermal energy input and internal reflux rates allowed us to perform reproducible distillation processes and to produce fruit spirit products with similar volatile compound compositions.

Besides sensor and control devices for energy and mass flow, sensors for the detection of accumulating foam levels were installed in the distillation system. In addition to the detection of foams, the structure of the foams is of interest, as this correlates with their stability. In particular, the liquid fraction in foams has a significant influence on the structure and stability of foams. However, currently the measurement of liquid fraction in foams requires complex measurement methods. Easily applicable methods for industrial use are missing. Therefore, in this work, a novel minimally invasive method was developed to determine liquid fraction in foam. The method is based on a modified level sensor, which measures the capacity of the surrounding medium. The liquid fraction can be inferred from the capacity of the surrounding medium. The modified sensor was calibrated using electrical conductivity measurement. The correlation between the sensor output signal and the measured liquid fraction indicated a high accuracy. While the applicability of this method was successfully demonstrated, some factors affecting the sensor signal still need to be investigated.

The digitization of the column still allowed the study of foam formations, as well as foam-promoting operating conditions and substrate properties on an industrial scale subsequent to the laboratory scale experiments.

In the first step for a foam management system, the inhibition of foams by modification of substrate properties was investigated. In experiments various physical and rheological parameters of mashes as well as other foam-relevant parameters were determined. The aim was to derive a possible link with foam formation. It was shown that the viscosity and viscosity-determining compounds of the substrate have a significant influence on the foaming behavior of mashes. Rye mash was used as the demonstration medium in these experiments. In rye mash the compound pentosan was, in particular, influencing the viscosity. The experiments

demonstrated, that the degradation of pentosans prior to distillation resulted in a decrease in viscosity and reduced foam accumulation.

Next to foam-promoting substrate properties, foam-promoting operating conditions were investigated. The aim was to link passive process parameters to foam formations. On a laboratory scale, the foam formation in rye mashes was investigated as a function of passive process parameters and operating conditions, respectively, during distillation. It was demonstrated, that foam formations only occurred in a narrow temperature range of 89.5 – 98.2 °C. Additionally, foam formations were significantly lower with reduced energy input. The findings of the lab scale experiments were applied to develop foam-resilient heating profiles for distillations in the column still. In addition, it was focused on the separation effectiveness and economic efficiency of the new heating profiles, particularly with regard to process duration and the quality of the distillates obtained. Promising foam-resilient heating profiles were transferred to different substrates and their effectiveness was tested. Based on the findings, recommendations for distilleries for a foam-resilient distillation process could be derived, as well as predictions regarding effects on the product quality and process effectiveness.

As the last step, active measures for foam destruction utilizing ultrasound were investigated. Ultrasound was introduced into the column at the level of the foam retention device of the distillation unit. The introduction of ultrasound into the column at the level of the foam retention device resulted in a reduction of foams. The observed decrease in foams was attributed to ultrasound-induced drainage of the liquid phase and subsequent destruction of the foam. However, also limitations of the method were found, e.g. limited area of effect. Further research is needed to validate the results and overcome these limitations.

Overall, it was shown that foam management, which is not based on chemical defoamers, is possible in foam formation under boiling conditions in distillation processes. Several proposed measures, including inhibition, reduction, and destruction of foams were proposed. By combining them a holistic foam management is feasible.

Zusammenfassung

Bei Destillationsprozessen kommt es bei verschiedenen Substraten zur Schaumbildung. Ihre Intensität hängt von Substrateigenschaften und Prozessparametern ab. Eine konkrete Vorhersage des Schaumpotentials kann aufgrund der physikalischen, chemischen und biochemischen Komplexität der Einflussfaktoren nur näherungsweise erfolgen. Schaumbildungen beeinflussen sowohl die Auslegung als auch den Betrieb von Destillationsanlagen, da Schäume verschiedene unerwünschte Auswirkungen auf den Prozess und das Produkt haben können.

In dieser Arbeit wurde die Schaumbildung unter Siedebedingungen in Destillationsanlagen der Spirituosenindustrie untersucht und verschiedene Methoden zur Schaumkontrolle für ein ganzheitliches Schaummanagementsystem entwickelt. Alle Methoden zur Schaumkontrolle wurden einzeln untersucht und für eine Minimierung der Schaumbildung in Destillationsprozessen optimiert. Ziel war es, den Destillationsprozess resistenter gegen schaumbedingte Prozessunterbrechungen zu machen.

Zur Untersuchung der Schaumbildung in Destillationsprozessen wurden Experimente im Labormaßstab und an einem Brenngerät durchgeführt. Da bisher die Reproduzierbarkeit bei Destillationsprozessen von Spirituosen ein Problem darstellt, musste hierfür zunächst eine Lösung erarbeitet werden. In dieser Arbeit konnten durch Digitalisierung des Brenngeräts Destillationen reproduzierbar durchgeführt werden. Die Digitalisierung umfasste den Einbau mehrerer Sensoren und Geräte zur Messung und Regelung von Energie- und Massenströmen. Insbesondere die präzise Steuerung der thermischen Energiezufuhr und der Rückflussrate in der Destillationskolonne ermöglichte es, reproduzierbare Destillationsprozesse durchzuführen und Obstbrände mit gleichbleibender Zusammensetzung der flüchtigen Verbindungen herzustellen.

Neben der Mess- und Regeltechnik für Energie- und Massenstrom wurden in der Destillationsanlage Sensoren zur Erfassung von Schäumen installiert. Neben der Detektion von Schäumen war die Messung der Struktur der Schäume von Interesse, da diese ihrer Stabilität beeinflusst. Insbesondere der Flüssigkeitsanteil in Schäumen hat einen erheblichen Einfluss auf die Struktur und die Stabilität von Schäumen. Allerdings gibt es zur Messung des Flüssigkeitsanteils in Schäumen derzeit nur komplexe Messmethoden. Einfach einzusetzende Methoden für den industriellen Einsatz fehlen. Daher wurde in dieser Arbeit eine neuartige, minimal-invasive Methode zur Bestimmung des Flüssigkeitsanteils in Schäumen entwickelt. Die Methode basiert auf einem modifizierten Füllstandssensor, der die Kapazität des ihn umgebenden Mediums misst. Über die Kapazitätsmessung des Schaumes kann auf den Flüssigkeitsanteil des Schaumes rückgeschlossen werden. Der modifizierte Sensor wurde mit Hilfe einer elektrischen Leitfähigkeitsmessung kalibriert. Eine hohe Korrelation zwischen dem Sensorsignal und dem gemessenen Flüssigkeitsanteil konnte gezeigt werden. Obwohl die Anwendbarkeit dieser Methode erfolgreich demonstriert wurde, müssen einige Faktoren, die das Sensorsignal beeinflussen, noch untersucht werden.

Die Digitalisierung des Brenngeräts ermöglichte die Untersuchung von Schaumbildung, sowie von schaumfördernden Betriebsbedingungen und Substrateigenschaften im industriellen Maßstab neben Experimenten im Labormaßstab.

Als erstes Element eines Schaummanagementsystem wurde die Inhibition von Schaumbildung durch Veränderung der Substrateigenschaften untersucht. In Versuchen wurden verschiedene physikalische und rheologische Parameter von Maischen sowie weitere schaumrelevante Parameter bestimmt. Ziel war es, einen möglichen Zusammenhang mit dem Schaumbildungsvermögen der Substrate herzustellen. Es zeigte sich, dass die Viskosität und viskositätsbestimmende Verbindungen im Substrat einen wesentlichen Einfluss auf das Schaumverhalten haben. Als Demonstrationsmedium für diese Versuche wurde Roggenmaische verwendet. In Roggenmaische war insbesondere die Verbindung Pentosan viskositätsbestimmend. In Versuchen konnte gezeigt werden, dass der Abbau von Pentosanen vor der Destillation zu einer Verringerung der Viskosität und einer geringeren Schaumbildung führte.

Neben den schaumfördernden Substrateigenschaften wurden auch schaumfördernde Betriebsbedingungen untersucht. Ziel war es, passive Prozessparameter bzw. daraus resultierende Betriebsbedingungen mit Schaumbildung zu korrelieren. Im Labormaßstab wurde die Schaumbildung in Roggenmaischen in Abhängigkeit von passiven Prozessparametern bzw. Betriebsbedingungen während der Destillation untersucht. Es zeigte sich, dass Schaumbildung nur in einem engen Temperaturbereich von 89,5 - 98,2 °C auftrat. Außerdem war die Schaumbildung bei reduziertem Energieeintrag signifikant reduziert. Die Erkenntnisse aus den Laborversuchen wurden genutzt, um schaumresistente Heizprofile für Destillationen mit dem Brenngerät zu entwickeln. Darüber hinaus wurde die Trenneffektivität und die Wirtschaftlichkeit der neuen Heizprofile, insbesondere im Hinblick auf die Prozessdauer und die Qualität der gewonnenen Destillate, untersucht. Vielversprechende schaumresistente Heizprofile wurden auf unterschiedlichen Substraten angewendet um ihre allgemeine Wirksamkeit zu prüfen. Aus den Ergebnissen konnten Empfehlungen für Brennereien für einen schaumresistenten Destillationsprozess abgeleitet, sowie Vorhersagen über Auswirkungen auf die Produktqualität und Prozesseffektivität durch Änderung der passiven Prozessparameter gemacht werden.

In einem letzten Schritt wurden aktive Maßnahmen zur Schaumzerstörung mit Hilfe von Ultraschall untersucht. Der Ultraschall wurde auf Höhe der Schaumrückhaltevorrichtung des brenngeräts in die Kolonne eingebracht. Die Einführung von Ultraschall in die Kolonne auf der Höhe der Schaumrückhaltevorrichtung führte zu einer Zerstörung von Schaumbildungen. Der beobachtete Rückgang der Schaumbildung wurde auf die durch den Ultraschall induzierte Entwässerung der flüssigen Phase und damit einhergehende Zerstörung des Schaums zurückgeführt. Es wurden jedoch auch Limitierungen der Methode festgestellt, z.B. ein begrenzter Wirkungsbereich. Weitere Forschungsarbeiten sind erforderlich, um die Ergebnisse zu validieren und diese Limitierungen zu überwinden.

Insgesamt wurde durch diese Arbeit gezeigt, dass ein Schaummanagement, das nicht auf chemischen Entschäumen basiert, bei der Schaumbildung unter Siedebedingungen in Destillationsprozessen möglich ist. Es wurden mehrere Maßnahmen vorgeschlagen, darunter die Inhibierung, Reduzierung und Zerstörung von Schaum. Durch deren Kombination ist ein ganzheitliches Schaummanagement möglich.

References

- [1] N. Kockmann, History of Distillation, in: Distillation, Elsevier, 2014: pp. 1–43. <https://doi.org/10.1016/B978-0-12-386547-2.00001-6>.
- [2] R.J. Forbes, A short history of the art of distillation: from the beginnings up to the death of Cellier Blumenthal, Brill, Leiden, 1970. <https://doi.org/10.1093/bjps/III.11.273>.
- [3] H. Brunschwygk, Hie anfahren ist das Buch genant Liber de arte distillandi: von der Künst der Distillierung, Strassburg, 1500. urn:nbn:de:bvb:12-bsb00031146-3.
- [4] W.H. Ryff, Das new groß Distillier Buch, wolgegründter künstlicher Distillation, Franckfurt, Egenolff, 1545. urn:nbn:de:bvb:12-bsb11069395-2.
- [5] J. French, The art of distillation, London, 1651.
- [6] N. Spaho, Distillation Techniques in the Fruit Spirits Production, in: Distillation - Innovative Applications and Modeling, InTech, 2017. <https://doi.org/10.5772/66774>.
- [7] Statistisches Bundesamt, Anzahl der Spirituosenbrennereien in Deutschland in den Jahren 2007/08 bis 2015/2016., (2017). <https://de.statista.com>, 31.07.2022.
- [8] Statistisches Bundesamt, Produktion von Spirituosen in Deutschland in den Jahren 1970 bis 2016., (2017). <https://de.statista.com>, 31.07.2022.
- [9] BMEL, Zukunftschancen für Klein- und Obstbrenner, 2015. <https://www.bmel.de/SharedDocs/Pressemitteilungen/2015/061-BLBranntweinmonopol.%0Ahtml>, 31.07.2022.
- [10] T. Senn, Erfolgreiche Klein- und Obstbrennerei – Herausforderungen in der Brennereitechnologie, in: Fachtagung Klein- Und Obstbrennereien in Baden-Württemberg Mit Zukunft, Gengenbach, 2017. <http://www.lvwobw.de/pb/,Lde/Startseite/Fachinformationen/Klein-+und+Obstbrennereien+in+Baden-Wuerttemberg+mit+Zukunft>, 31.07.2022.
- [11] Bundesvereinigung der Deutschen Ernährungsindustrie e.V. (BVE), Fakt: ist - Lebensmittelqualität, Berlin, 2016.
- [12] DLG e.V., Preisträger Spirituosen 2022, (2022).
- [13] DLG e.V., Preisträger Spirituosen 2021, (2022).
- [14] E. Kirschbaum, Destillier- und Rektifiziertchnik, Springer Berlin Heidelberg, Berlin, Heidelberg, 1969. <https://doi.org/10.1007/978-3-662-11458-2>.
- [15] H.J. Pieper, E.-E. Bruchmann, E. Kolb, Technologie der Obstbrennerei, Eugen Ulmer GmbH & Co., Stuttgart, 1977.

- [16] G. Ströhmer, M.E. Haug, H.-J. Junker, B. Riemer, *Spirituosentechnologie*, 7th ed., Behr's...Verlag, Hamburg, 2019.
- [17] N. Christoph, C. Bauer-Christoph, Flavour of spirit drinks: raw materials, fermentation, distillation, and ageing, in: R.G. Berger (Ed.), *Flavours and Fragrances*, Springer-Verlag, Berlin, 2007: pp. 219–239.
- [18] B. Willner, M. Granvogl, P. Schieberle, Characterization of the Key Aroma Compounds in Bartlett Pear Brandies by Means of the Sensomics Concept, *Journal of Agricultural and Food Chemistry*. 61 (2013) 9583–9593. <https://doi.org/10.1021/jf403024t>.
- [19] H. Woidich, W. Pfannhauser, R. Eberhardt, *Aroma compounds in Williams pear brandy: analysis by capillary chromatography and mass spectrometry*, Klosterneuburg, 1978.
- [20] I.K. Cigić, L. Zupančič-Kralj, Changes in odour of bartlett pear brandy influenced by sunlight irradiation, *Chemosphere*. 38 (1999) 1299–1303. [https://doi.org/10.1016/S0045-6535\(98\)00549-9](https://doi.org/10.1016/S0045-6535(98)00549-9).
- [21] R. Rodríguez Madrera, A.P. Lobo, J.J.M. Alonso, Effect of cider maturation on the chemical and sensory characteristics of fresh cider spirits, *Food Research International*. 43 (2010) 70–78. <https://doi.org/10.1016/j.foodres.2009.08.014>.
- [22] P.X. Etiévant, Wine, in: H. Maarse (Ed.), *Volatile Compounds in Foods and Beverages*, TNO-CIVO Food Analysis Institute, Zeist, 1991: pp. 483–546.
- [23] I. Nykänen, L. Nykänen, Distilled beverages, in: H. Maarse (Ed.), *Volatile Compounds in Foods and Beverages*, TNO-CIVO Food Analysis Institute, Zeist, 1991: pp. 547–580.
- [24] H. Maarse, C.A. Vissche, *Volatile Compounds in Food: Qualitative and Quantitative Data*, TNO-CIVO Food Analysis Institute, Zeist, 1990.
- [25] F. López, J.J. Rodríguez-Bencomo, I. Orriols, J.R. Pérez-Correa, Fruit Brandies, in: *Science and Technology of Fruit Wine Production*, Elsevier, 2017: pp. 531–556. <https://doi.org/10.1016/B978-0-12-800850-8.00010-7>.
- [26] A. Dunkel, M. Steinhaus, M. Kotthoff, B. Nowak, D. Krautwurst, P. Schieberle, T. Hofmann, Nature's Chemical Signatures in Human Olfaction: A Foodborne Perspective for Future Biotechnology, *Angewandte Chemie International Edition*. 53 (2014) 7124–7143. <https://doi.org/10.1002/anie.201309508>.
- [27] R. Leaute, Distillation in Alambic, *American Journal of Enology and Viticulture*. 41 (1990) 90–103.
- [28] L. García-Llobodanin, J. Roca, J.R. López, J.R. Pérez-Correa, F. López, The lack of reproducibility of different distillation techniques and its impact on pear spirit composition, *International Journal of Food Science and Technology*. 46 (2011) 1956–1963. <https://doi.org/10.1111/j.1365-2621.2011.02707.x>.

- [29] Y. Arrieta-Garay, C. López-Vázquez, P. Blanco, J.R. Pérez-Correa, I. Orriols, F. López, Kiwi spirits with stronger floral and fruity characters were obtained with a packed column distillation system, *Journal of the Institute of Brewing*. 120 (2014) 111–118. <https://doi.org/10.1002/jib.117>.
- [30] Y. Arrieta-Garay, L. García-Llobodanin, J.R. Pérez-Correa, C. López-Vázquez, I. Orriols, F. López, Aromatically Enhanced Pear Distillates from Blanquilla and Conference Varieties Using a Packed Column, *Journal of Agricultural and Food Chemistry*. 61 (2013) 4936–4942. <https://doi.org/10.1021/jf304619e>.
- [31] Y. Arrieta-Garay, P. Blanco, C. López-Vázquez, J.J. Rodríguez-Bencomo, J.R. Pérez-Correa, F. López, I. Orriols, Effects of Distillation System and Yeast Strain on the Aroma Profile of Albariño (*Vitis vinifera* L.) Grape Pomace Spirits, *Journal of Agricultural and Food Chemistry*. 62 (2014) 10552–10560. <https://doi.org/10.1021/jf502919n>.
- [32] J.J. Rodríguez-Bencomo, J.R. Pérez-Correa, I. Orriols, F. López, Spirit Distillation Strategies for Aroma Improvement Using Variable Internal Column Reflux, *Food and Bioprocess Technology*. 9 (2016) 1885–1892. <https://doi.org/10.1007/s11947-016-1776-0>.
- [33] P.C. Wankat, *Separation Process Engineering*, Pearson Education, New Jersey, 2010.
- [34] H. Tanner, H.R. Brunner, *Fruit Distillation Today*, 3rd ed., Chemical and Administration Society, 1982.
- [35] M.J. Claus, K.A. Berglund, Defining still parameters using chemcad batch distillation model for modeling fruit spirits distillations, *Journal of Food Process Engineering*. 32 (2009) 881–892. <https://doi.org/10.1111/j.1745-4530.2008.00251.x>.
- [36] P. Matias-Guiu, J.J. Rodríguez-Bencomo, I. Orriols, J.R. Pérez-Correa, F. López, Floral aroma improvement of Muscat spirits by packed column distillation with variable internal reflux, *Food Chemistry*. 213 (2016) 40–48. <https://doi.org/10.1016/j.foodchem.2016.06.054>.
- [37] A. Prins, Principles of foam stability, in: E. Dickinson, G. Stainsby (Eds.), *Advances in Food Emulsions and Foams*, Elsevier Applied Science, London, 1988: pp. 91–122.
- [38] E. Dickinson, Stability and rheological implications of electrostatic milk protein–polysaccharide interactions, *Trends in Food Science & Technology*. 9 (1998) 347–354. [https://doi.org/10.1016/S0924-2244\(98\)00057-0](https://doi.org/10.1016/S0924-2244(98)00057-0).
- [39] E. Dickinson, Hydrocolloids at interfaces and the influence on the properties of dispersed systems, *Food Hydrocolloids*. 17 (2003) 25–39. [https://doi.org/10.1016/S0268-005X\(01\)00120-5](https://doi.org/10.1016/S0268-005X(01)00120-5).
- [40] F.M. Nunes, M.A. Coimbra, Influence of polysaccharide composition in foam stability of espresso coffee, *Carbohydrate Polymers*. 37 (1998) 283–285. [https://doi.org/10.1016/S0144-8617\(98\)00072-1](https://doi.org/10.1016/S0144-8617(98)00072-1).

- [41] A. Ye, Complexation between milk proteins and polysaccharides via electrostatic interaction: Principles and applications - A review, *International Journal of Food Science and Technology*. 43 (2008) 406–415. <https://doi.org/10.1111/j.1365-2621.2006.01454.x>.
- [42] Q.P. Nguyen, A. V. Alexandrov, P.L. Zitha, P.K. Currie, Experimental and Modeling Studies on Foam in Porous Media: A Review, in: *SPE International Symposium on Formation Damage Control*, Society of Petroleum Engineers, 2000. <https://doi.org/10.2118/58799-MS>.
- [43] L.L. Schramm, F. Wassmuth, Foams: Basic Principles, in: *Foams: Fundamentals and Applications in the Petroleum Industry*, 1994: pp. 3–45. <https://doi.org/10.1021/ba-1994-0242.ch001>.
- [44] J.A. Gallego-Juárez, G. Rodríguez, E. Riera, A. Cardoni, Ultrasonic defoaming and debubbling in food processing and other applications, in: *Power Ultrasonics*, Elsevier, 2015: pp. 793–814. <https://doi.org/10.1016/B978-1-78242-028-6.00026-0>.
- [45] A. Hilberer, S.-H. Chao, Antifoaming Agents, in: *Encyclopedia of Polymer Science and Technology*, John Wiley & Sons, Inc., Hoboken, NJ, USA, 2012: pp. 60–65. <https://doi.org/10.1002/0471440264.pst411.pub2>.
- [46] H.Z. Kister, What caused tower malfunctions in the last 50 years?, *Chemical Engineering Research and Design*. 81 (2003) 5–26. <https://doi.org/10.1205/026387603321158159>.
- [47] G.H. Miller, *Whisky Science*, Springer International Publishing, Cham, 2019. <https://doi.org/10.1007/978-3-030-13732-8>.
- [48] H.Z. Kister, Common Techniques for Distillation Troubleshooting, in: *Distillation: Operation and Applications*, 2014: pp. 37–101. <https://doi.org/10.1016/B978-0-12-386876-3.00002-8>.
- [49] P. Schidrowitz, F. Kaye, The Distillation of Whisky, *Journal of the Institute of Brewing*. 12 (1906) 496–517. <https://doi.org/10.1002/j.2050-0416.1906.tb02170.x>.
- [50] M. Kaltschmitt, H. Hartmann, H. Hofbauer, *Energie aus Biomasse*, Springer Berlin Heidelberg, Berlin, Heidelberg, 2016. <https://doi.org/10.1007/978-3-662-47438-9>.
- [51] L.L. Simon, H. Kencse, K. Hungerbuhler, Optimal rectification column, reboiler vessel, connection pipe selection and optimal control of batch distillation considering hydraulic limitations, *Chemical Engineering and Processing: Process Intensification*. 48 (2009) 938–949. <https://doi.org/10.1016/j.cep.2008.12.006>.
- [52] P. Dürr, W. Albrecht, M. Gössinger, K. Hagmann, D. Pulver, G. Scholten, *Technologie der Obstbrennerei*, 3rd ed., Ulmer, Stuttgart, 2010.
- [53] A. Hilberer, S.-H. Chao, Antifoaming Agents, in: *Encyclopedia of Polymer Science and Technology*, John Wiley & Sons, Inc., Hoboken, NJ, USA, 2012: pp. 60–65. <https://doi.org/10.1002/0471440264.pst411.pub2>.

- [54] A. Prins, M. van den Tempel, , in: IVth International Congress on Sur-Face Active Substances, Brussels, 1964: p. 1119.
- [55] N.D. Denkov, K.G. Marinova, S.S. Tcholakova, Mechanistic understanding of the modes of action of foam control agents, *Advances in Colloid and Interface Science*. 206 (2014) 57–67. <https://doi.org/10.1016/j.cis.2013.08.004>.
- [56] P.R. Garrett, *Defoaming: Theory and Industrial Applications*, CRC Press, Boca Raton, 1992.
- [57] M. Andriot, S.H. Chao, A. Colas, S. Cray, F. de Buyl, J.V.Jr. DeGroot, A. Dupont, T. Easton, J.L. Garaud, E. Gerlach, F. Gubbels, M. Jungk, S. Leadley, J.P. Lecomte, B. Lenoble, R. Meeks, A. Mountney, G. Shearer, S. Stassen, C. Stevens, X. Thomas, A.T. Wolf, *Silicones in Industrial Applications*, in: R. de Jaeger, M. Gleria (Eds.), *Silicon-Based Inorganic Polymers*, Nova Science, New York, 2008: p. 97.
- [58] S.J. Routledge, D.R. Poyner, R.M. Bill, Antifoams: the overlooked additive?, *Pharmaceutical Bioprocessing*. 2 (2014) 111–114. <https://doi.org/10.2217/PBP.14.5>.
- [59] J. Rocker, A. Mahmoudkhani, L. Bava, B. Wilson, Low Environmental Impact Nonsilicone Defoamers for Use in Oil/Gas/Water Separators, in: *SPE Eastern Regional Meeting*, Society of Petroleum Engineers, 2011. <https://doi.org/10.2118/149462-MS>.
- [60] M.H. Pahl, D. Franke, Schaum und Schaumzerstörung - ein Überblick, *Chemie Ingenieur Technik*. 67 (1995) 300–312. <https://doi.org/10.1002/cite.330670306>.
- [61] F. Vardar-Sukan, Foaming: Consequences, prevention and destruction, *Biotechnology Advances*. 16 (1998) 913–948. [https://doi.org/10.1016/S0734-9750\(98\)00010-X](https://doi.org/10.1016/S0734-9750(98)00010-X).
- [62] C. Miller, Antifoaming in aqueous foams, *Current Opinion in Colloid & Interface Science*. 13 (2008) 177–182. <https://doi.org/10.1016/j.cocis.2007.11.007>.
- [63] J. Wang, A. v. Nguyen, S. Farrokhpay, A critical review of the growth, drainage and collapse of foams, *Advances in Colloid and Interface Science*. 228 (2016) 55–70. <https://doi.org/10.1016/j.cis.2015.11.009>.
- [64] B. Furchner, A. Mersmann, Mechanische Schaumzerstörung, *Chemie Ingenieur Technik*. 58 (1986) 332–333. <https://doi.org/10.1002/cite.330580416>.
- [65] N.P. Ghildyal, B.K. Lonsane, N.G. Karanth, Foam Control in Submerged Fermentation: State of the Art, in: 1988: pp. 173–222. [https://doi.org/10.1016/S0065-2164\(08\)70207-7](https://doi.org/10.1016/S0065-2164(08)70207-7).
- [66] D. Weaire, S. Hutzler, *The Physics of Foams*, Oxford University Press, 2001. <https://doi.org/10.1063/1.1366070>.

- [67] A.-L. Fameau, A. Salonen, Effect of particles and aggregated structures on the foam stability and aging, *Comptes Rendus Physique*. 15 (2014) 748–760. <https://doi.org/10.1016/j.crhy.2014.09.009>.
- [68] C.I. Nindo, J. Tang, J.R. Powers, P.S. Takhar, Rheological properties of blueberry puree for processing applications, *LWT - Food Science and Technology*. 40 (2007) 292–299. <https://doi.org/10.1016/j.lwt.2005.10.003>.
- [69] A. M. Goula, K. G. Adamopoulos, Rheological Models of Kiwifruit Juice for Processing Applications, *Journal of Food Processing & Technology*. 02 (2011). <https://doi.org/10.4172/2157-7110.1000106>.
- [70] C. Hill, J. Eastoe, Foams: From nature to industry, *Advances in Colloid and Interface Science*. 247 (2017) 496–513. <https://doi.org/10.1016/j.cis.2017.05.013>.
- [71] M. López-Barajas, A. Viu-Marco, E. López-Tamames, S. Buxaderas, M.C. de la Torre-Boronat, Foaming in Grape Juices of White Varieties, *Journal of Agricultural and Food Chemistry*. 45 (1997) 2526–2529. <https://doi.org/10.1021/jf9607369>.
- [72] M. López-Barajas, E. López-Tamames, S. Buxaderas, G. Suberbiola, M.C. de la Torre-Boronat, Influence of Wine Polysaccharides of Different Molecular Mass on Wine Foaming, *American Journal of Enology and Viticulture*. 52 (2001).
- [73] B. Dollet, C. Raufaste, Rheology of aqueous foams, *Comptes Rendus Physique*. 15 (2014) 731–747. <https://doi.org/10.1016/j.crhy.2014.09.008>.
- [74] G. Katgert, B.P. Tighe, M. van Hecke, The jamming perspective on wet foams, *Soft Matter*. 9 (2013) 9739. <https://doi.org/10.1039/c3sm51543e>.
- [75] D. Langevin, Aqueous foams and foam films stabilised by surfactants. Gravity-free studies, *Comptes Rendus Mécanique*. 345 (2017) 47–55. <https://doi.org/10.1016/j.crme.2016.10.009>.
- [76] R. Lemlich, A theory for the limiting conductivity of polyhedral foam at low density, *Journal of Colloid and Interface Science*. 64 (1977) 107–110. [https://doi.org/10.1016/0021-9797\(78\)90339-9](https://doi.org/10.1016/0021-9797(78)90339-9).
- [77] R. Phelan, D. Weaire, E.A.J.F. Peters, G. Verbist, The conductivity of a foam, *Journal of Physics: Condensed Matter*. 8 (1996) 475–482.
- [78] J.C. Maxwell, *A Treatise on Electricity and Magnetism*, Oxford University Press, Oxford, 1998.
- [79] K. Feitosa, S. Marze, A. Saint-Jalmes, D.J. Durian, Electrical conductivity of dispersions: from dry foams to dilute suspensions, *Journal of Physics: Condensed Matter*. 17 (2005) 6301–6305. <https://doi.org/10.1088/0953-8984/17/41/001>.

- [80] M.U. Vera, A. Saint-Jalmes, D.J. Durian, Scattering optics of foam, *Applied Optics*. 40 (2001) 4210. <https://doi.org/10.1364/AO.40.004210>.
- [81] E. Forel, E. Rio, M. Schneider, S. Beguin, D. Weaire, S. Hutzler, W. Drenckhan, The surface tells it all: relationship between volume and surface fraction of liquid dispersions, *Soft Matter*. 12 (2016) 8025–8029. <https://doi.org/10.1039/C6SM01451H>.
- [82] H. Emmerich, L. Schaller, R. Nauber, L. Knüpfer, S. Heitkam, J. Czarske, L. Büttner, Linear, spatio-temporally resolved ultrasound measurement of the liquid fraction distribution in froth, *Tm - Technisches Messen*. 88 (2021) 562–570. <https://doi.org/10.1515/teme-2021-0047>.
- [83] E. Solórzano, S. Pardo-Alonso, J.A. de Saja, M.A. Rodríguez-Pérez, Study of aqueous foams evolution by means of X-ray radioscopy, *Colloids and Surfaces A: Physicochemical and Engineering Aspects*. 438 (2013) 159–166. <https://doi.org/10.1016/j.colsurfa.2013.01.052>.
- [84] S. Heitkam, M. Rudolph, T. Lappan, M. Sarma, S. Eckert, P. Trtik, E. Lehmann, P. Vontobel, K. Eckert, Neutron imaging of froth structure and particle motion, *Minerals Engineering*. 119 (2018) 126–129. <https://doi.org/10.1016/j.mineng.2018.01.021>.
- [85] Y. Yang, Y. Xiang, G. Chu, H. Zou, Y. Luo, M. Arowo, J.-F. Chen, A noninvasive X-ray technique for determination of liquid holdup in a rotating packed bed, *Chemical Engineering Science*. 138 (2015) 244–255. <https://doi.org/10.1016/j.ces.2015.07.044>.
- [86] D. Osorio, J.R. Pérez-Correa, L.T. Biegler, E. Agosin, Wine Distillates: Practical Operating Recipe Formulation for Stills, *Journal of Agricultural and Food Chemistry*. 53 (2005) 6326–6331. <https://doi.org/10.1021/jf047788f>.
- [87] M. Balcerek, K. Pielech-Przybylska, P. Patelski, U. Dziekońska-Kubczak, E. Strąk, The effect of distillation conditions and alcohol content in ‘heart’ fractions on the concentration of aroma volatiles and undesirable compounds in plum brandies, *Journal of the Institute of Brewing*. 123 (2017) 452–463. <https://doi.org/10.1002/jib.441>.
- [88] R. Luna, F. López, J.R. Pérez-Correa, Minimizing methanol content in experimental charentais alembic distillations, *Journal of Industrial and Engineering Chemistry*. 57 (2018) 160–170. <https://doi.org/10.1016/j.jiec.2017.08.018>.
- [89] R. Luna, P. Matias-Guiu, F. López, J.R. Pérez-Correa, Quality aroma improvement of Muscat wine spirits: A new approach using first-principles model-based design and multi-objective dynamic optimisation through multi-variable analysis techniques, *Food and Bioproducts Processing*. 115 (2019) 208–222.
- [90] G. Niggemann, A. Rix, R. Meier, Distillation of Specialty Chemicals, in: *Distillation*, Elsevier, 2014: pp. 297–335. <https://doi.org/10.1016/B978-0-12-386876-3.00007-7>.

- [91] Z. Jiang, R. Agrawal, Process intensification in multicomponent distillation: A review of recent advancements, *Chemical Engineering Research and Design*. 147 (2019) 122–145. <https://doi.org/10.1016/j.cherd.2019.04.023>.
- [92] P.H. Tsarouhas, I.S. Arvanitoyannis, Z.D. Ampatzis, A case study of investigating reliability and maintainability in a Greek juice bottling medium size enterprise (MSE), *Journal of Food Engineering*. 95 (2009) 479–488. <https://doi.org/10.1016/j.jfoodeng.2009.06.011>.
- [93] spiritsEUROPE, The faces & places of a vibrant sector., Brussels, Belgium, 2020.
- [94] Destatis, Arbeitsunterlage zur Alkoholsteuerstatistik 2018, 2019.
- [95] N. Spaho, P. Dürr, S. Grba, E. Velagić-Habul, M. Blesić, Effects of distillation cut on the distribution of higher alcohols and esters in brandy produced from three plum varieties, *Journal of the Institute of Brewing*. 119 (2013) 48–56. <https://doi.org/10.1002/jib.62>.
- [96] W.L. McCabe, J.C. Smith, P. Harriott, Unit operations of chemical engineering. , McGraw-Hill, New York, USA, 1993.
- [97] K.A. Jacques, T.P. Lyons, D.R. Kelsall, The alcohol textbook: a reference for the beverage, fuel and industrial alcohol industries, Nottingham University Press, Nottingham, UK, 2003.
- [98] S. Spotar, A. Rahman, O.C. Gee, K.K. Jun, S. Manickam, A revisit to the separation of a binary mixture of ethanol–water using ultrasonic distillation as a separation process, *Chemical Engineering and Processing: Process Intensification*. 87 (2015) 45–50. <https://doi.org/10.1016/j.cep.2014.11.004>.
- [99] D. Heller, S. Roj, J. Switulla, R. Kölling, D. Einfalt, Tackling Foam-Based Process Disruptions in Spirit Distillation by Thermal Energy Input Adaptations, *Food and Bioprocess Technology*. 15 (2022) 821–832. <https://doi.org/10.1007/s11947-022-02785-5>.
- [100] P.C. Wankat, Equilibrium Staged Separations: Separations in Chemical Engineering, Prentice Hall, Hobonk, USA, 1988.
- [101] A. Liebminger, C. Philipp, S. Sari, M. Holstein, V. Dietrich, M. Goessinger, In-line conductivity measurement to select the best distillation technique for improving the quality of apricot brandies, *European Food Research and Technology*. 247 (2021) 1987–1997. <https://doi.org/10.1007/s00217-021-03766-2>.
- [102] T.L. Peters, Comparison of continuous extractors for the extraction and concentration of trace organics from water, *Analytical Laboratories*. 54 (1982) 1913–1914.

- [103] R.P. Reddy, J.H. Lienhard, The Peak Boiling Heat Flux in Saturated Ethanol–Water Mixtures, *Journal of Heat Transfer*. 111 (1989) 480–486. <https://doi.org/10.1115/1.3250702>.
- [104] D.S. Sholl, R.P. Lively, Seven chemical separations to change the world, *Nature*. 532 (2016) 435–437. <https://doi.org/10.1038/532435a>.
- [105] P. Bastidas, J. Parra, I. Gil, G. Rodríguez, Alcohol Distillation Plant Simulation: Thermal and Hydraulic Studies, *Procedia Engineering*. 42 (2012) 80–89. <https://doi.org/10.1016/j.proeng.2012.07.397>.
- [106] A. Liebminger, M. Holstein, V. Dietrich, M. Goessinger, Automated separation of tail fraction for fruit distillates by means of in-line conductivity measurement, *International Journal of Food Science & Technology*. 55 (2020) 3484–3492. <https://doi.org/10.1111/ijfs.14682>.
- [107] N. Spaho, D. Đukic-Ratković, N. Nikićević, M. Blesić, V. Tešević, B. Mijatović, M. Smajić Murtić, Aroma compounds in barrel aged apple distillates from two different distillation techniques, *Journal of the Institute of Brewing*. 125 (2019) 389–397. <https://doi.org/10.1002/jib.573>.
- [108] M. Balcerk, K. Pielech-Przybylska, P. Patelski, U. Dziekońska-Kubczak, E. Strąk, The effect of distillation conditions and alcohol content in ‘heart’ fractions on the concentration of aroma volatiles and undesirable compounds in plum brandies, *Journal of the Institute of Brewing*. 123 (2017) 452–463. <https://doi.org/10.1002/jib.441>.
- [109] D. Einfalt, K. Meissner, L. Kurz, K. Intani, J. Müller, Fruit Spirit Production from Coffee Cherries—Process Analysis and Sensory Evaluation, *Beverages*. 6 (2020) 57. <https://doi.org/10.3390/beverages6030057>.
- [110] VDLUFA, *Method Book III - The chemical analysis of feedstuffs*, 3., VDLUFA Verlag., Darmstadt, 1997.
- [111] ICC -International Association for Cereal Science and Technology, 104/1 Determination of Ash in Cereals and Cereal Products, 1960.
- [112] M.M. Bradford, A rapid and sensitive method for the quantitation of microgram quantities of protein utilizing the principle of protein-dye binding, *Analytical Biochemistry*. 72 (1976) 248–254. [https://doi.org/10.1016/0003-2697\(76\)90527-3](https://doi.org/10.1016/0003-2697(76)90527-3).
- [113] Y.Y. Lim, T.T. Lim, J.J. Tee, Antioxidant properties of several tropical fruits: A comparative study, *Food Chemistry*. 103 (2007) 1003–1008. <https://doi.org/10.1016/j.foodchem.2006.08.038>.
- [114] G. Ferrari, O. Lablanquie, R. Cantagrel, J. Ledauphin, T. Payot, N. Fournier, E. Guichard, Determination of Key Odorant Compounds in Freshly Distilled Cognac Using GC-O, GC-MS, and Sensory Evaluation, *Journal of Agricultural and Food Chemistry*. 52 (2004) 5670–5676. <https://doi.org/10.1021/jf049512d>.

- [115] H. Zhang, Z. Wang, O. Liu, Development and validation of a GC–FID method for quantitative analysis of oleic acid and related fatty acids, *Journal of Pharmaceutical Analysis*. 5 (2015) 223–230. <https://doi.org/10.1016/j.jpha.2015.01.005>.
- [116] J.A. Kirwan, D.I. Broadhurst, R.L. Davidson, M.R. Viant, Characterising and correcting batch variation in an automated direct infusion mass spectrometry (DIMS) metabolomics workflow, *Analytical and Bioanalytical Chemistry*. 405 (2013) 5147–5157. <https://doi.org/10.1007/s00216-013-6856-7>.
- [117] R. Mesnage, M. Arno, G.-E. Séralini, M.N. Antoniou, Transcriptome and metabolome analysis of liver and kidneys of rats chronically fed NK603 Roundup-tolerant genetically modified maize, *Environmental Sciences Europe*. 29 (2017) 6. <https://doi.org/10.1186/s12302-017-0105-1>.
- [118] H.M. Parsons, D.R. Ekman, T.W. Collette, M.R. Viant, Spectral relative standard deviation: a practical benchmark in metabolomics, *Analyst*. 134 (2009) 478–485. <https://doi.org/10.1039/B808986H>.
- [119] L. García-Llobodanin, T. Senn, M. Ferrando, C. Güell, F. López, Influence of the fermentation pH on the final quality of Blanquilla pear spirits, *International Journal of Food Science & Technology*. 45 (2010) 839–848. <https://doi.org/10.1111/j.1365-2621.2010.02206.x>.
- [120] L.F. Hernández-Gómez, J. Úbeda, A. Briones, Melon fruit distillates: comparison of different distillation methods, *Food Chemistry*. 82 (2003) 539–543. [https://doi.org/10.1016/S0308-8146\(03\)00008-6](https://doi.org/10.1016/S0308-8146(03)00008-6).
- [121] P. Awad, V. Athès, M.E. Decloux, G. Ferrari, G. Snackers, P. Raguenaud, P. Giampaoli, Evolution of Volatile Compounds during the Distillation of Cognac Spirit, *Journal of Agricultural and Food Chemistry*. 65 (2017) 7736–7748. <https://doi.org/10.1021/acs.jafc.7b02406>.
- [122] W.F. Duarte, J.C. Amorim, L. de Assis Lago, D.R. Dias, R.F. Schwan, Optimization of Fermentation Conditions for Production of the Jabuticaba (*Myrciaria cauliflora*) Spirit Using the Response Surface Methodology, *Journal of Food Science*. 76 (2011) C782–C790. <https://doi.org/10.1111/j.1750-3841.2011.02169.x>.
- [123] C.C.A. do A. Santos, W.F. Duarte, S.C. Carreiro, R.F. Schwan, Inoculated fermentation of orange juice (*Citrus sinensis* L.) for production of a citric fruit spirit, *Journal of the Institute of Brewing*. 119 (2013) 280–287. <https://doi.org/10.1002/jib.89>.
- [124] M.J. Claus, K.A. Berglund, Fruit brandy production by batch column distillation with reflux, *Journal of Food Process Engineering*. 28 (2005) 53–67. <https://doi.org/10.1111/j.1745-4530.2005.00377.x>.
- [125] L. Butkhup, M. Jeenphakdee, S. Jorjong, S. Samappito, W. Samappito, S. Chowtivannakul, HS-SPME-GC-MS analysis of volatile aromatic compounds in alcohol

- related beverages made with mulberry fruits, *Food Science and Biotechnology*. 20 (2011) 1021–1032. <https://doi.org/10.1007/s10068-011-0140-4>.
- [126] M.G. Lambrechts, I.S. Pretorius, Yeast and its Importance to Wine Aroma - A Review, *South African Journal of Enology & Viticulture*. 21 (2019). <https://doi.org/10.21548/21-1-3560>.
- [127] H. Maarse, *Volatile Compounds in Foods and Beverages*, Routledge, London, UK, 2017. <https://doi.org/10.1201/9780203734285>.
- [128] L. Nykänen, Formation and Occurrence of Flavor Compounds in Wine and Distilled Alcoholic Beverages, *American Journal of Enology and Viticulture*. 37 (1986) 84–96.
- [129] L. Nykänen, H. Suomalainen, *Aroma of Beer, Wine and Distilled Alcoholic Beverages*, Akademie-Verlag, Berlin, Germany, 1983.
- [130] P. Blumenthal, M. Steger, D. Einfalt, J. Rieke-Zapp, A. Quintanilla Bellucci, K. Sommerfeld, S. Schwarz, D. Lachenmeier, Methanol Mitigation during Manufacturing of Fruit Spirits with Special Consideration of Novel Coffee Cherry Spirits, *Molecules*. 26 (2021) 2585. <https://doi.org/10.3390/molecules26092585>.
- [131] European Parliament and Council, Regulation (EU) 2019/787 of the European Parliament and of the Council of 17 April 2019 on the definition, description, presentation and labelling of spirit drinks, the use of the names of spirit drinks in the presentation and labelling of other foodstuffs, the protection of geographical indications for spirit drinks, the use of ethyl alcohol and distillates of agricultural origin in alcoholic beverages, and repealing Regulation (EC) No 110/2008, *Off. J. Europ. Union*, 2019.
- [132] D. Exerowa, P.M. Kruglyakov, Technological Application of Foams: Physicochemical Ground, in: *Foam and Foam Films*, 5th ed., Studies in Interface Science, 1998: pp. 656–737. [https://doi.org/10.1016/S1383-7303\(98\)80013-6](https://doi.org/10.1016/S1383-7303(98)80013-6).
- [133] E.A.J.F. Peters, *Theoretical and experimental contributions to the understanding of foam drainage*, Eindhoven University of Technology, 1995.
- [134] S.J. Neethling, H.T. Lee, J.J. Cilliers, A foam drainage equation generalized for all liquid contents, *Journal of Physics: Condensed Matter*. 14 (2002) 331–342. <https://doi.org/10.1088/0953-8984/14/3/304>.
- [135] A.-L. Biance, A. Delbos, O. Pitois, How Topological Rearrangements and Liquid Fraction Control Liquid Foam Stability, *Physical Review Letters*. 106 (2011) 068301. <https://doi.org/10.1103/PhysRevLett.106.068301>.
- [136] www.baumer.com/de/de/p/14200 (Accessed on January 31,2022), (n.d.).
- [137] I. Cantat, S. Cohen-Addad, F. Elias, F. Graner, R. Höhler, O. Pitois, F. Rouyer, A. Saint-Jalmes, R. Flatman, *Foams: Structure and Dynamics*, Oxford University Press, 2013. <https://doi.org/10.1093/acprof:oso/9780199662890.001.0001>.

- [138] K. Steck, M. Hamann, S. Andrieux, P. Muller, P. Kékicheff, C. Stubenrauch, W. Drenckhan, Fluorocarbon Vapors Slow Down Coalescence in Foams, *Advanced Materials Interfaces*. 8 (2021) 2100723. <https://doi.org/10.1002/admi.202100723>.
- [139] W. Drenckhan, A. Saint-Jalmes, The science of foaming, *Advances in Colloid and Interface Science*. 222 (2015) 228–259. <https://doi.org/10.1016/j.cis.2015.04.001>.
- [140] T. Gaillard, C. Honorez, M. Jumeau, F. Elias, W. Drenckhan, A simple technique for the automation of bubble size measurements, *Colloids and Surfaces A: Physicochemical and Engineering Aspects*. 473 (2015) 68–74. <https://doi.org/10.1016/j.colsurfa.2015.01.089>.
- [141] S. Heitkam, K. Eckert, Convective instability in sheared foam, *Journal of Fluid Mechanics*. 911 (2021) A54. <https://doi.org/10.1017/jfm.2020.1062>.
- [142] D.G. Archer, P. Wang, The Dielectric Constant of Water and Debye-Hückel Limiting Law Slopes, *Journal of Physical and Chemical Reference Data*. 19 (1990) 371–411. <https://doi.org/10.1063/1.555853>.
- [143] J.-M. Lourtioz, H. Benisty, V. Berger, J.-M. Gérard, D. Maystre, A. Tcheltnokov, D. Pagnoux, *Photonic Crystals: Towards Nanoscale Photonic Devices*, Springer Berlin Heidelberg, Berlin, Heidelberg, 2005. <https://doi.org/10.1007/978-3-540-78347-3>.
- [144] Q.P. Nguyen, A. v. Alexandrov, P.L. Zitha, P.K. Currie, Experimental and Modeling Studies on Foam in Porous Media: A Review, in: *SPE International Symposium on Formation Damage Control*, Society of Petroleum Engineers, 2000. <https://doi.org/10.2118/58799-MS>.
- [145] J.A. Gallego-Juárez, G. Rodríguez, E. Riera, A. Cardoni, Ultrasonic defoaming and debubbling in food processing and other applications, in: *Power Ultrasonics*, Elsevier, 2015: pp. 793–814. <https://doi.org/10.1016/B978-1-78242-028-6.00026-0>.
- [146] G.H. Miller, *Whisky Science*, Springer International Publishing, Cham, 2019. <https://doi.org/10.1007/978-3-030-13732-8>.
- [147] K. Autio, Functional Aspects of Cereal Cell-Wall Polysaccharides, in: *Carbohydrates in Food*, Second Edition, CRC Press, 2006: pp. 167–207. <https://doi.org/10.1201/9781420015058.ch5>.
- [148] H.-D. Belitz, W. Grosch, *Food Chemistry*, 3rd ed., Springer Berlin Heidelberg, Berlin, Heidelberg, 1999. <https://doi.org/10.1007/978-3-662-07281-3>.
- [149] R.W. Cawley, The role of wheat flour pentosans in baking. II.—Effect of added flour pentosans and other gums on gluten-starch loaves, *Journal of the Science of Food and Agriculture*. 15 (1964) 834–838. <https://doi.org/10.1002/jsfa.2740151204>.
- [150] E. Denli, R. Ercan, Effect of added pentosans isolated from wheat and rye grain on some properties of bread, *European Food Research and Technology*. 212 (2001) 374–376. <https://doi.org/10.1007/s002170000281>.

- [151] T. Maeda, N. Morita, Characteristics of Pentosan in Polished Wheat Flour and Its Improving Effects on Breadmaking, *Journal of Applied Glycoscience*. 53 (2006) 21–26. <https://doi.org/10.5458/jag.53.21>.
- [152] S. Vanhamel, G. Cleemput, J.A. Delcour, M. Nys, P.L. Darius, Physicochemical and functional properties of rye nonstarch polysaccharides. IV. The effect of high molecular weight water-soluble pentosans on wheat-bread quality in a straight-dough procedure, *Cereal Chemistry*. 70 (1993) 306–311. http://www.aaccnet.org/publications/cc/backissues/1993/documents/70_306.pdf.
- [153] M. Izydorczyk, C.G. Biliaderis, W. Bushuk, Physical Properties of Water-Soluble Pentosans from Different Wheat Varieties, *Cereal Chem.* 68 (1991) 145–150. <http://www.aaccnet.org/publications/cc/backissues/1991/Documents/CC1991a30.html>.
- [154] AOAC, Official methods of analysis of the Association of Official Agricultural Chemists, Washington, D.C., 1960.
- [155] R. Jäger, E. Unger, Ueber Pentosanbestimmung, *Berichte Der Deutschen Chemischen Gesellschaft*. 35 (1902) 4440–4443. <https://doi.org/10.1002/cber.190203504106>.
- [156] AGF, Bestimmung des Proteingehaltes mittels DUMAS-Verbrennungsmethode: Standardmethode der Arbeitsgemeinschaft Getreideforschung e.V., Detmold, 1999.
- [157] T. Senn, H. Pieper, Ethanol-Classical methods, in: H. Rehm, G. Reed (Eds.), *Biotechnology - Products of Primary Metabolism*, VCH, Weinheim, 1996: pp. 109–110.
- [158] U.K. Laemmli, Cleavage of Structural Proteins during the Assembly of the Head of Bacteriophage T4, *Nature*. 227 (1970) 680–685. <https://doi.org/10.1038/227680a0>.
- [159] H.B. Hansen, B. Møller, S.B. Andersen, J.R. Jørgensen, Å. Hansen, Grain Characteristics, Chemical Composition, and Functional Properties, of Rye (*Secale cereale* L.) As Influenced by Genotype and Harvest Year, *Journal of Agricultural and Food Chemistry*. 52 (2004) 2282–2291. <https://doi.org/10.1021/jf0307191>.
- [160] S. Bengtsson, P. Aman, Isolation and chemical characterization of water-soluble arabinoxylans in rye grain, *Carbohydrate Polymers*. 12 (1990) 267–277. [https://doi.org/10.1016/0144-8617\(90\)90068-4](https://doi.org/10.1016/0144-8617(90)90068-4).
- [161] R. Marchal, C. Descoins, P. Jeandet, Effect of the temperature on the Champagne wine foaming properties, in: *Vino Analytica Scientia Congress*, Aveiro, Portugal, 2003.
- [162] F. Brissonnet, A. Maujean, Identification of some foam-active compounds in a Champagne base wine, *American Journal of Enology and Viticulture*. 42 (1991) 97–102.
- [163] D.E. Evans, M.C. Sheehan, D.C. Stewart, The Impact of Malt Derived Proteins on Beer Foam Quality. Part II: The Influence of Malt Foam-positive Proteins and Non-starch Polysaccharides on Beer Foam Quality, *Journal of the Institute of Brewing*. 105 (1999) 171–178. <https://doi.org/10.1002/j.2050-0416.1999.tb00016.x>.

- [164] M. Lewis, A. Lewis, Correlation of beer foam with other beer properties, *Master Brewers Association of the Americas*. 40 (2003) 114–124.
- [165] D.K. Sarker, P.J. Wilde, D.C. Clark, Enhancement of protein foam stability by formation of wheat arabinoxylan-protein crosslinks, *Cereal Chemistry*. 75 (1998) 493–499. <https://doi.org/10.1094/CCHEM.1998.75.4.493>.
- [166] F. Meuser, K.G. Busch, H. Fuhrmeister, K. Rubach, Foam-forming capacity of substances present in rye, *Cereal Chemistry*. 78 (2001) 50–54. <https://doi.org/10.1094/CCHEM.2001.78.1.50>.
- [167] A.E. Dorsey, Control of foam during fermentation by the application of ultrasonic energy, *Journal of Biochemical and Microbiological Technology and Engineering*. 1 (1959) 289–295. <https://doi.org/10.1002/jbmt.390010305>.
- [168] P.F. Stanbury, A. Whitaker, S.J. Hall, *Principles of Fermentation Technology*, Second Edi, Pergamon, 1995. <https://doi.org/10.1016/C2009-0-11099-1>.
- [169] D. Murray, Grain whisky distillation, in: *Whisky*, Elsevier, 2014: pp. 179–198. <https://doi.org/10.1016/B978-0-12-401735-1.00010-6>.
- [170] H.J. Pieper, E.-E. Bruchmann, E. Kolb, *Technologie der Obstbrennerei*, Eugen Ulmer GmbH & Co., Stuttgart, 1977.
- [171] D. Heller, D. Einfalt, Foam-Resilient Distillation Processes—Influence of Pentosan and Thermal Energy Input on Foam Accumulation in Rye Mash Distillation, *Food and Bioprocess Technology*. (2021). <https://doi.org/10.1007/s11947-021-02660-9>.
- [172] A.P. Neilson, D.A. Lonergan, S.S. Nielsen, Laboratory Standard Operating Procedures, in: 2017: pp. 3–20. https://doi.org/10.1007/978-3-319-44127-6_1.
- [173] Deutsche Institut für Normung e.V., DIN 53019:2008-09 Messung von Viskositäten und Fließkurven mit Rotationsviskosimetern - Teil 1: Grundlagen und Messgeometrie, 2009.
- [174] A. Sluiter, B. Hames, R. Ruiz, C. Scarlata, J. Sluiter, D. Templeton, Technical Report NREL/TP-510-42622: Determination of Ash in Biomass, National Renewable Energy Laboratory (NREL). (2008).
- [175] R.I. Aylott, W.M. MacKenzie, Analytical strategies to confirm the generic authenticity of Scotch whisky, *Journal of the Institute of Brewing*. 116 (2010) 215–229. <https://doi.org/10.1002/j.2050-0416.2010.tb00424.x>.
- [176] A. Douady, C. Puentes, P. Awad, M. Esteban-Decloux, Batch distillation of spirits: experimental study and simulation of the behaviour of volatile aroma compounds, *Journal of the Institute of Brewing*. 125 (2019) 268–283. <https://doi.org/10.1002/jib.560>.
- [177] E.S.P. Nascimento, D.R. Cardoso, D.W. Franco, Quantitative ester analysis in cachaça and distilled spirits by Gas Chromatography-Mass Spectrometry (GC-MS), *Journal of*

- Agricultural and Food Chemistry. 56 (2008) 5488–5493. <https://doi.org/10.1021/jf800551d>.
- [178] J.J. Rodríguez-Bencomo, J.R. Pérez-Correa, I. Orriols, F. López, Spirit Distillation Strategies for Aroma Improvement Using Variable Internal Column Reflux, *Food and Bioprocess Technology*. 9 (2016) 1885–1892. <https://doi.org/10.1007/s11947-016-1776-0>.
- [179] N. Spaho, Distillation Techniques in the Fruit Spirits Production, in: *Distillation - Innovative Applications and Modeling*, InTech, 2017. <https://doi.org/10.5772/66774>.
- [180] P. Scherübel, *Mysterium Methanol - Ein ständiger Begleiter im Obstbrand?*, TU Graz, 2018.
- [181] H. Leuner, C. Gerstenberg, K. Lechner, C. McHardy, C. Rauh, J.-U. Repke, Overcoming unwanted foam in industrial processes of the chemical and food industry – an ongoing survey, *Chemical Engineering Research and Design*. 163 (2020) 281–294. <https://doi.org/10.1016/j.cherd.2020.09.006>.
- [182] M.J. Lockett, *Distillation tray fundamentals*, Cambridge University Press, New York, 1986. <https://doi.org/10.1002/cjce.5450660130>.
- [183] C. McHardy, J. Thünnesen, T. Horneber, J. Kostova, M.A. Hussein, A. Delgado, C. Rauh, Active control of foams by physically based destruction mechanisms, *PAMM*. 18 (2018). <https://doi.org/10.1002/pamm.201800351>.
- [184] M. Zlokarnik, *Scale-Up in Chemical Engineering*, Wiley-VCH Verlag GmbH & Co. KGaA, 2006. <https://doi.org/10.1002/352760815X>.
- [185] A.J. Wilson, *Foams: Physics, Chemistry and Structure*, Springer Science & Business Media, 2013.
- [186] L. Strodtsmann, R. Staud, T. Klinke, K. Jasch, S. Scholl, Quantification of evaporation-induced foaming ability, *Chemical Engineering Research and Design*. 179 (2022) 502–509. <https://doi.org/10.1016/j.cherd.2022.01.021>.
- [187] A.D. Wheatley, K.A. Johnson, C.I. Winstanley, Foaming in activated sludge plants treating dairy waste, *Environmental Technology Letters*. 9 (1988) 181–190. <https://doi.org/10.1080/09593338809384556>.
- [188] P. Tomtas, Formation and elimination of foam in the technological process of potato starch production, *PRZEMYSŁ SPOŻYWCZY*. 1 (2019) 26–32. <https://doi.org/10.15199/65.2019.1.5>.
- [189] S. Takesono, M. Onodera, J. Nagai, K. Yamagiwa, A. Mori, A. Ohkawa, Relation between mechanical foam-breaking difficulty and the foaming characteristics of solutions, *Journal of Fermentation and Bioengineering*. 75 (1993) 314–318. [https://doi.org/10.1016/0922-338X\(93\)90158-5](https://doi.org/10.1016/0922-338X(93)90158-5).

- [190] P.R. Garrett, Defoaming: Antifoams and mechanical methods, *Current Opinion in Colloid & Interface Science*. 20 (2015) 81–91. <https://doi.org/10.1016/j.cocis.2015.03.007>.
- [191] J.R. Rosenau, L.F. Whitney, J.R. Haight, Potato Juice Processing, in: *Proceedings Eighth National Symposium on Food Processing Wastes: March 30 - April 1*, U. S. Environmental Protection Agency, Office of Research and Development, Industrial Environmental Research Laboratory, Seattle, Washington, 1977.
- [192] W.L. Emkey, *Chemical-free foam control system and method*, 2015.
- [193] R.L. Whistler, J.N. Bemiller, E.F. Paschall, *Starch: Chemistry and Technology*, 2nd ed., Elsevier, Academic Press, Orlando, 1984. <https://doi.org/10.1016/C2009-0-02983-3>.
- [194] R.M.G. Voucher, A.L. Weiner, Foam control by acoustic and aerodynamic means, *British Chemical Engineering*. 8 (1963) 808–812.
- [195] N. Sandor, H.N. Stein, Foam Destruction by Ultrasonic Vibrations, *Journal of Colloid and Interface Science*. 161 (1993) 265–267. <https://doi.org/10.1006/jcis.1993.1465>.
- [196] M.D. Morey, N.S. Deshpande, M. Barigou, Foam Destabilization by Mechanical and Ultrasonic Vibrations, *Journal of Colloid and Interface Science*. 219 (1999) 90–98. <https://doi.org/10.1006/jcis.1999.6451>.
- [197] V.N. Khmelev, A.N. Galakhov, A. v. Shalunov, A.A. Romashkin, Compact Ultrasonic Drier for Low Temperature Dehydration of Products in Food Industry, in: *International Conference and Seminar of Young Specialists on Micro/Nanotechnologies and Electron Devices*, IEEE, Erlagol, Altai, Russia, 2011: pp. 225–229.
- [198] G. Rodríguez, E. Riera, J.A. Gallego-Juárez, V.M. Acosta, A. Pinto, I. Martínez, A. Blanco, Experimental study of defoaming by air-borne power ultrasonic technology, *Physics Procedia*. 3 (2010) 135–139. <https://doi.org/10.1016/j.phpro.2010.01.019>.
- [199] P.K. Chendke, H.S. Fogler, Second-order sonochemical phenomena—extensions of previous work and applications in industrial processing, *The Chemical Engineering Journal*. 8 (1974) 165–178. [https://doi.org/10.1016/0300-9467\(74\)85022-7](https://doi.org/10.1016/0300-9467(74)85022-7).
- [200] S. v. Komarov, M. Kuwabara, M. Sano, Control of Foam Height by Using Sound Waves., *ISIJ International*. 39 (1999) 1207–1216. <https://doi.org/10.2355/isijinternational.39.1207>.
- [201] H. Medwin, Acoustical determinations of bubble-size spectra, *J Acoust Soc Am*. 62 (1977) 1041–1044. <https://doi.org/10.1121/1.381617>.
- [202] T.G. Leighton, *Derivation of the Rayleigh-Plesset equation in terms of volume*, ISVR Technical Reports, 308, Southampton, UK, 2007.

- [203] H.A. Vaidya, Ö. Ertunç, T. Lichtenegger, A. Delgado, A. Skupin, The penetration of acoustic cavitation bubbles into micrometer-scale cavities, *Ultrasonics*. 67 (2016) 190–198. <https://doi.org/10.1016/j.ultras.2015.12.009>.
- [204] J.G. McDaniel, I. Akhatov, R.G. Holt, Inviscid dynamics of a wet foam drop with monodisperse bubble size distribution, *Physics of Fluids*. 14 (2002) 1886–1894. <https://doi.org/10.1063/1.1475315>.
- [205] J. Pierre, B. Dollet, V. Leroy, Resonant Acoustic Propagation and Negative Density in Liquid Foams, *Physical Review Letters*. 112 (2014) 148307. <https://doi.org/10.1103/PhysRevLett.112.148307>.
- [206] I. ben Salem, R.-M. Guillermic, C. Sample, V. Leroy, A. Saint-Jalmes, B. Dollet, Propagation of ultrasound in aqueous foams: bubble size dependence and resonance effects, *Soft Matter*. 9 (2013) 1194–1202. <https://doi.org/10.1039/C2SM25545F>.
- [207] E. Morelle, A. Rudolph, C. McHardy, C. Rauh, Detection and prediction of foam evolution during the bottling of noncarbonated beverages using artificial neural networks, *Food and Bioprocess Processing*. 128 (2021) 63–76. <https://doi.org/10.1016/j.fbp.2021.03.017>.
- [208] E.B. Matzke, The three-dimensional shape of bubbles in foam; an analysis of the role of surface forces in three-dimensional cell shape determination, *American Journal of Botany*. 33 (1946) 58–80. <https://doi.org/10.1002/j.1537-2197.1946.tb10347.x>.
- [209] A.M. Kraynik, D.A. Reinelt, F. van Swol, Structure of random monodisperse foam, *Physical Review E*. 67 (2003) 031403. <https://doi.org/10.1103/PhysRevE.67.031403>.
- [210] H.M. Princen, Rheology of foams and highly concentrated emulsions. II. experimental study of the yield stress and wall effects for concentrated oil-in-water emulsions, *Journal of Colloid and Interface Science*. 105 (1985) 150–171. [https://doi.org/10.1016/0021-9797\(85\)90358-3](https://doi.org/10.1016/0021-9797(85)90358-3).
- [211] J. Thünnesen, B. Gatternig, A. Delgado, Ultrasonic Effects on Foam Formation of Fruit Juices during Bottling, *Eng. 2* (2021) 356–371. <https://doi.org/10.3390/eng2030023>.
- [212] C.E. Lockwood, P.M. Bummer, M. Jay, Purification of Proteins Using Foam Fractionation, *Pharmaceutical Research*. 14 (1997) 1511–1515. <https://doi.org/10.1023/A:1012109830424>.
- [213] T. Runowski, M.H. Pahl, Lineare Stabilitätsanalyse der Strömung einer drainierenden Schaumlamelle, *Chemie Ingenieur Technik*. 76 (2004) 1068–1072. <https://doi.org/10.1002/cite.200403425>.
- [214] A. Boudaoud, Y. Couder, M. ben Amar, Self-Adaptation in Vibrating Soap Films, *Physical Review Letters*. 82 (1999) 3847–3850. <https://doi.org/10.1103/PhysRevLett.82.3847>.

- [215] C. Gaulon, C. Derec, T. Combriat, P. Marmottant, F. Elias, Sound and vision: visualization of music with a soap film, *European Journal of Physics*. 38 (2017) 045804. <https://doi.org/10.1088/1361-6404/aa7147>.
- [216] C.Y. Ng, H. Park, L. Wang, Dynamic Stabilization of Foam Films with Acoustic Sound, *Langmuir*. 36 (2020) 2966–2973. <https://doi.org/10.1021/acs.langmuir.9b03767>.
- [217] K.B. Kann, Sound waves in foams, *Colloids and Surfaces A: Physicochemical and Engineering Aspects*. 263 (2005) 315–319. <https://doi.org/10.1016/j.colsurfa.2005.04.010>.
- [218] Y. Couder, J.M. Chomaz, M. Rabaud, On the hydrodynamics of soap films, *Physica D: Nonlinear Phenomena*. 37 (1989) 384–405. [https://doi.org/10.1016/0167-2789\(89\)90144-9](https://doi.org/10.1016/0167-2789(89)90144-9).
- [219] V.O. Afenchenko, A.B. Ezersky, S. v. Kiyashko, M.I. Rabinovich, P.D. Weidman, The generation of two-dimensional vortices by transverse oscillation of a soap film, *Physics of Fluids*. 10 (1998) 390–399. <https://doi.org/10.1063/1.869571>.
- [220] J.-L. Joye, G.J. Hirasaki, C.A. Miller, Asymmetric Drainage in Foam Films, *Langmuir*. 10 (1994) 3174–3179. <https://doi.org/10.1021/la00021a046>.
- [221] S.L. Umbach, E.A. Davis, J. Gordon, P. Callaghan, Water self-diffusion coefficients and dielectric properties determined for starch-gluten-water mixtures heated by microwave by conventional methods, *Cereal Chemistry*. 69 (1992) 637–642.
- [222] N. Mujica, S. Fauve, Sound velocity and absorption in a coarsening foam, *Physical Review E*. 66 (2002) 21404. <https://doi.org/10.1103/PhysRevE.66.021404>.
- [223] A.C. Dedhia, P. v Ambulgekar, A.B. Pandit, Static foam destruction: role of ultrasound, *Ultrasonics Sonochemistry*. 11 (2004) 67–75. [https://doi.org/10.1016/S1350-4177\(03\)00134-2](https://doi.org/10.1016/S1350-4177(03)00134-2).
- [224] J.B. Winterburn, P.J. Martin, Mechanisms of ultrasound foam interactions, *Asia-Pacific Journal of Chemical Engineering*. 4 (2009) 184–190. <https://doi.org/10.1002/apj.225>.
- [225] M. Nakata, N. Tanimura, D. Koyama, M.P. Krafft, Adsorption and Desorption of a Phospholipid from Single Microbubbles under Pulsed Ultrasound Irradiation for Ultrasound-Triggered Drug Delivery, *Langmuir*. 35 (2019) 10007–10013. <https://doi.org/10.1021/acs.langmuir.8b03621>.
- [226] J.Z. Sostaric, P. Riesz, Adsorption of Surfactants at the Gas/Solution Interface of Cavitation Bubbles: An Ultrasound Intensity-Independent Frequency Effect in Sonochemistry, *The Journal of Physical Chemistry B*. 106 (2002) 12537–12548. <https://doi.org/10.1021/jp022106h>.

- [227] D. Sunartio, M. Ashokkumar, F. Grieser, Study of the Coalescence of Acoustic Bubbles as a Function of Frequency, Power, and Water-Soluble Additives, *J Am Chem Soc.* 129 (2007) 6031–6036. <https://doi.org/10.1021/ja068980w>.
- [228] R.E. Apfel, Acoustic cavitation prediction, *J Acoust Soc Am.* 69 (1981) 1624–1633. <https://doi.org/10.1121/1.385939>.

Acknowledgments

Die letzten Seiten der vorliegenden Arbeit, welche im Zeitraum Januar 2019 bis Oktober 2022 am Fachgebiet Hefegenetik & Gärungstechnologie der Universität Hohenheim unter der Leitung von Herrn Prof. Ralf Kölling entstanden ist, möchte ich dafür nutzen mich bei all jenen zu bedanken, welche zum Gelingen jener beigetragen haben.

Vor allem gilt mein Dank *Herrn Prof. Ralf Kölling* für die Möglichkeit meine Promotion an seinem Fachgebiet durchzuführen. Im Speziellen möchte ich mich für die zahlreichen, interessanten Debatten (sowohl über hochkomplexe Thematiken als auch über Thematiken trivialer Natur) und die immerwährende Hilfsbereitschaft bedanken.

Dr. Daniel Einfalt möchte ich ebenso für die Möglichkeit der Promotion, insbesondere im Hinblick auf mein Promotionsprojekt und die Themastellung, danken. Auch für die Unterstützung beim Anfertigen wissenschaftlicher Publikationen und die hervorragende Zusammenarbeit möchte ich mich herzlich bedanken.

Allen weiteren am Fachgebiet danke ich für ihre Hilfsbereitschaft, Freundlichkeit und den freundschaftlichen Umgang. Besonders bedanken möchte ich mich bei *Frau Julia Pesl* für die tatkräftige Unterstützung und für das stets offene Ohr; bei *Herrn Luis Hoppert* für all die wissenschaftlichen und nicht wissenschaftlichen Gespräche in den gemeinsamen Bürojahren und bei *Frau Ana Vidakovic* für die geistige Unterstützung auf den letzten Metern.

Ein ganz besonderer Dank gilt *meinen Eltern Jörg und Anita Heller* für ihre fortwährende Unterstützung auf meinem akademischen Weg und in allen anderen Bereichen. Auch möchte ich mich bei ihnen für die stetige Motivation und Geduld bedanken.

An letzter Stelle, doch am wichtigsten, möchte ich *meiner Frau Laura Heller* und *meinem Sohn Ben Heller* danken. Es wären zu viele Gründe, warum ich ihnen danken müsste, um alle hier aufzuführen, weshalb ich einfach nur sage: Danke, dass ihr da seid.

Eidesstattliche Versicherung



UNIVERSITÄT
HOHENHEIM

Eidesstattliche Versicherung gemäß § 7 Absatz 7 der Promotionsordnung der Universität Hohenheim zum Dr. rer. nat.

1. Bei der eingereichten Dissertation zum Thema

Foam management in distillation plants

handelt es sich um meine eigenständig erbrachte Leistung.

2. Ich habe nur die angegebenen Quellen und Hilfsmittel benutzt und mich keiner unzulässigen Hilfe Dritter bedient. Insbesondere habe ich wörtlich oder sinngemäß aus anderen Werken übernommene Inhalte als solche kenntlich gemacht.

3. Ich habe nicht die Hilfe einer kommerziellen Promotionsvermittlung oder -beratung in Anspruch genommen.

4. Die Bedeutung der eidesstattlichen Versicherung und der strafrechtlichen Folgen einer unrichtigen oder unvollständigen eidesstattlichen Versicherung sind mir bekannt.

Die Richtigkeit der vorstehenden Erklärung bestätige ich: Ich versichere an Eides statt, dass ich nach bestem Wissen die reine Wahrheit erklärt und nichts verschwiegen habe.

Ort und Datum

Unterschrift

Curriculum Vitae

Personal data

Name **Daniel Heller**
Date of Birth **23.08.1993**
Place of Birth **Waiblingen**



Education

2018 – (2022) **University of Hohenheim**
Yeast Genetics and Fermentation Technology
Doctorate (Dr. rer. nat.)

2016 - 2018 **University of Hohenheim**
Master of Science
'Food Science and Engineering'

2012 - 2015 **University of Hohenheim**
Bachelor of Science
'Lebensmittelwissenschaft und Biotechnologie'

Professional experience

2022 **Project Manager R&D**
GEA Brewery Systems GmbH

2018 - 2022 **Research Associate**
University of Hohenheim
Yeast Genetics and Fermentation Technology

2016 **Intern - Product development: fruit preparations**
Zott SE & Co. KG

2015 - 2016 **Employee – Quality Assurance/Quality Management**
Hengstenberg GmbH & Co. KG

Awards and honors

2018 **'Collaudatio'** for outstanding achievements in the master's program

Publications

Staud, R., Heller, D., Knüpfer, L., Heitkam, S., Einfalt, D., Jasch, K. and Scholl, S. Minimal-Invasive Method for the Evaluation of Liquid Fractions in Foams with a Point Level Sensor. *Chem. Eng. Technol* 45, 1397-1403 (2022).
<https://doi.org/10.1002/ceat.202200072>

Thünnesen, J., Gerstenberg, C., Heller, D., Leuner, H., Einfalt, D., McHardy, C., Gatternig, B., Rauh, C., Repke, J. and Delgado, A. Resonant Ultrasonic Defoaming in Aqueous Evaporation/Boiling Processes at Different Size Scales. *Chem. Eng. Technol* 45, 1380-1388 (2022).
<https://doi.org/10.1002/ceat.202200068>

Heller, D., Roj, S., Switulla, J., Kölling, R. and Einfalt, D. Tackling Foam-Based Process Disruptions in Spirit Distillation by Thermal Energy Input Adaptations. *Food Bioprocess Technol* 15, 821–832 (2022).
<https://doi.org/10.1007/s11947-022-02785-5>

Heller D. and Einfalt D. Reproducibility of Fruit Spirit Distillation Processes. *Beverages*, 8(2), 20 (2022).
<https://doi.org/10.3390/beverages8020020>

Heller, D. and Einfalt, D. Foam-Resilient Distillation Processes—Influence of Pentosan and Thermal Energy Input on Foam Accumulation in Rye Mash Distillation. *Food Bioprocess Technol* 14, 1640–1647 (2021).
<https://doi.org/10.1007/s11947-021-02660-9>

Bohn, J., Roj, S.; Hoppert, L., Heller, D. and Einfalt, D. Absorbance Spectroscopy of Heads, Hearts and Tails Fractions in Fruit Spirits. *Beverages* 7, 21 (2021).
<http://dx.doi.org/10.3390/beverages7020021>

Heller, D. and Einfalt, D. Wildflower mixtures for bioethanol production – Pretreatment and enzymatic hydrolysis. *Biomass and Bioenergy* 141, 105727 (2020)
<https://doi.org/10.1016/j.biombioe.2020.105727>

Place, Date

Daniel Heller